THE ROLE OF NEUTROPHIL RECRUITMENT IN THE PATHOGENESIS OF *Salmonella enterica* SEROTYPE *Typhimurium*-INDUCED ENTERITIS IN CALVES

A Dissertation

by

JAIRO EDUARDO DOS SANTOS NUNES

Submitted to the Office of Graduate Studies of
Texas A&M University
in partial fulfillment of the requirements for the degree of

DOCTOR OF PHILOSOPHY

December 2007

Major Subject: Veterinary Pathology

THE ROLE OF NEUTROPHIL RECRUITMENT IN THE PATHOGENESIS OF *Salmonella enterica* SEROTYPE *Typhimurium*-INDUCED ENTERITIS IN CALVES

A Dissertation

by

JAIRO EDUARDO DOS SANTOS NUNES

Submitted to the Office of Graduate Studies of
Texas A&M University
in partial fulfillment of the requirements for the degree of

DOCTOR OF PHILOSOPHY

Approved by:

Chair of committee,	L. Garry Adams
Committee Members,	Renée M. Tsolis
	Andreas J. Baumler
	Robert C. Burghardt
Head of Department,	Gerald Bratton

December 2007

Major Subject: Veterinary Pathology

ABSTRACT

The Role of Neutrophil Recruitment in the Pathogenesis of *Salmonella enterica* Serotype *Typhimurium*-Induced Enteritis in Calves. (December 2007)

Jairo Eduardo dos Santos Nunes, D.V.M., Universidade Federal de Uberlândia; M.Sc., Universidade Federal de Minas Gerais

Chair of Advisory Committee: L. Garry Adams

The role of neutrophils in the pathogenesis of *Salmonella typhimurium*-induced ruminant and human enteritis and diarrhea remains incompletely understood. To address this question, the *in vivo* bovine ligated ileal loop model of non-typhoidal salmonellosis was used in calves with the naturally-occurring Bovine Leukocyte Adhesion Deficiency (BLAD) mutation whose neutrophils are unable to extravasate and infiltrate the extravascular matrix. Data obtained from BLAD calves were compared to those from genetically normal calves negative for the BLAD mutation. Morphologic studies showed that the absence of significant tissue influx of neutrophils in intestine infected by *S. typhimurium* resulted in less tissue damage, reduced luminal fluid accumulation, and increased bacterial invasion compared to regular calves. Study of gene expression profile of cytokines by quantitative Real-Time PCR (qRTPCR) revealed that the massive tissue influx of neutrophils during acute infection is mainly driven by the CXC chemokine GRO-α especially in the last stages of

acute infection and to a lesser extent, IL-8. In contrast, the pro-inflammatory cytokines IL-1β and TNF-α were not significantly correlated with the presence or absence of tissue neutrophils.

The precise *in situ* localization of gene expression of these major cytokines and chemokines was investigated by qRTCPR from specific groups of intestinal cells captured by Laser Capture Microdissection in *S. typhimurium*-infected ileal loops from BLAD animals. Our data confirmed that gene expression of IL-8, GRO-α, and IL-1β was predominantly localized to enterocytes of crypts with less expression in enterocytes of villi tips and cells that form the domed villi were not an important source of TNF-α gene expression. Microarray technology was used to determine the global transcriptional profile of bovine intestinal loops inoculated with *S. typhimurium*. The host samples were hybridized on a 13K bovine-specific oligoarray and microarray data was analyzed using a suite of gene expression analysis and modeling tools. Analysis of our data revealed that the tissue influx of neutrophils in ileal loops greatly influenced the host gene expression. Major differences in gene expression in relevant fields of *Salmonella* research including inflammation and immune response, Toll-like receptor signaling, cytokine profiles, apoptosis, and intracellular defense against infection are discussed.

This work is dedicated to my lovely wife Josely, my father Celio, my mother Carmem, and to my blessed baby daughter, Rafaella, who has arrived this year to complete our lives

ACKNOWLEDGEMENTS

I am very grateful to the chair of my advisory committee, Dr. Garry Adams, for his guidance, support, friendship, and above all, for always trusting in my potential to seek my professional goals. I also extend my gratitude to the other members of my committee, Dr. Robert Burghardt, Dr. Renee Tsolis, and Dr. Andreas Baumler, for their constant support throughout my program.

My special appreciation is for my adorable wife, Josely, for her infinite support and kindness in all moments.

This work would never have been possible without the help of my friends from Dr. Adams' laboratory, including the terrific scientists Sara Lawhon, Sangeeta Khare, Carlos Rossetti, Tamara Gull, Quynhtien Tran, and Sarah Luciano, in addition to Alan Patranella, Roberta Pugh, Doris Hunter, and Tiffany Fausett.

I am very grateful to many other friends, including Rosemary Vollmar for providing the histologic sections, Ross Payne and Helga Bhatkar for processing and helping with the transmission and scanning electron microscopy respectively, Jenni Weeks for the assistance with the microarrays, Mary Ronsonet for helping with general inquiries, Beth Suehs and Jeanine Malazzo for their patience and countless assistance with visa regulations, and Drs. Bryan Kamery and Ken Drake from Seralogix Inc., Austin, for performing the microarray analysis and helping with the interpretation of microarray data.

Finally, I would like to express my gratitude to all current and former faculty, residents, and staff from the Pathology Diagnostic Laboratory and Clinical Pathology Laboratory at Texas A&M University for their invaluable encouragement, making possible the successful completion of my residency program and board preparation. I thank Joanne Mansell, John Edwards, Brian Porter, Kelly Credille, Roy Pool, Wayne Corapi, Ralph Storts, George Stoica, Brad Weeks, Robert Dunstan, John Mackie, Allan Kessell, Malcolm Lancaster, Lars Mecklenburg, Ann Kier, Mark Johnson, Karen Russell, Shashi Ramaiah, Fred Clubb, Cheryl Chamblee, Sharon Dickerson, Odete Mendes, Eric Hansen, Laura Kennedy, Melanie Buote, Heather Shive, David Calise, Fabiano Oliveira, Gabriel Gomez, Aline Rodrigues, Fabio Aloisio, Karen Trainor, Catherine Pfent, Elisabeth Cienava, Elisabeth Spangler, Mary Nabity, Angela Wilcox, Seth Chapman, Barbara Lewis, Lynne Cassone, David Vogt, Ken Turner, and David Cruz.

TABLE OF CONTENTS

Page

LIST OF FIGURES

FIGURE Page

FIGURE Page

LIST OF TABLES

CHAPTER I

INTRODUCTION

Salmonellosis

Salmonellosis is one of the most common food-borne bacterial diseases in the world (47, 59, 180) and a major cause of enteric disease in both humans and animals (48). In humans, an estimated 1.4 million new cases and 500 deaths occur annually in the United States alone (121). Approximately 40,000 cases of enteric human Salmonellosis are reported to the Center of Disease Control (CDC) every year (87). Recent data published by the CDC reporting the prevalence of food-born disease outbreaks from 1998-2002 identified a bacterial etiology in 18% of all outbreaks, with Salmonella accounting for almost half of these (63). Despite the fact that Salmonellosis is a recognizable notifiable disease, the number of reported cases is believed to be highly underestimated since CDC estimates the occurrence of approximately 38 unreported cases for every case reported to national surveillance throughout the United States (87).

This dissertation follows the style of Infection and Immunity.

Worldwide, non-typhoidal Salmonellosis causes 1.3 billion new cases each year resulting in 3 million deaths (143). Humans are often infected by consumption of animal products (76) and cattle constitute an import reservoir for human infections (214). Approximately 95% of human *Salmonella* infections are food-borne, accounting for 30% of all deaths caused by food-borne infections in the United States (121). In cattle, particularly in calves, *S. typhimurium* is a major cause of calf morbidity and mortality (174, 214). Medical and productivity costs as a result of *Salmonella* infections in humans and cattle result in annual losses in the range of 0.6 to 3.5 billion dollars (121).

Currently, more than 2,400 *Salmonella* serotypes have been identified (22). According to the most recent classification adopted by the CDC, all serotypes belong to two species only, namely *S. enterica*, which is represented by more than 2,400 serotypes, *and S. bongori* represented by 20 serotypes (22). *S. enterica* is further subdivided in six subspecies which are numbered I, II, IIa, IIb, IV, and VI, and named *enterica, salamae, arizonae, diarizonae, houtenae,* and *indica* respectively (22). Warm-blooded animals are infected with serotypes that belong to subspecies I (22). In this dissertation, the simplified denotation *S. typhimurium* will be used to replace *Salmonella enterica* subsp. *enterica* ser. Typhimurium, with the same rule being applied to other serotypes within the subspecies enterica hereafter.

Salmonella enterica encompasses a diverse range of bacteria that cause a spectrum of diseases in many hosts (15). Despite the large numbers of serovars identified to date, clinical disease in humans and animals results from

infection by relatively few serovars, which can be divided in three major groups based upon host prevalence (192). The first group is formed by host-specific serovars that typically cause clinical disease in a limited number of phylogenetically related species. Common serovars in this group include Typhi and Gallinarum, which result almost exclusively in systemic disease in humans and fowls respectively. The second group consists of host-restricted strains that primarily result in clinical disease in one or two closely related host species but may also occasionally cause disease in other hosts. Typical serovars in this group include Dublin and Cholerasuis, which primarily cause systemic disease in ruminants and pigs respectively, yet may potentially infect other animal species and humans. The third group is composed of ubiquitous serovars that commonly induce gastroenteritis in a broad range of unrelated and related host species such as Typhimurium and Enteritidis.

Salmonellosis in humans has two principal clinical manifestations known as typhoidal and non-typhoidal diseases (21). The most prevalent typhoidal Salmonella serovars, Typhi and Paratyphi, cause severe systemic illness that can lead to death (21). A recent study revised the global burden of typhoid fever and concluded that an estimated 20 million cases and 200,000 deaths occurs worldwide each year as a result of typhoidal Salmonellosis, with south-central Asia and south-east Asia showing the highest incidence of the disease (34). Non-typhoidal Salmonellosis is typically characterized by a self-limiting gastroenteritis, although serious complications, including systemic disease and death may occur in immunocompromised people (86, 148).

According to a recent worldwide study reported to the World Health Organization (WHO) global Salmonella survey, serovar Enteritidis is the most common human isolate of non-typhoidal Salmonellosis followed by Typhimurium and Newport (180). The same study identified serovar Typhimurium as the most frequent non-human isolate followed by Heidelberg and Enteritidis.

Salmonellosis in cattle occurs world widely and has been associated primarily with serovars Typhimurium, Dublin, and Newport to a lesser extent (24, 154). The peak of disease incidence in calves infected with S. typhimurium is at three weeks of age, whereas spread of S. dublin in infected calves is slower resulting in disease peak at 4-5 weeks of age (217). Clinical signs in young calves vary, but regardless of the serovar, the enteric form of the disease typically predominates, with diarrhea being the most important clinical manifestation of infection (216). Infection of calves with the host-adapted S. dublin; however, may cause a septicemic systemic disease affecting a variety of organs in the absence of enteric involvement, causing most commonly meningoencephalitis, polyarthritis, osteomyelitis, and pneumonia (154). In addition, infection with S. dublin in pregnant cows and heifers may cause abortion (84).

Clinical signs are typically divided into three forms based on the duration of infection and final outcome, named peracute, acute, and chronic (90). Peracute infections are often manifested as death in the absence of clinical signs and a clinical course of less than two days (200). Acute infections are typically manifested as a diarrheal disease and the mortality rate depends on the

presence or absence of treatment, ranging between 10 to 60% (200). The chronic form of the disease is usually less severe, more common in older calves, and may or not be associated with diarrhea (200).

Pathologic findings as a result of S. typhimurium infection in calves are limited to the intestine (187). Post-mortem examination in early stages of infection reveals congestion and fluid distention of the jejunum and ileum followed by formation of a fibrinous pseudomembrane within the lumen, typically attached to the surface of Peyer's patches in the ileal mucosa (215). In addition, mesenteric lymph nodes are often enlarged (215). Histologically, villi blunting precedes massive tissue influx of neutrophils, followed by transmigration of neutrophils into crypts and lumen, Peyer's Patch necrosis, and ultimately mucosal necrosis (164).

Pathogenesis of *S. typhimurium*-induced Enteritis

Although the complete mechanism of *Salmonella*-induced diarrhea is still unclear, the pathogenesis of *S. typhimurium*-induced enteritis has been extensively investigated and partially characterized by various studies using the bovine model of *Salmonella*-induced diarrhea (161, 164). The disease in cattle is a useful model for *Salmonella*-induced enteritis and diarrhea in humans, because the clinical manifestations of the disease are similar in both species (165). In both

humans and cattle, infection with *S. typhimurium* remains localized to the intestine and manifests as an acute neutrophilic enteritis and diarrhea (161). In contrast, mice infected with *S. typhimurium* develop a systemic disease with characteristic absence of diarrhea, similarly to human typhoid fever caused by the serotypes Typhi, Paratyphi A, B, and C (10, 91, 221).

The ligated intestinal loop model in calves have been used in most studies on the pathogenesis of S. typhimurium-induced enteritis using the bovine model (159, 163, 164, 191, 221-223). The model allows molecular and morphologic characterization of the host and agent responses to infection in the same animal under several distinct experimental conditions, such as distinct bacterial backgrounds and different times post-infection. It has been used to study the pathogenesis of S. typhimurium-induced enteritis is several species besides the bovine, including pigs (20, 123, 124), sheep (193), mice (147), and rabbits (45, 67, 202).

Shortly after infection in calves, as early as 5 minutes (54), S. typhimurium colonize the intestine, preferentially the ileum, where a higher density of gut-associated lymphoid tissue represented by the ileal Peyer's patches is present (161, 164). Once believed to invade only M-cells, it has now become well established based on studies using the bovine and swine models, that S. typhimurium can infect a variety of intestinal cells, including goblet cells, enterocytes of absorptive and domed villi, as well as macrophages and neutrophils in the lamina propria (54, 123, 124, 164). Intestinal cellular invasion is followed by villi blunting and activation of pro-inflammatory cytokines and CXC

chemokines (IL-8, GROα, GROγ, and GCP-1) that promote massive tissue influx of neutrophils peaking at 4 hours post-infection (164, 221, 222). Extravasated neutrophils transmigrate through the epithelial barrier formed by enterocytes, infiltrating into crypts and the lumen (164). Severe neutrophilic enteritis is followed by detachment of surface enterocytes with disruption of epithelial basement membrane, fibrin and fluid exudation into the lumen resulting in pseudomembrane formation, and ultimately necrosis of the mucosa and diarrhea (164).

Ultrastructural studies have demonstrated that Salmonella, when in contact with the epithelial barrier, induce cytoskeleton changes in enterocytes resulting in apical membrane ruffling formation, a process culminating in bacterial engulfment (54, 78, 164). In addition, bacterial attachment is often associated with loss of microvilli (164). Studies in the swine model suggest that invading S. typhimurium has a specific affinity to sites of cell extrusion (124). After invasion, Salmonella reside in acidified membrane-bound compartments called Salmonella-containing vacuoles (SCV) (205). Recent evidence based on S. typhimurium infection in dendritic cells suggest that wild type virulent strains are contained in spacious phagosomes and are organized in groups of multiple organisms, whereas mutant strains with attenuated virulence remains within tight phagosomes that closely follow the contour of the bacteria and occur mainly as single profiles (101).

The major virulent genes required by S. enterica to cause infections in susceptible hosts are carried on discrete regions of the chromosome called

Salmonella pathogenicity islands (128). Salmonella pathogenicity islands (SPI) are essential for host cell invasion and intracellular pathogenesis (80). Although 14 SPIs has been identified to date, SPI-1 and SPI-2 are considered central to the virulence of S. enterica in mammals (128), because they both encode a dedicated protein secretion system, termed type III secretion system (TTSS), which determine the ability of S. typhimurium successfully invade and colonize the intestine (57, 75, 89). During infection, the activated TTSS resembles a needle-like structure that enable Salmonella to translocate SPI-encoded effector proteins directly into the host cell cytoplasm, where the proteins manipulate the host cell signaling (56-58). The TTSS has a complex structure composed of several proteins that interact to form a base, inner rod, and a needle allowing delivery of effector proteins into host cells (58). The TTSS has been described in variety of pathogenic and symbiotic bacteria, as well as plants, nematodes, and insects (58). In S. typhimurium, the base is composed of three proteins: InvG that makes up the outer rings plus PrgH and PrgJ, which supposedly form the rest of the structure (114). The putative inner rod protein and needle proteins are PrgJ and PrgI respectively (58, 105). In addition, a regulatory protein named InvJ is required for appropriate assembly of the complex but is not part of the final structure (58, 105).

Two major types of TTSS are important during the pathogenesis of Salmonella infections, the TTSS-1 and TTSS-2 (58). TTSS-1 is encoded by SPI-1 and is essential for S. typhimurium invasion (56) and enteritis in the bovine model (187). Other functions being attributed to TTSS-1 with a role in Salmonella

pathogenesis include reorganization of host cell structure and invasion of fibroblasts and epithelial cells (81), transmigration of polymorphonuclear granulocytes (PMNs) across epithelial cell layers (107), and cell death (94). In contrast, the SPI-2-encoded type III secretion system, termed TTSS-2, plays a essential role in facilitating the replication of intracellular bacteria within membrane-bound SCV (205) and is required for Salmonella replication within host cells and establishment of systemic infection in the murine typhoid model (53).

The TTSS-1 is required for invasion of the bovine intestine (207), triggering the production of CXC chemokines, neutrophil recruitment (187, 221, 222), fluid accumulation, and diarrhea (187, 206, 222). In the bovine model, strains carrying mutations in effector proteins translocated by TTSS-1 such as SipA, SopA, SopB, SopD or SopE2 had markedly reduced enteropathogenicity resulting in attenuated fluid accumulation (223). Since mutations impairing components of the TTSS-1 complex result in similarly attenuated strains during oral infections in calves, it is hypothesized that S. typhimurium TTSS-1 functions mainly to translocate six effector proteins; SipA, SopA, SopB, SopD, SopE, and SopE2, into host cells during bovine enteritis (149).

The molecular pathogenesis of intestinal epithelium invasion is beginning to be characterized. Studies using non-polarized human epithelial cell lines concluded that the genes SopB, SopE, and SopE2 are required for invasion (224), whereas SopD and SopA does not appear to be required (150). A series of elegant studies have demonstrated that SopE, SopE2, and SopB, upon delivery

by the TTSS-1, activate specific Rho Family GTPases (Rac1, RhoG, and Cdc42) that mediate invasion-related cellular responses such as actin remodeling, macropinocytosis, and nuclear responses (144). Accordingly, SopE and SopE2 are guanine nucleotide exchange factors that directly activate Rac1 and Cdc42. Rac1 is required for S. typhimurium entry and activation of Cdc42 results in nuclear responses within host cells, such as production of IL-8. It was also demonstrated in these studies that SopB, an inositol phosphatase, indirectly activates RhoG by directly stimulating SH3-containing guanine nucleotide exchange factor, an exchange factor for RhoG. This indirect action of SopB over RhoG plays a central role in actin cytoskeleton remodeling during infection accounting for the SopD-dependent invasion phenotype. SipA has also been shown to play a role in invasion by directly interacting with the structural components of the actin filaments inducing cytoskeleton rearrangements (225, 226). In addition, there is also evidence that SopA and SopD contribute to invasion in non-polarized cells, but similar results were not observed in polarized colon carcinoma cell lines (150).

In calves, transepithelial migration of S. typhimurium after invasion occurs rapidly as opposed to evidence of persistence and replication within SCV as reported in *in vitro* studies (149). The bacteria are first seen in the apical border and rapidly transit to a basolateral location at or before one hour post-infection, followed by invasion of lamina propria at one to four hours post-infection (161, 164). The molecular mechanisms governing CXC chemokine production and neutrophilic inflammation are yet poorly characterized. Strains

carrying mutations of *sipB*, *invH* or combined mutations of *sipA, sopA, sopB, sopD*, and *sopE2* induce markedly reduced inflammatory responses and fluid secretion in calves (206, 223). Evidence of the TTSS-1 translocated effector proteins SipA, SopE, and SopE2 contributing for S. typhimurium-induce enteritis is supported by studies employing the streptomycin-pretreated-mouse model (14, 76). This model has been proved to be useful to investigate the factors that contribute to trigger Salmonella-induced enteritis in vivo (21). Mutation of *sptP, avrA, sspH1* or *alrP* had no effect on enteritis and fluid secretion in calves suggesting that not all TTSS-1 protein-encoded genes are required for inflammation and diarrhea (221). Some in vitro studies using human intestinal epithelial cell lines found conflicting results since they demonstrate that mutants defective for translocation of TTSS-1 effector proteins induce the same levels of CXC chemokines production in wild type and mutant strains (65, 66, 220). In human epithelial cell lines, immune recognition of bacterial flagellin appears to be the dominant mechanism for CXC chemokine production (65, 66, 88, 183, 220).

Flagellin, a principal component of bacterial flagella, is part of pathogen-associated molecular patterns (PAMPs) which are expressed on several infectious agents, but not on the host (79). S. typhimurium flagellin is recognized by Toll-like receptor 5 (TLR5) (79), which is expressed in the basolateral area of intestinal epithelial cells (65). The restricted localization of the TLR5 in intestinal cells prevents its activation by PAMPs expressed in commensal intestinal bacteria (149). Despite the evidence showing the importance of flagellin triggering chemokine production, in vivo studies in calves

have found that S. typhimurium with inactivated TTSS-1 results in much stronger reduction of neutrophilic infiltration compared to a strain with inactivated flagellin (167), indicating that flagellin-mediated TLR5 activation is not the only mechanism contributing to enteritis (149). Similar to activation of the inflammatory response, the molecular mechanisms driving fluid secretion and diarrhea during Salmonella-induced enteritis is incompletely characterized. Fluid secretion in epithelial cells appear to be mediated by sopB through activation of chloride secretion (142), but there is paucity of current evidence supporting this finding.

Bovine Leukocyte Adhesion Deficiency

Bovine leukocyte adhesion deficiency (BLAD) is a lethal autosomal recessive congenital disease of Holstein cattle characterized by recurrent bacterial infections, delayed wound healing, stunted growth, and the characteristic marked and persistent neutrophilia (130, 132, 135). Affected calves have recurrent bacterial infections that fail to respond to conventional treatment (184) and usually die before reaching sexual maturity (68, 100, 182). The most commonly observed clinical manifestations of the disease in calves are gingivitis, alveolar periostitis, diarrhea, bronchopneumonia, peripheral lymphadenopathy, and chronic dermatitis (68, 130). Recurrent necrotic and indolent infections of

soft tissues affecting especially the oral mucous membrane and intestinal tract is considered the hallmark of BLAD (6, 14, 133, 135).

The condition was first recognized in a Holstein heifer in 1983 and called granulocytopathy, because a neutrophil dysfunction was suspected to be the cause (74). In 1987, several cases of bovine granulocytopathy syndrome characterized by defective inflammatory responses and impaired neutrophil functions were reported in Japan (138, 139, 182). In 1990, the cause of the condition was determined to be a lack of β2 integrin molecules expressed on the leukocytes, and it was renamed Bovine Leukocyte Adhesion Deficiency (99). Ever since, several cases of BLAD have been reported in Holsteins in several countries of Europe, Australia, USA, and Japan (132).

The causative genetic defect of BLAD is a single point mutation (adenine to guanine) at the position 383 of the of β2 integrin subunit CD18, which results in an aspartic acid to glycine substitution at amino acid 128 (D128G) (62, 132, 171). This mutation occurs within an extracellular region highly conserved among integrin β subunits, near 26 aminoacids identical in normal bovine, human and murine CD18 (171). A second silent single point mutation, cytosine to thymine, has also been identified between the normal and the BLAD allele at position 775 of the CD18 gene (171). Distinction between normal, carrier, and affected animals is normally determined though restriction analysis of PCR products amplified from position 383 of the CD18 gene (127, 181, 184). The carrier frequency of BLAD among Holstein cattle in the US had once reached 15% among bulls and 6% among cows, making this condition one of the most

common genetic diseases known in animal agriculture (171). Continuous screening of young bulls before entering artificial insemination stations has significantly reduced the incident of BLAD (146). BLAD is considered a good animal model for the remarkably similar condition in humans termed Leukocyte Adhesion Deficiency (LAD) (71) and for efficient control of genetic disorders mediated by a single recessive mode of inheritance (132).

The common beta subunit of β2 integrins, CD18, associates with four different alpha chains (CD11) to give rise to four distinct integrins: CD11a/CD18 (LFA-1), CD11b/CD18 (Mac-1), CD11c/CD18 (CR4), and CD11d/CD18 (70). LFA-1 is expressed in all leukocytes, particularly T and B lymphocytes, as well as many leukocyte-derived cells such as macrophages (11, 132). Neutrophils express LFA-1, Mac-1, and CR4; however, Mac-1 is expressed at significant higher levels in activated neutrophils (55). Mac-1 and CR4 are also expressed in neutrophils, monocytes/macrophages, and natural killer cells (180). While CR4 is the most prominent integrin expressed in activated tissue macrophages (11), CD11d/CD18, is abundant in peripheral blood CD8+ lymphocytes as well as in some tissue-compartmentalized macrophages (196).

Since association between subunits CD11 and CD18 within activated leukocytes is critical for expression of the β2 integrin heterodimer on the cell surface (176), the defective CD18 subunit of BLAD calves result in deficient expression of all four classes of β2 integrins on leukocytes of affected calves (4, 33, 71). Binding of β2 integrins on the neutrophil surface to intercellular adhesion molecule 1 (ICAM-1) on vascular endothelium is required for neutrophil

emigration into sites of inflammation, therefore BLAD calves have impaired extravasation of neutrophils into sites of inflammation (135). A notable exception occurs in lungs of calves experimentally infected with the bacteria Mannheimia haemolytica, the etiologic agent of Bovine Pneumonic Pasteurellosis. Accordingly, studies using BLAD calves have demonstrated that β2 integrin-ICAM-1 adherence mediates neutrophil extravasation and infiltration into the bronchi during Pneumonic Pasteurellosis, but it is not required for neutrophil infiltration into the bronchioles and alveoli (2, 3).

In addition to deficient extravasation, BLAD calf neutrophils have marked functional abnormalities including severely decreased adherence, chemotactic movements, phagocytosis, luminol-dependent chemiluminescent response, and O(2-)- producing activities (135). Adherence and chemotactic responses of mononuclear phagocytes from cattle with BLAD are also markedly reduced (137). Although delayed and impaired, antibody production was found to take place in immunized BLAD calves, indicating lymphocyte reactivity (131). Immune stimulation of BLAD calves revealed severely delayed and defective antigen-specific immune responses (131). Neutrophils from BLAD also have significantly decreased expression of L-selectin compared to control calves (134). Regarding BLAD carriers, β2 integrin expression on neutrophils from heterozygous animals is 56 to 99% compared to neutrophils from normal cows (33); however, leukocytes from BLAD carriers had no detectable functional differences when compared with normal controls (172).

The Role of Neutrophils in *S. typhimurium*-induced Enteritis

Despite the fact that massive neutrophilic influx is the histopathologic hallmark of *S. typhimurium*-induced enteritis in humans and calves (190), the role of neutrophils in the pathogenesis of non-typhoidal Salmonellosis remains to be better characterized. In addition, the mechanisms leading to the massive neutrophil recruitment is uncertain to date. One proposed mechanism is that *S. typhimurium* triggers the massive neutrophil influx into tissues by activating gene expression of pro-inflammatory cytokines in intestinal cells through the action of translocated effector proteins (190). A second hypothesis suggests that *S. typhimurium* has a more passive role by proposing that activation of neutrophilic inflammation occurs as a result of binding of *Salmonella* PAMPs to pathogen recognition receptors in cells of the lamina propria (190).

Studies using the ligated ileal loop model in calves infected with *S. typhimurium* suggest that the massive tissue influx of neutrophils lead to loss of epithelial integrity resulting in effusion of a protein-rich exudates into the intestinal lumen, thereby contributing to diarrhea (222). Corroborative evidence that neutrophil influx contribute to diarrhea is supported by studies in rabbit ligated ileal loops showing that treatment with nitrogen mustard, an inhibitor of neutrophil influx, inhibited fluid secretion induced by *Salmonella* (202). Alternatively, neutrophils may contribute to diarrhea by stimulating chloride secretion in intestinal epithelial cells (112). Accordingly, activated neutrophils in the lumen

release a neutrophil-derived secretagogue identified as 5'-AMP, which induces electrogenic chloride secretion in the intestinal epithelia resulting in secretory diarrhea (112). Diarrhea has also been associated with the inositol phosphatase activity of SopB, which may directly trigger chloride secretion through changes in phosphatidylinositol signaling (142).

While much evidence points to the harmful effects of neutrophil influx to the host during non-typhoidal Salmonellosis, this response is likely important to reduce infection and prevent systemic spread (149). Infection of rabbit ligated ileal loops with *Shigella flexneri* demonstrated that neutrophil influx is essential for preventing bacterial dissemination within the lamina propria (157). Regardless of these findings, neutrophils are in general not considered effective in the control of intracellular pathogens despite being an important component of innate immunity (26). Investigation of the role of neutrophils in the murine model of typhoidal Salmonellosis suggests that neutrophils are unable to control systemic spread and replication of *S. typhimurium* in organs with large bacterial loads, whereas the rapid neutrophil influx observed in the intestine of non-typhoidal models of Salmonellosis prevents the spread of the pathogen (26).

Objectives

Based on the current literature available on the pathogenesis of *S. typhimurium*-induced enteritis, it is clear that the contribution of neutrophils remains incompletely understood. The overall goal of this work is to better characterize the role of neutrophil recruitment in the bovine model of non-typhoidal Salmonellosis. The BLAD calf is used here as a model for absence or markedly reduced neutrophil influx into sites of infection, allowing determination of molecular and morphologic changes induced independently of neutrophilic inflammation. Chapter II of this dissertation evaluates the *in vivo* host response to S. typhimurium at the morphologic and immunologic levels with emphasis in the kinetics of changes induced by infection in the absence of neutrophils as well as determination of gene expression of major pro-inflammatory cytokines during infection. Chapter III identifies the *in vivo* contribution of specific cell types targeted by *S. typhimurium* during intestinal infection by demonstrating the influence of neutrophils over the gene expression of pro-inflammatory cytokines. Chapter IV identifies the most relevant *in vivo* differentially expressed genes and their dynamic temporal relationship during *S. typhimurium* infection in the absence of significant neutrophilic enteritis.

CHAPTER II

MORPHOLOGIC AND CYTOKINE PROFILE CHARACTERIZATION OF *Salmonella typhimurium* INFECTION IN CALVES WITH BOVINE LEUKOCYTE ADHESION DEFICIENCY

Introduction

Salmonella enterica serovar Typhimurium (hereafter *S. typhimurium)* is the most frequent non-human isolate and among the three most common human isolate of non-typhoidal salmonellosis (180). The non-typhoidal form of salmonellosis is characterized by a self-limiting enterocolitis with diarrhea in the absence of systemic disease (31). This form results in between 200 million and 1.3 billion cases including 3 million deaths each year worldwide (210). Moreover, *S. typhimurium* is a major cause of calf morbidity and mortality resulting in significant economic losses (121). The 2004 Salmonella report published by the Center of Disease Control (CDC) reported cattle as the most commonly identified source for *Salmonella spp.*, including *S. typhimurium,* which was the most frequent serovar isolated from humans in that year. According to a CDC analysis on the impact of foodborne illnesses, non-typhoidal salmonellosis

accounted for 25.6% of hospitalizations and 30.6% of deaths due to known foodborne pathogens in the United States (121). The disease is markedly similar in both humans and cattle, making the calf an excellent model to study the non-typhoidal form of salmonellosis (165, 221).

The morphologic changes and profile of selected chemokines, as well as pro- and anti-inflammatory cytokines have been characterized in calves by using the ileal loop model of *S. typhimurium*-induced enteritis (161, 164). Accordingly, infection of ileal Peyer's patches by *S. typhimurium* results in severe tissue influx of neutrophils, which is thought to play a significant role in the pathogenesis of enteritis and diarrhea induced by *S. typhimurium* infections (161, 164). The massive tissue influx of neutrophils was associated with increased expression the CXC chemokines IL-8, GROα, GROγ, and GCP-2, the pro-inflammatory cytokine IL-1β, and anti-inflammatory cytokines IL-1Ra and IL-4 (164). In a similar study using the same model, the CXC chemokine GROα was considered the most important stimulus for tissue influx of neutrophils (221). *In vivo* studies using the ligated intestinal loop model in rabbits also found that *Salmonella*-induced fluid secretion and diarrhea is inhibited by depletion of neutrophilic pool by nitrogen mustard (202).

Hypothetically, the tissue influx of neutrophils induces loss of epithelial integrity and effusion of a protein rich exudate into the intestinal lumen contributing to diarrhea (222). Alternatively, neutrophils may contribute to diarrhea by directly stimulating chloride secretion in intestinal epithelial cells. Mice experimentally infected with *S. typhimurium* typically develop the typhoid

form of salmonellosis characterized by systemic disease with a mild monocytic enteritis, minimal intestinal infiltration of neutrophils, and mild epithelial damage (221). The classic lack of diarrhea observed in these animals corroborates with evidence that neutrophil influx plays a major role in fluid secretion. In addition, infection by *S. typhimurium* in mice elicit intestinal gene expression of CC chemokines, which are mainly chemoattractant to mononuclear cells, rather than neutrophilic chemoattractants (CXC chemokines) (221), indicating that these striking differences in host responses to infection are a reflection of the distinctive cytokine profile in infected calves and mice.

Salmonella effector proteins encoded by genes *sipA (sspA), sopA, sopB (sigD), sopD*, and *sopE2* are components of the invasion-associated type III secretion system (TTSS-1), which is required for eliciting neutrophil influx and fluid accumulation in bovine ligated ileal loops (60, 96, 163, 213, 223). Calves infected with a *S. typhimurium* carrying simultaneous mutations in all TTSS-1-associated genes (*sipAsopABDE2* mutant or ZA21) had markedly attenuated tissue influx of neutrophils, mild epithelial damage, and severely reduced fluid secretion (221, 222). The presence of these genes is also required for CXC chemokine gene expression in bovine but not in murine intestinal tissue (221). In addition, orally infected calves infected by *Salmonella* strains carrying mutations in structural components of the TTSS-1 (*prgH*) have attenuated pathogenicity similar to the mutant strain ZA21 (187, 188), highlighting the importance of this secretion system in the pathogenesis of *S. typhimurium*-induced enteritis.

To develop a better understanding of the host response to non-typhoidal salmonellosis, with particular emphasis in the role played by neutrophils, we employed the ligated ileal loop model in calves with bovine leukocyte adhesion deficiency (BLAD). BLAD is an autosomal recessive congenital condition of Holstein cattle characterized by an impaired extravasation of neutrophils into sites of inflammation (135). The condition is caused by a single point mutation (adenine to guanine) at position 383 of the common β2 integrin subunit CD18, resulting in defective expression of β2 integrin in the surface of leukocytes (62, 132, 171). Since binding of β2 integrin expressed in the surface of activated neutrophils to intracellular adhesion molecule-1 (ICAM-1) expressed in activated endothelial cells is required for extravasation of neutrophils into sites of inflammation, the defective expression of β2 integrin in BLAD neutrophils render these animals incapable of mounting an adequate neutrophilic response against bacterial infections (62, 135). Here, we used BLAD calves as a "neutrophil knockout" model to describe the histologic and ultrastructural changes, and the profile of gene expression of major chemokines and pro-inflammatory cytokines in bovine Peyer's patches infected with *S. typhimurium*.

Materials and Methods

Bacterial strains and growth conditions

Strains of *S. typhimurium* used in this study included the Wild Type strain IR715 (ATCC 14028 wild type *nal*) (178) and the mutant strain ZA21 (Δ*sipAsopABDE2* - ATCC 14028 *nal*) (223). All strains were grown in Luria-Bertani (LB) medium with nalidixic acid antibiotic (50 mg/liter) under agitation (250 rpm) overnight at 37^{o}C; 50 μl of the culture was inoculated into 5 ml of fresh LB medium and subculture for additional 4 hours before inoculation.

Animals, surgical procedure, and sampling

A total of four BLAD Holstein calves, 1 to 5 weeks of age, represented by both genders, weighting approximately 35 to 55 Kg were used in these experiments. All calves were homozygous for the BLAD defect (CD18 -/-) as determined by a PCR-based DNA test combined with restriction enzyme analysis (99, 171). Embryo transfer technology (168) was used to generate 3 BLAD calves present in this study. The other calf as well as all BLAD embryos were donated by the USDA/ARS National Animal Disease Center (NADC) –

Ames, IA. The calves were kept clinically healthy before the experiments at the Large Animal Hospital of the College of Veterinary Medicine, Texas A&M University, College Station, TX, and negative for *Salmonella spp.* as determined by fecal culture using enrichment in tetrathionate broth (Difco, Detroit, MI). Calves were fed antibiotic-free milk replacer twice a day, water *ad libitum*, and fasted 24 hours prior to experimental surgeries. The ligated ileal loop surgical procedure was employed as previously described (164, 166). Briefly, anesthesia was induced with propofol (Abbot Laboratories, Chigaco, IL) followed by placement of endotracheal tube and maintenance with isofluorane (Abbot Laboratories, Chigaco, IL) for the duration of the experiment. A laparotomy was performed, the ileum and jejunum were exposed and 16-20 loops, 5 to 8 cm long, were ligated in the ileum and distal jejunum, intercalated with 1-2 cm loops. The loops were injected with 3 ml of either sterile LB broth (control loops) or LB containing approximately 0.75 x 10^9 colony-forming units (cfu) of the *S. typhimurium* strains previously described. Loops were replaced into the abdominal cavity and excised at 1, 4, 8, and 12 hours post-infection (HPI). Samples for bacteriologic culture, histopathology, transmission and scanning electron microscopy, and quantitative real time PCR (qRT-PCR) were collected. Data collected from bacteriology, fluid secretion, gene expression of cytokines and chemokines were compared to four control, age-matched, male Holstein calves negative for the BLAD defect (CD18 +/+) submitted to similar experimental protocols.

Fluid secretion, bacteriologic culture, and histopathology

Excised loops were opened and the amount of accumulated fluid was measured in metric units. Two 6 mm biopsy punches were taken from the intestinal mucosa and submucosa along the anti-mesenteric side, including the Peyer's patches, washed 3 times in 5 ml of phosphate buffer saline (PBS), homogenized in 900 μl of PBS, serially diluted, and plated onto nalidixic acid (50 mg/liter) containing LB plates (223) for cfu enumeration. Intestinal samples were fixed in neutral 10% buffered formalin, processed according to routine procedures for paraffin embedding, sectioned at 4-5 μm, and stained with hematoxylin and eosin (H&E).

Scanning and transmission electron microscopy

Several small fragments of the intestinal samples were fixed overnight at 4^{o}C in a solution composed of 5% glutaraldehyde and 4% paraformaldehyde in 0.1M sodium cacodylate buffer and processed as previously described (164). Briefly, after fixation, samples were washed 3 times with 0.1M sodium cacodylate buffer and post fixed for 2 hours at 4^{o}C in 1% osmium tetroxide in 0.1M sodium cacodylate buffer. For transmission electron

microscopy, the samples were stained overnight at 4°C in a saturated uranyl acetate solution, dehydrated in graduated series of ethanol solutions and propylene oxide, and embedded in Epon-Araldite. Sections 0.5 μm thick were stained with toluidine blue and examined under light microscopy for selection of microscopic fields that included villi, lamina propria with crypts, muscularis mucosa, and submucosa. Blocks were trimmed to produce thin sections (60-90 nm), mounted onto copper grids, stained with uranyl acetate and lead citrate, and examined with a Zeiss 10C transmission electron microscope. For scanning electron microscopy, samples were dehydrated, dried, coated with approximately 500 Å thin layer of AuPd and examined with a JEOL JSM-6400 scanning electron microscope at an accelerating voltage of 15 kV.

Real time polymerase chain reaction (qRTPCR)

As a source of host RNA, six to eight 6 mm biopsy punches were taken from the intestinal samples including Peyer's patches. Punches were immediately cleaned to remove debris, minced into small pieces with a sterile scalpel or razor blade, immersed in 500 μl of 4°C TRI-reagent® (Ambion, Foster City, CA) and further homogenized using a tissue grinder. The RNA was extracted the same day according to TRI-reagent manufacturer instructions, the pellet was resuspended in nuclease-free water (Ambion, Foster City, CA), and

contaminant DNA was removed by RNase-free DNase I treatment (Ambion, Foster City, CA) according to manufacturer's instructions. Samples were stored at -80^{o}C until used. The resultant DNA-free RNA was quantified using a NanoDrop® ND-1000 spectrophotometer (NanoDrop Technologies, Wilmington, DE) and assessment of RNA quality was determined using an Agilent 2100 Bioanalyser (Agilent Technologies, Santa Clara, CA).

Selected RNA samples of adequate quality from each condition was used to determine the gene expression levels of IL-8, GRO-α, IL-1β, and TNF-α by qRTPCR as previously described (221). Briefly, 2 μg of RNA was reverse transcribed at 48 ^{o}C for 30 min with random hexamer primers and Multiscribe Reverse Transcriptase (Applied biosystems, Foster City, CA). The resultant cDNA at concentration of 40 ηg per sample was mixed with 4 SmartMix beads per sample (Cepheid, Sunnyvale, CA), SYBRGreen-I 0.2x (Invitrogen Corporation, Carlsbad, CA) and 500 nM of each primer set (Table 1). The qRTPCR reaction was performed using a Smart Cycler II (Cepheid, Sunnyvale, CA). The quantitative gene expression of each cytokine and chemokine was normalized to the internal control glyceraldehyde-3-phosphate dehydrogenase (GAPDH). The normalized levels of gene expression in infected tissues were calculated relative to uninfected control tissues as previously described (221).

Statistical analysis

The effects of *S. typhimurium* wild type (WT) and *sipAsopABDE2* mutant (MT) infection on intestinal invasion, fluid secretion, and gene expression of cytokines and chemokines were analyzed by calculation of geometric means and standard deviation, followed by the use of a Student's *t* test to determine differences with statistical significance ($p < 0.05$).

Table 1- Primer sequences used in qRTPCR to study the gene expression of *S. typhimurium* infected bovine intestine.

Target	Primer sequence[a]	Amplicon size (bp)
GAPDH	TTCTGGCAAAGTGGACATCGT	114
	GCCTTGACTGTGCCGTTGA	
GRO-α	CACTGCGACCAAACCGAAGT	153
	GTATCAAGAAGCTCGTTCCAT	
IL-8	TGCTTTTTTGTTTTCGGTTTTTG	71
	AACAGGCACTCGGGAATCCT	
IL-1β	CCAGCCTGGCAAAAACCAT	201
	CCGGAAATTGGTTCCACAGT	
TNF-α	GTTCCTCACCCACACCATCAG	283
	GGTAGTCCGGCAGGTTGATC	

[a]Sequences for bovine genes were obtained from GenBank. Top row represents forward primers and bottom row shows reverse primers.

Results

Morphologic findings

Histologic evaluation of intestinal sections of BLAD Calves (CD18 -/-) calves was limited to the distal jejunal and ileal mucosa and submucosa. Morphologic changes in the muscular layers were disregarded to avoid inclusion of artifacts resultant from surgical manipulation and the use of electrocautery for loop excision. All sections from uninfected control loops were histologically within normal limits. Histologic lesions in BLAD calves were not observed in tissues infected by any of the strains used (WT and MT) at 1 HPI. At this time point, the absorptive villi retained normal morphology showing no evidence of blunting (Figs. 1A, B, C), and inflammatory infiltrates were not observed. The first histologic changes were detected at 4 HPI, characterized by mild blunting of the absorptive villi in WT-infected tissues from three animals (Fig. 2A). In addition to blunting, mild exudation of fibrin into the lumen admixed with karyorrhectic cellular debris (pseudomembrane formation) and infrequent detachment of enterocytes from the basal membrane was occasionally observed in WT-infected samples (Fig. 2B). Histologic lesions were not detected in any of the MT-infected tissues in this time point, as well as in the WT-infected loop from one animal. As with 1 HPI, inflammation was not significant in any tissues examined regardless the strain.

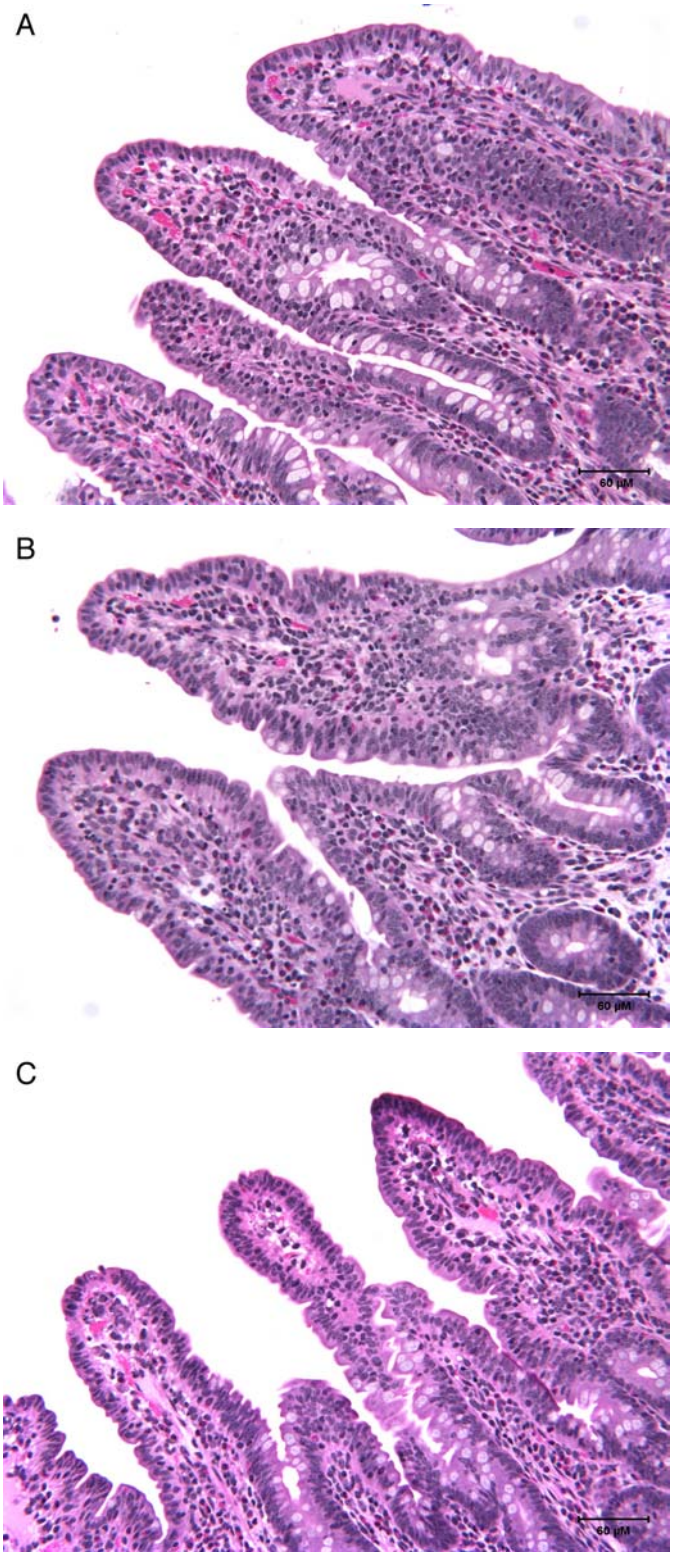

Figure 1: Normal histologic appearance of absorptive villi in uninfected control (A), WT- (B), and MT-infected samples. 1 hour post-infection. BLAD calf (CD18 -/-). H&E.

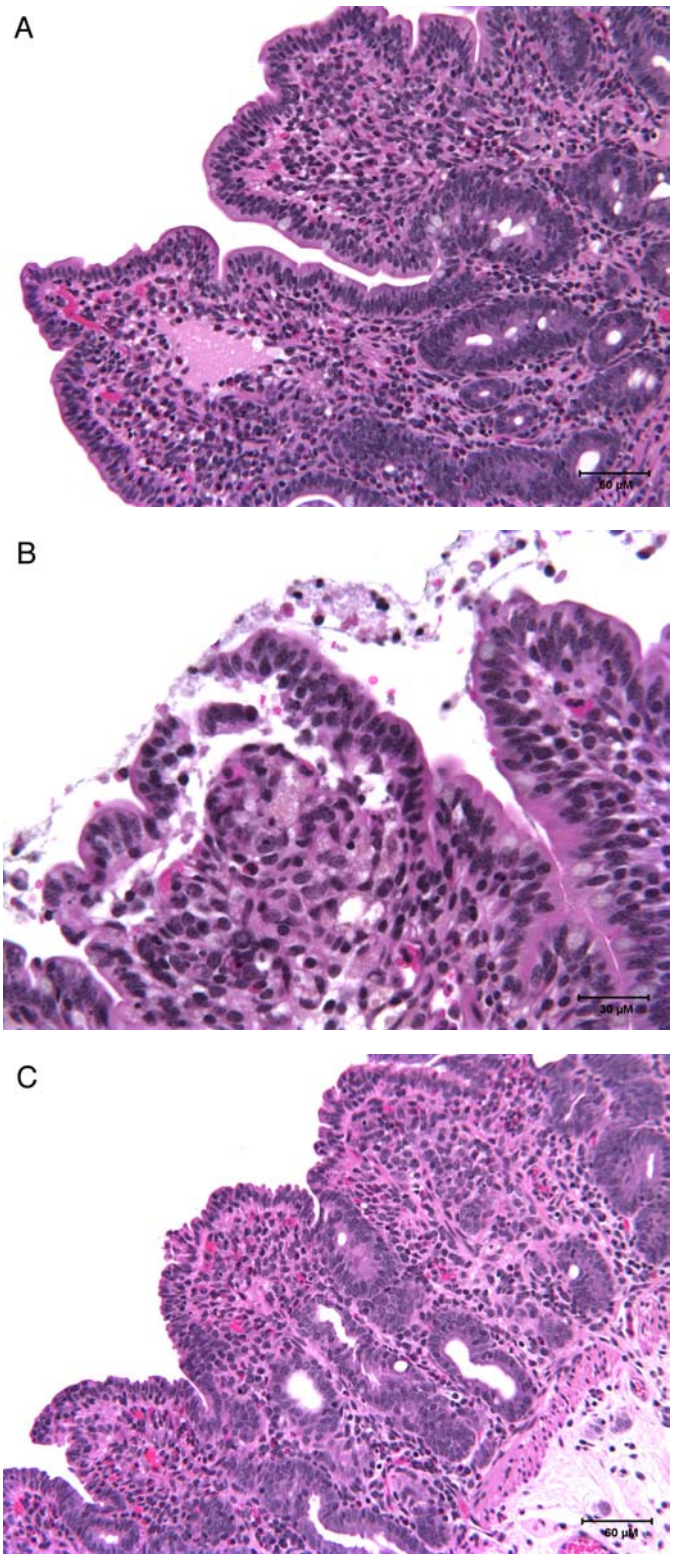

Figure 2: Mild villi blunting (A) and detachment of enterocytes at the tip of absorptive villi with fibrinous pseudomembrane formation (B) in WT-infected samples. 4 hours post-infection. Marked blunting, shortening, and fusion of villi in WT-infected samples (C). 8 hours post-infection. BLAD calf (CD18 -/-). H&E.

Marked histologic lesions began to be detected at 8 HPI in BLAD calves. In general, while both WT- and MT-infected loops had similar lesions, the severity of changes was markedly reduced in tissues infected by the MT strain, particularly in 2 animals, which exhibited mild changes when compared to uninfected control samples. In addition, differences in severity of lesions for both WT- and MT-infected tissues were evident with two calves having marked lesions whereas the other two calves generally had similar but milder lesions. Villi were often markedly blunt, shortened, and fused (Fig. 2C). Enterocytes along tips of absorptive and domed villi were occasionally detached from the basement membrane and replaced or disrupted by karyorrhectic and pyknotic cellular debris indicating necrosis. Necrosis appeared first at the tips and progressed towards the basolateral surface of villi (Fig. 3A). Necrotic debris was also occasionally evident scattered in the lamina propria on both absorptive and domed villi (Fig. 3B). Inflammation was generally mild and limited to a few perivascular neutrophils in the submucosa. Neutrophils were rarely observed in the lamina propria. Occasional crypts contained a few desquamated enterocytes and necrotic debris. Crypts filled with viable and degenerate neutrophils (crypt abscesses) were not observed in any of the samples.

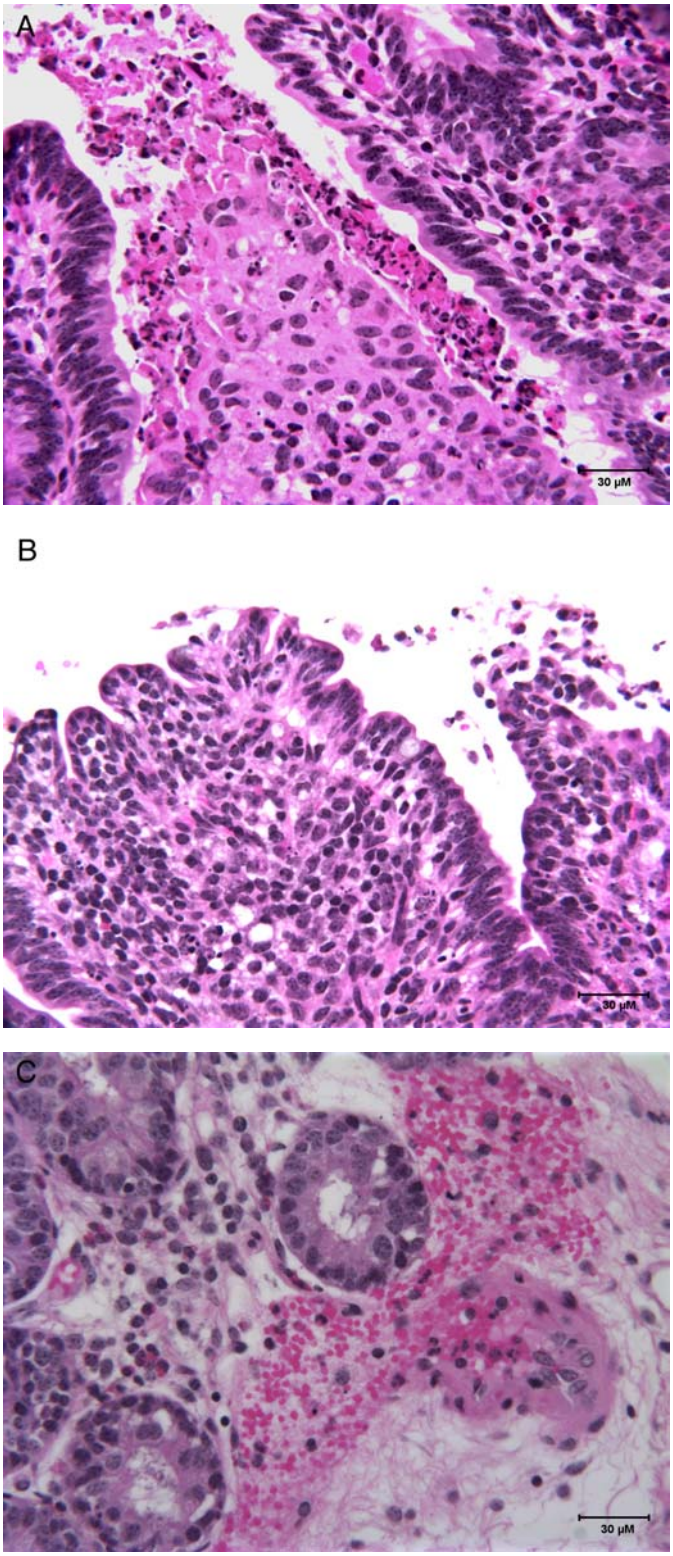

Figure 3: Necrosis of villi tips and basolateral surface (A), scattered necrosis in throughout the villi lamina propria (B), and vascular necrosis with extravasation of neutrophils and erythrocytes into the submucosa (C) in WT-infected samples. 8 hours post-infection. BLAD calf (CD18 -/-). H&E.

A few mucosal and several submucosal small blood vessels (arterioles, capillaries, and venules) contained fibrin thrombi and were often packed with circulating neutrophils. Occasionally, these vessels had walls disrupted by fibrin and necrotic debris (vasculitis with fibrinoid necrosis) allowing neutrophil extravasation (Fig. 3C). The submucosa was expanded by edema, fibrin, and occasional hemorrhage. A fibrinous pseudomembrane, often meager, admixed with a few desquamated enterocytes, covered the lumen in some animals.

No histologic lesions were observed in the submucosal lymphoid tissue (Peyer's patches) in any of the samples at any time point (Figs 4A and 4B). At 12 HPI, the mucosa was markedly collapsed and reduced in thickness resulting often in complete atrophy and fusion of villi (Fig. 4C). Vascular lesions similarly to the ones observed at 8 HPI were more frequently seen in the submucosa. These vessels were often surrounded by large numbers of neutrophils, abundant fibrin, edema, and occasional hemorrhage. As with 8 HPI, necrotic enterocytes tended to concentrate along the entire surface of villi in WT-infected samples contrasting the preferential occurrence at tips of villi in MT-infected samples. Other lesions observed were similar to the ones described above at 8 HPI for both WT- and MT-infected loops.

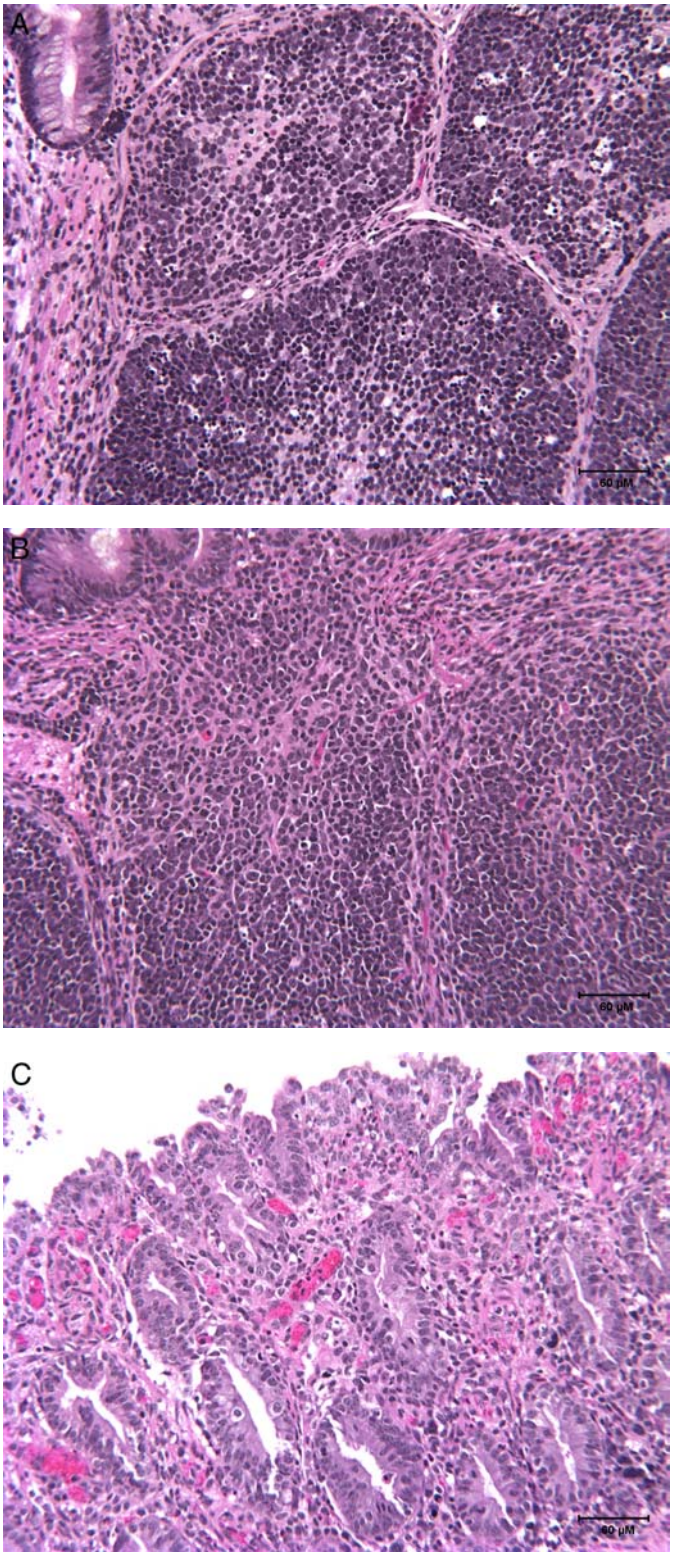

Figure 4: Normal appearance of Peyer's patches in uninfected control (A) and WT-infected sample (B). 8 hours post-infection. Severe villi atrophy in WT-infected sample (C). 12 hours post-infection. BLAD calf (CD18 -/-). H&E.

Ultrastructurally, evidence of WT *S. typhimurium* invasion was observed in epithelial cells at 1 HPI in most sections evaluated. In contrast, invading or internalized MT bacteria were infrequently seen at any time point. Invasion of epithelial cells was often associated with disruption of microvilli and apical membrane ruffle formation (Fig. 4, A-B). Invasive bacteria commonly targeted both enterocytes at tips of villi and M-cells in the domed villi of the follicle associated epithelium overlying Peyer's patches, while goblet cells were rarely infected. Invading organisms were located in membrane-bound vacuoles of two types, either spacious vacuoles containing multiple organisms or within tight phagosomes that closely followed the contour of the bacteria. Epithelial cells containing bacteria often displayed variable degrees of degenerative changes including cell swelling, rarefaction of cytoplasm, mitochondrial swelling with disruption of cristae, and dilation of endoplasmatic reticulum (Fig. 4C). Occasional WT and rare MT-bacteria were also observed within phagocytic cells in the subepithelial location in the lamina propria. Bacteria were rarely found in lymphoid follicles that compose Peyer's patches at any time point. A few infiltrating inflammatory cells within the lamina propria were occasionally observed at later time points, most of which were macrophages and lymphocytes, with rare occurrence of neutrophils (Fig. 4D). The lamina propria and submucosa were often expanded by clear spaces accompanied by breakdown of collagen fibers indicating edema (Fig. 4D). Cells with features of apoptosis and phagocytic cells containing apoptotic bodies were commonly seen

in all samples, but more often in infected tissues regardless the bacterial strain, yet bacteria were not found to be associated with these cells.

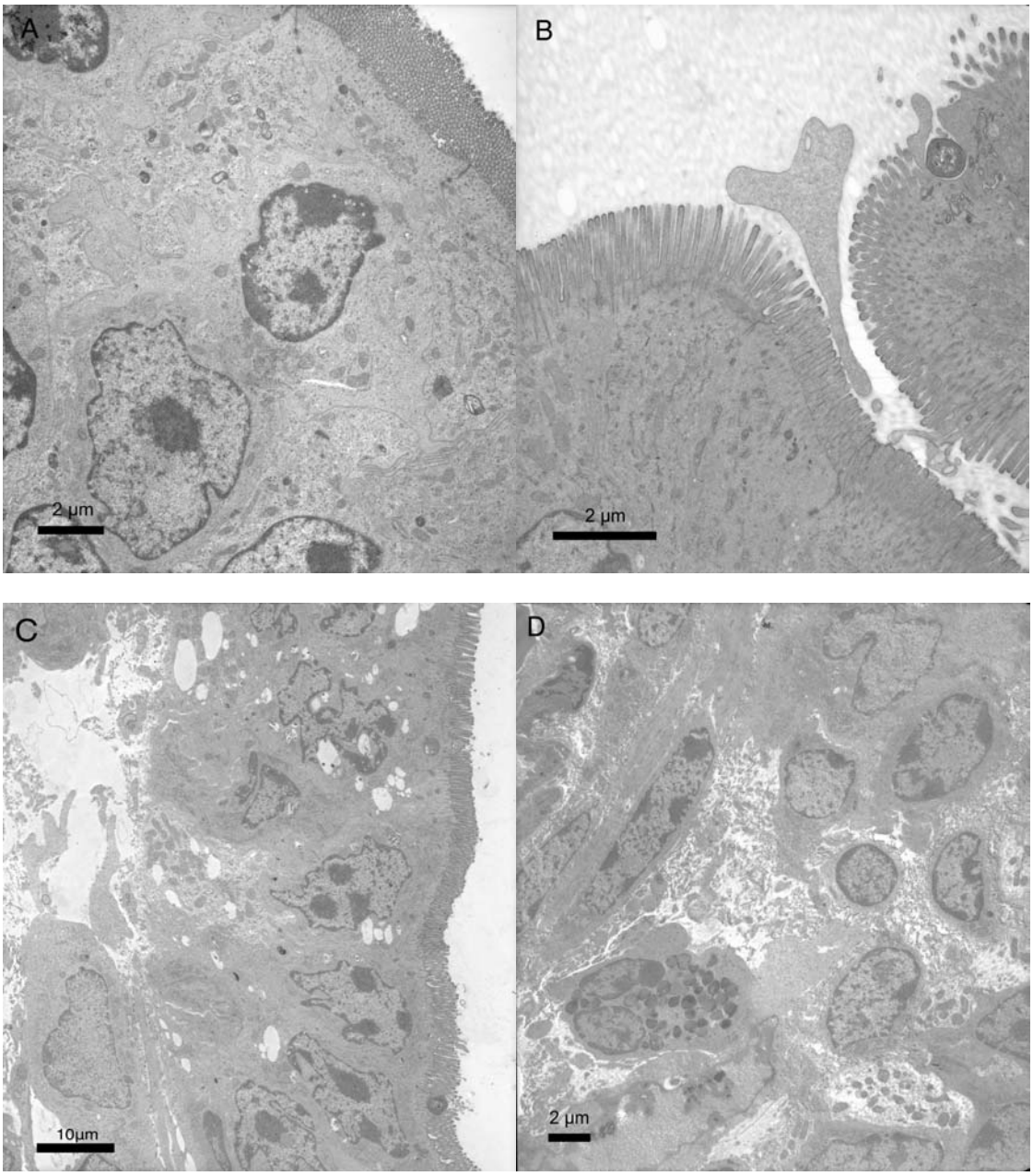

Figure 5: Transmission electron micrographs of normal enterocytes in the tip of villi from an uninfected control sample (A) and WT-infected samples (B-D). Upon contact with the apical portion of enterocytes, *S. typhimurium* disrupted the brush border and induced membrane ruffle formation (B). Infected cells showed evidence of degeneration including cytoplasmic swelling, rarefaction, loss of organelles, and dilation of endoplasmatic reticulum (C). The lamina propria often exhibited clear spaces with breakdown of collagen fibers (edema) and rare neutrophils (D). 1 hour post-infection. BLAD calf (CD18 -/-).

Analysis of mucosal surface by scanning electron microscopy confirmed the presence of villi blunting beginning at 4 HPI in WT-infected samples and 8 hours in MT-infected samples. At 12 hours, both strains induced marked villi blunting and luminal fibrin exudation (Figs. 5 A-B).

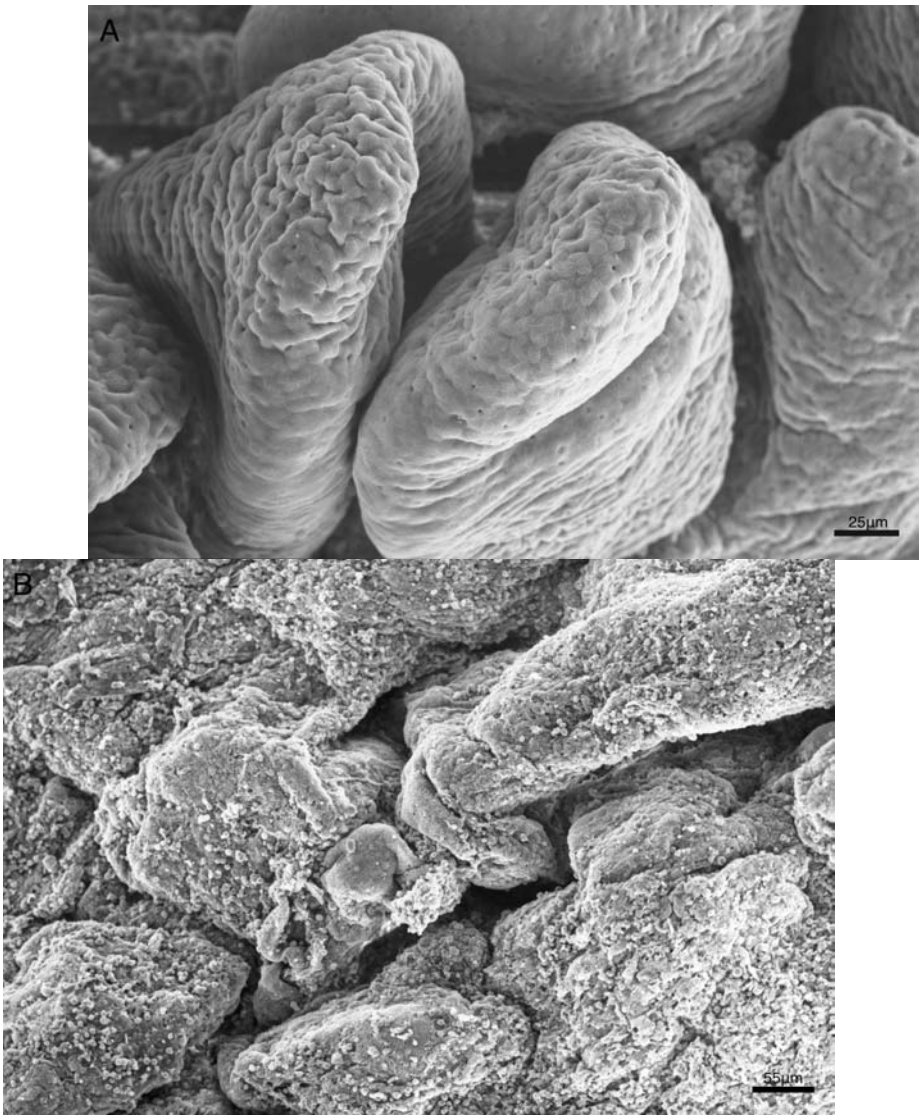

Figure 6: Scanning electron micrograph of the intestinal mucosa depicting normal appearance of villi in an uninfected control sample at 1 hour post-infection (A) compared to an WT-infected sample at 12 hours post-infection (B). Note in (B) the severe villi atrophy and luminal fibrin exudation (pseudomembrane formation). BLAD calf (CD18 -/-).

Tissue invasion and fluid secretion

The results of *S. typhimurium* invasion in the intestinal samples are summarized in Figure 6. In general for both WT and MT bacteria, a higher number of organisms invaded the mucosa in BLAD calves as compared to control; however, the difference was not statistically significant at most time points except to WT-infected tissues at 4 HPI. The WT strain was also found to be significantly more invasive than MT bacteria in control calves at all time points, except 1 hour post-infection. In contrast, in BLAD calves, the WT strain was significantly more invasive than MT at 1 HPI only.

Quantification of the amount of fluid accumulated within the intestinal lumen for each sample demonstrated that fluid secretion in WT-infected samples is significantly reduced in BLAD calves compared to control calves at 8 and 12 HPI (Fig. 7). While control calves had significantly increased fluid secretion in WT compared to MT-infected samples at late time points (4 and 8 hours), a significant difference between WT and MT-infected tissues in BLAD calves was observed only at 4 hour post-infection (Fig. 7).

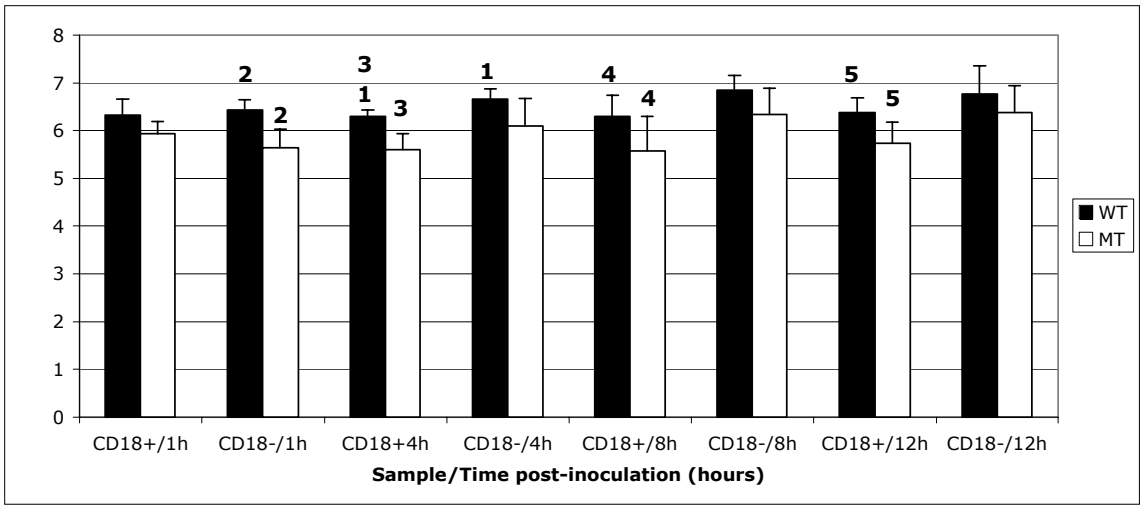

Figure 7: Wild type (WT) and mutant (MT) *S. typhimurium* mucosal invasion in BLAD (CD18 -/-) and control calves (CD18 +/+) at 1, 4, 8 and 12 hours post-infection. Conditions labeled with the same number are statistically different ($P < 0.05$).

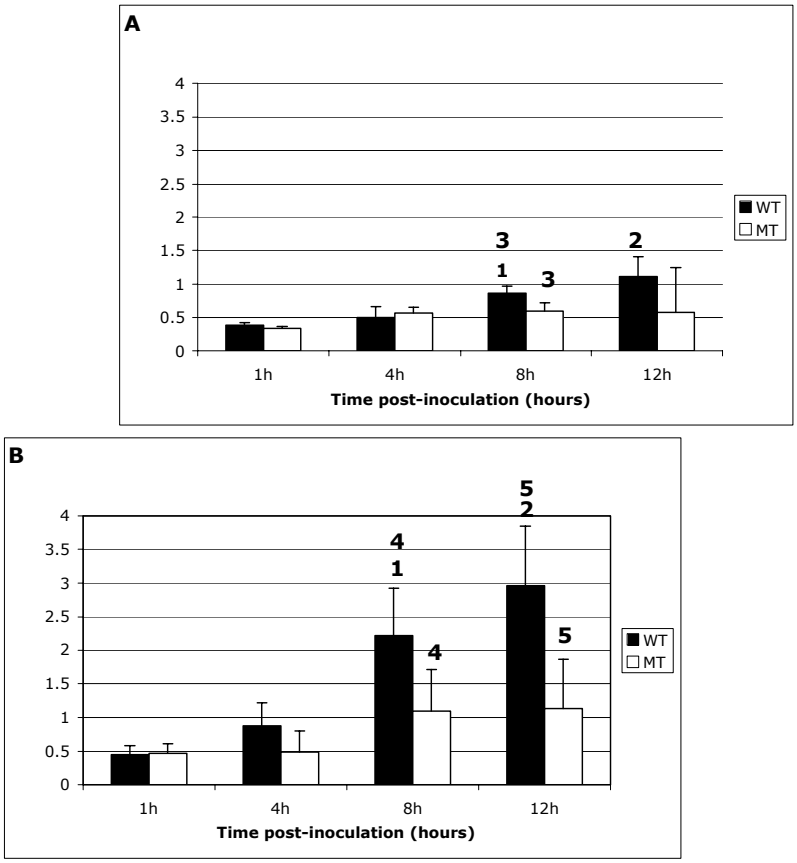

Figure 8: Wild type (WT) and mutant (MT) *S. typhimurium* fluid accumulation in BLAD (A) and control calves (B) at 1, 4, 8 and 12 hours post-infection. Conditions labeled with the same number are statistically different ($P < 0.05$).

Chemokine and cytokine profile

Quantitative gene expression of major pro-inflammatory cytokines (IL-1β & TNF-α) and chemokines (IL-8 & GRO-α) was determined by Real-Time PCR technology. IL-8 gene expression in WT-infected samples was significantly higher in BLAD compared to control calves at 4 and 12 HPI (Fig. 8). In addition, samples from BLAD calves had significant differences in IL-8 gene expression between WT and MT-infected tissues (Fig. 8), showing higher expression in MT and WT infected samples at 1 and 8 HPI respectively (Fig. 8). Gene expression of GRO-α was significantly higher in control calves compared to BLAD in WT-infected samples at 12 HPI only (Fig. 9). In addition, at this time point, GRO-α gene expression in control calves was higher in WT compared to MT-infected samples at 12 HPI (Fig. 9).

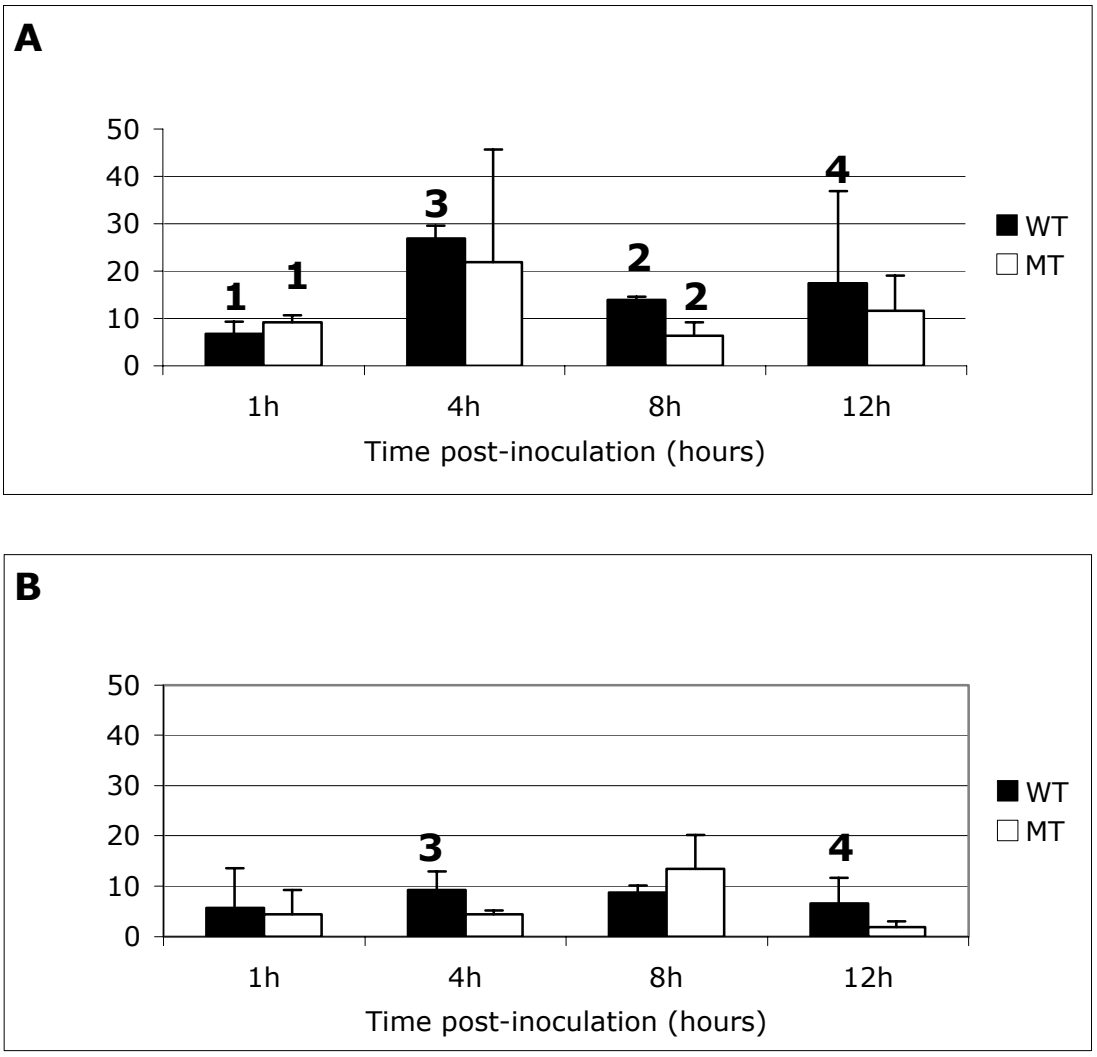

Figure 9: Wild type (WT) and mutant (MT) *S. typhimurium*-induced IL-8 gene expression in BLAD (A) and control calves (B) at 1, 4, 8 and 12 hours post-infection. Conditions labeled with the same number are statistically different ($P < 0.05$).

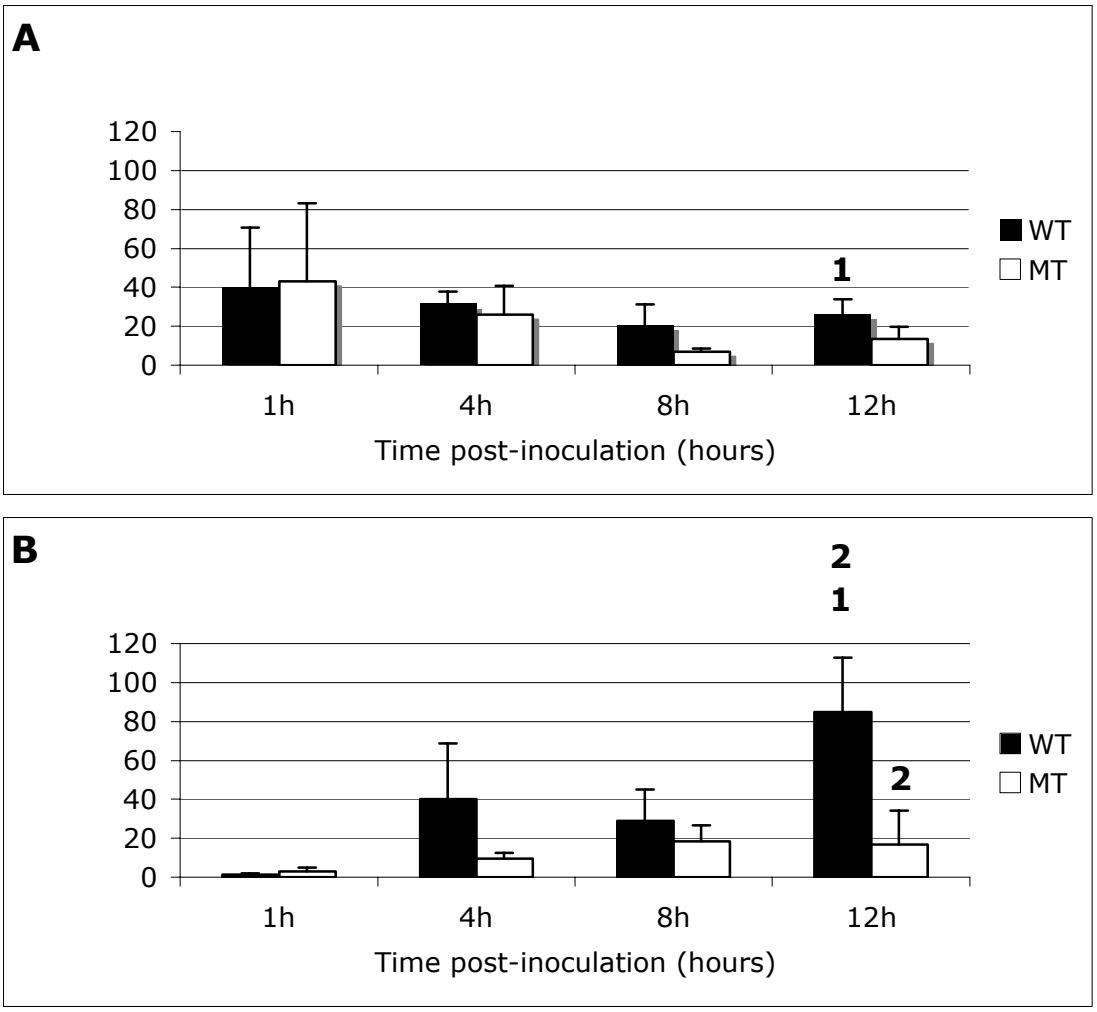

Figure 10: Wild type (WT) and mutant (MT) *S. typhimurium*-induced GRO-α gene expression in BLAD (A) and control calves (B) at 1, 4, 8 and 12 hours post-infection. Conditions labeled with the same number are statistically different ($P < 0.05$).

Significant statistical differences in IL-1β gene expression were not observed comparing any samples from BLAD and control calves (Fig. 10). Although not significant, the levels of IL-1β gene expression was generally higher in control animals than BLAD calves for most samples at most time points (Fig. 10). The gene expression of TNF-α, another major pro-inflammatory cytokine, was variable depending on the animal genotype. At 1 HPI, WT-infected samples

had higher expression in BLAD compared to control calves whereas the opposite, i.e. higher expression in control than BLAD, was detected in WT-infected samples at 4 HPI (Fig. 11).

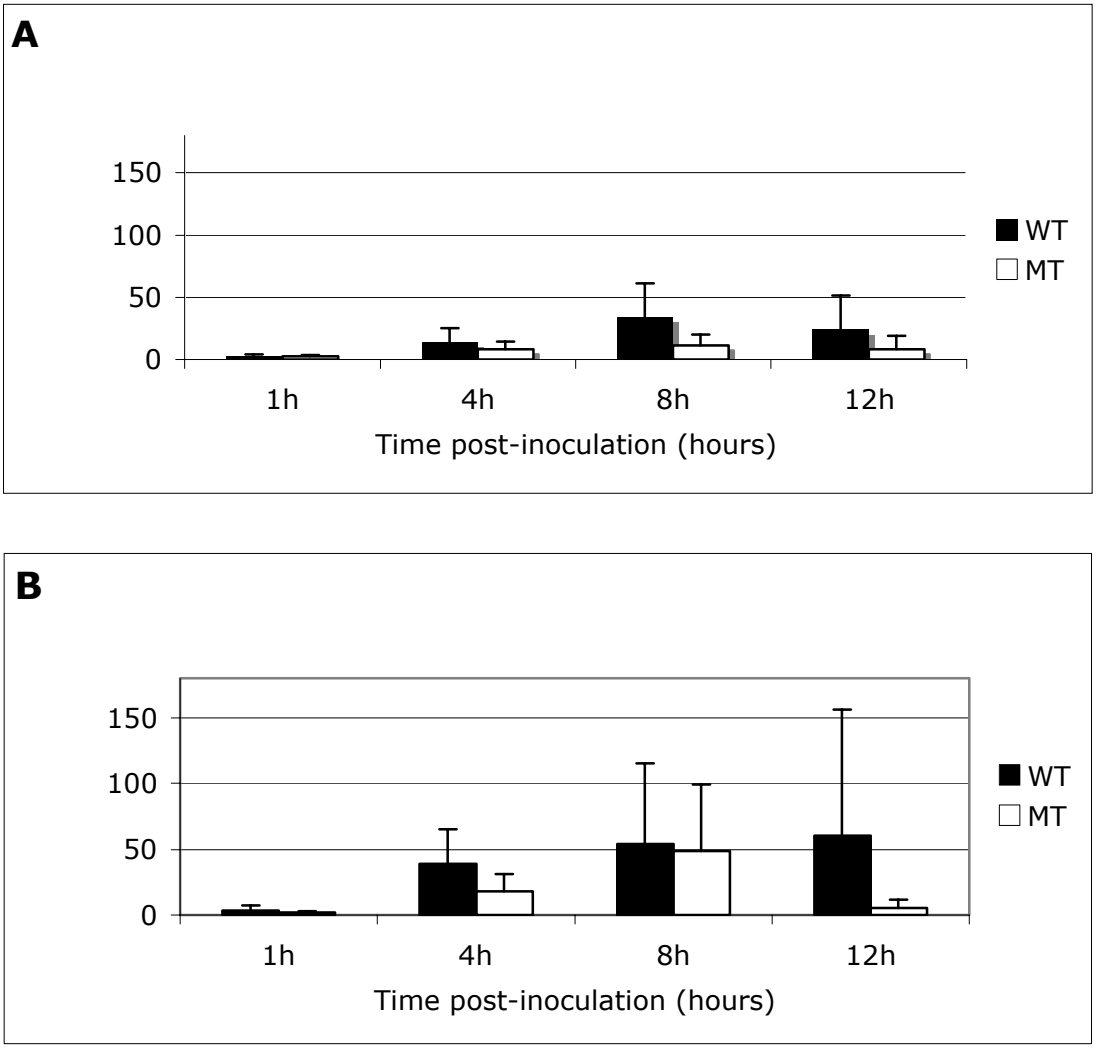

Figure 11: Wild type (WT) and mutant (MT) *S. typhimurium*-induced IL-1β gene expression in BLAD (A) and control calves (B) at 1, 4, 8 and 12 hours post-infection. Conditions labeled with the same number are statistically different ($P < 0.05$).

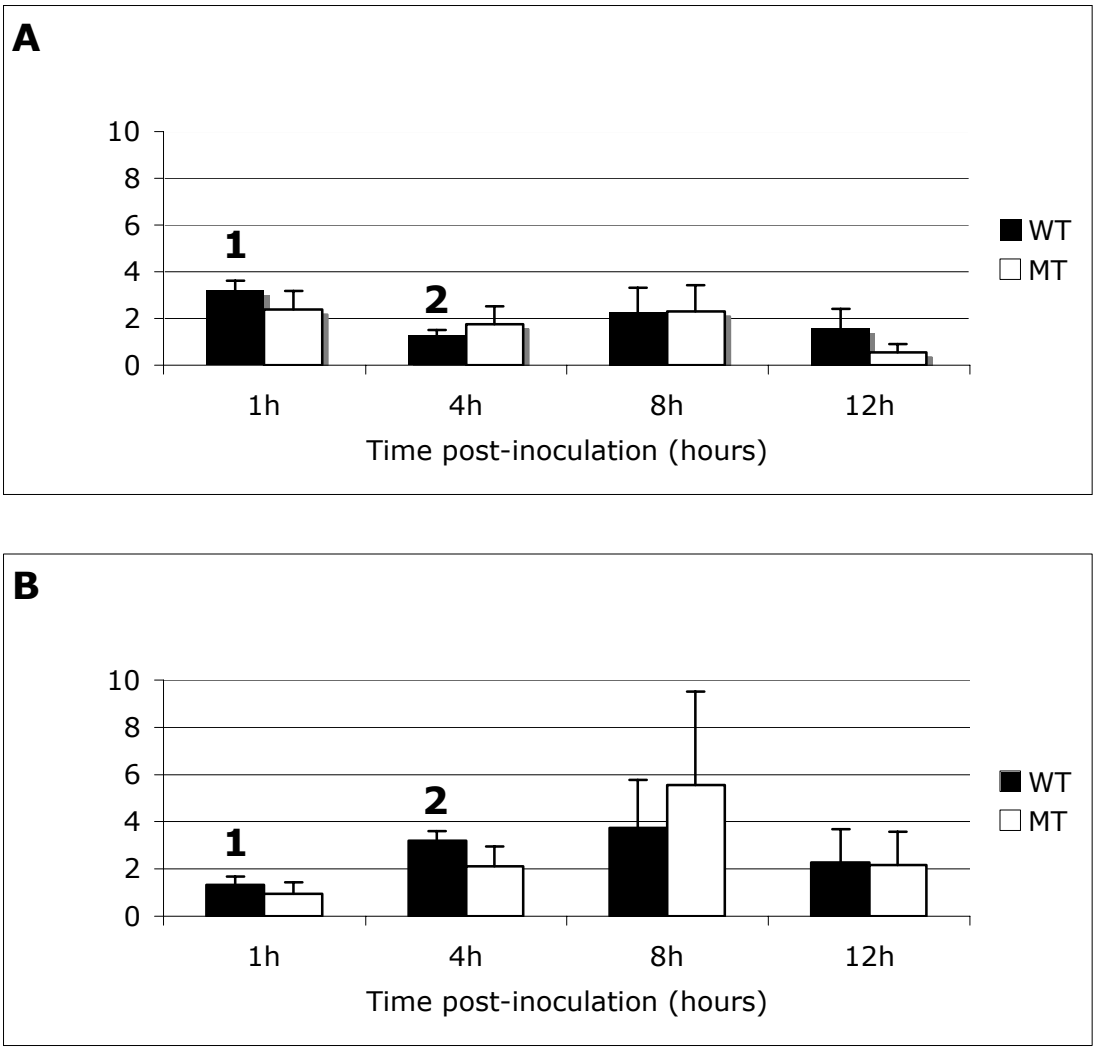

Figure 12: Wild type (WT) and mutant (MT) *S. typhimurium*-induced TNF-α gene expression in BLAD (A) and control calves (B) at 1, 4, 8 and 12 hours post-infection. Conditions labeled with the same number are statistically different ($P < 0.05$).

Discussion

The acute morphologic changes induced by *S. typhimurium* infection in calves as well as the profile of cytokines and chemokines have been well documented in previous studies using the ligated intestinal loop model (32,

78, 163, 164, 221, 223). Currently, the massive tissue influx of neutrophils is considered the histopathological hallmark of typhoidal salmonellosis (190). The typical neutrophilic influx has been suggested to represent the major event triggering tissue necrosis and diarrhea (161, 164, 222). Here we described the morphologic changes induced by *S. typhimurium* infection in BLAD calves, which essentially lack tissue neutrophils.

Our findings demonstrate remarkable morphologic differences in the intestine in the absence of tissue influx of neutrophils. While the first histologic lesions of villi blunting in normal calves (CD18 +/+) appeared as early as 15 minutes post-infection (164), blunting in BLAD calves was absent at 1 HPI and first detected at 4 HPI (WT-infected samples only). Moreover, the MT strain, well-known for its attenuated pathogenicity, induced the first detectable blunting at 8 HPI. In addition to blunting, detachment of epithelial cells in BLAD calves infected with WT strain was mainly observed at 8 HPI with only occasional occurrence at 4 hours. In contrast, this finding was commonly observed at 3 HPI (164) and first detected as early as 1 hour in normal calves (221).

Although evidence of neutrophil extravasation in BLAD calves with experimental Pasteurellosis has been reported to occur in the lungs (2, 3, 5), significant mucosal neutrophilic inflammation was not observed in any of the infected intestinal tissues. When present, neutrophils were limited to the perivascular connective tissue in the submucosa at 8 and 12 HPI, always associated with vascular lesions. Our data suggest that submucosal extravasation of neutrophils was caused by loss of vascular integrity secondary

to vasculitis, formation of fibrin thrombi, and vascular necrosis. Vasculitis and thrombosis has been previously reported in BLAD calves with dermatitis (6).

The typical widespread necrosis of the uppermost mucosa with complete loss of the intestinal epithelium extending to crypts reported at 8-12 hours in *S. typhimurium*-infected calves (187, 222) was not observed in BLAD calves. In contrast, necrosis in BLAD samples was limited to tips of villi, progressing to the basolateral surface, and a few scattered foci in the lamina propria, presumably reflecting the pattern of bacterial invasion and dissemination. Instead of massive mucosal necrosis, the most impressive morphologic change in BLAD tissue at 12 HPI was complete atrophy and fusion of villi. This finding indicates that changes in villi morphology during non-typhoidal salmonellosis can be induced by epithelial invasion in the absence of neutrophilic inflammation. Ultrastructurally, lesions in enterocytes induced by *S. typhimurium* infection in BLAD calves, including attachment and disruption of the brush border, apical membrane ruffling formation, and cellular degeneration, were similar to the ones reported in normal calves submitted to similar experimental conditions (164). Moreover, the published data identifying cell tropism of *S. typhimurium* for M-cells in the follicle-associated epithelium of Peyer's patches and epithelial cells at the tips of absorptive villi (54, 164) was confirmed in our BLAD samples.

The most remarkable and surprising morphologic difference between the typical lesions of *S. typhimurium*-induced enteritis in normal calves compared to animals in this study was the complete absence of Peyer's patches lesions in BLAD calves. Acute salmonellosis in calves is typically associated with

lymphocyte depletion in Peyer's patches follicles (164) progressing to necrosis in chronic stages of infection (215). The absence of significant lesions in BLAD calves suggests that Peyer's patch necrosis in salmonellosis occurs as a consequence of neutrophilic infiltration within lymphoid follicles as opposed to bacterial infection of cells being transported into the lymphoid follicles. This hypothesis is supported by evidence that neutrophilic infiltration in Peyer's patch-infected samples precedes lymphoid depletion and necrosis in calves (164).

Invasion of *S. typhimurium* in bovine ligated ileal loops is dependent on the synergistic effects of TTSS-1-encoded effector proteins SipA, SopA, SopB, SopD, SopE, and SopE2 (149, 223). TTSS-1 effectors induces rearrangements in the host cell cytoskeleton resulting in apical membrane ruffle formation and macropinocytosis of the bacteria (52, 61). In this study, mucosal invasion of *Salmonella* was generally increased in BLAD compared to control calves, though statistically significant at only 4 HPI. In addition, for most time points, the MT strain carrying simultaneous mutations in the five major TTSS-1-encodes genes was not found to be significantly less invasive than the WT in BLAD calves as opposed to the higher invasiveness of WT compared to MT bacteria as confirmed by our data from control calves and as reported in the literature (221, 222). Collectively, these data suggest that tissue influx of neutrophils partially reduce mucosal invasion of WT *S. typhimurium* and largely contribute to prevention of invasion of the mutant strain. Our finding of no significant difference in invasiveness between WT and MT strain in control animals at 1 hour post-infection corroborates this concept, because the number

of tissue neutrophils to prevent MT invasion is markedly reduced at 1 hour post-infection compared to later time points. Even though all intestinal samples were serially washed in three different PBS solutions to reduce extracellular organisms, a possible limitation of our methodology to determine invasion is the absence of antibiotic treatment (gentamicin) of collected mucosal samples before culture to eliminate non-invaded bacteria potentially attached to the mucosa or luminal secretory material (mucus, fibrin, etc) (150). On the other hand, the consequences of gentamicin treatment to the intestinal mucosa and resident flora during the time between processing of samples and culture have not been determined and could potentially interfere with invasion. For instance, non-typhoidal salmonellosis in mice, which typically develop typhoidal systemic disease when infected by *S. typhimurium*, can be induced experimentally by oral treatment with high doses of the antibiotic streptomycin followed by infection with *S. typhimurium* (77), indicating that disruption of normal flora by antibiotics can dramatically change the host-agent interaction and potentially induce unexpected results.

The mechanism responsible for fluid secretion and diarrhea in non-typhoidal models of salmonellosis remains to be elucidated. Studies in bovine ligated ileal loops strongly support an exudative mechanism rather than secretory diarrhea (chloride secretion) as the most likely mechanism (222). Accordingly, the massive intestinal influx of neutrophils in caves infected with *S. typhimurium* results in necrosis with loss of epithelial integrity and diarrhea by an exudative mechanism (222). This hypothesis is supported by the pronounced loss of

plasma proteins after infection of calves by *S. typhimurium* indicating increased intestinal permeability associated with severe intestinal protein loss during infection (160). Our data provide strong evidence that fluid accumulation in BLAD calves is significantly reduced compared to control calves in late time points when inflammation is normally most severe, i.e. at 8 and 12 HPI. As with bacterial invasion, the markedly different degree of responses between WT and MT-infected samples observed in control animals were generally less evident in BLAD animals, supporting the hypothesis that neutrophil influx plays a crucial role in the pathogenesis of both strains, especially preventing pathologic effects caused by the MT strain. Our findings support the hypothesis of exudative diarrhea secondary to inflammation as the major contributor for fluid secretion in non-typhoidal salmonellosis. It is important to realize; however, that while markedly reduced, fluid secretion in BLAD calves still occurred. It is yet to be determined if the mild fluid accumulation observed in BLAD animals results from either secretory mechanisms, secondary to the necrosis and vascular lesions , or a combination thereof as commonly observed at 8 and 12 hours post-infection.

The type of inflammatory infiltrate that characterize a disease is controlled in part by the profile of inflammatory cytokines and chemokines (110). The pro-inflammatory cytokines IL-1β and TNF-α as well as potent neutrophil chemoattractants, the CXC chemokines IL-8 and GRO-α, have been suggested to play a major roles during *S. typhimurium*-induced enteritis and diarrhea in calves (161, 164, 222). Besides being often expressed in the bovine model of non-typhoidal salmonellosis, IL-8 gene expression is also induced by human

epithelial cell lines by the *S. typhimurium* TTSS-1 (85). We found that gene expression of IL-8 in WT-infected samples is significantly higher in BLAD than in control animals at 4 and 12 HPI. A possible interpretation of this finding is that the absence of tissue neutrophils in BLAD triggers a positive feedback mechanism for production of more IL-8 via unknown pathways in an attempt to recruit neutrophils necessary to control infection. This finding also suggests that neutrophils are unlikely to be the major source of IL-8 during *S. typhimurium* infection in calves since increased gene expression in BLAD occurred in the absence of significant tissue influx of neutrophils. Studies using the bovine ligated ileal loop model have identified the GRO-α chemokine as the major chemoattractant for neutrophils during *S. typhimurium*-induced enteritis (221). Our data on GRO-α gene expression in control calves confirm its high expression levels, up to 80 fold increase over control in WT-infected samples, especially in the later stages of acute infection, i.e. at 12 HPI. This finding suggests that the massive influx of neutrophils seen at the late phase of acute infection is mainly driven by GRO-α. In BLAD calves; however, the GRO-α gene expression at WT-infected samples at this late stage of infection was significantly reduced compared to control indicating that the neutrophil influx potentially may play a role in triggering GRO-α gene expression in the later phase of acute infection by either directly secreting this chemokine or stimulating its production in other cell types indirectly. IL-1β and TNF-α are classic pro-inflammatory cytokines increased during *Salmonella* infection in all organs studied to date using *in vivo* models of infection (40, 102, 164). Extensive evidence from studies in mice

indicates that these cytokines are essential for host defense against *Salmonella* infection (41). In bovine ligated ileal loops infected with *S. typhimurium*, the gene expression of these two cytokines was determined by conventional reverse transcription PCR. Accordingly, the expression of IL-1β was elevated at 3 and 6 HPI, whereas no changes in gene expression was detected for TNF-α after infection (159). Our data show that the gene expression levels of IL-1β in BLAD calves were lower than those of control animals, especially in WT-infected samples, at 2 hours and later time points. These data were expected in view of the essentially absent tissue inflammation in the BLAD calves; however, the differences in gene expression observed were not statistically different. The lack of statistical significance in the different expression levels of IL-1β between BLAD and control animals can be explained by the high standard deviation observed in our data as a result of marked individual variability. More experimental samples are necessary to increase the statistical power and confirm our findings regarding IL-1β gene expression. The TNF-α gene expression in our BLAD samples was variable in WT-infected samples, with significantly higher expression in BLAD at 1 HPI, but with the opposite relationship, i.e. higher expression occurring in control animals at 4 hour post-infection. These results, combined with our finding of no significant differences in TNF-α gene expression between BLAD and control calves at later time points suggest that neutrophil influx likely plays a minor role in the gene expression of this cytokine during *S. typhimurium*-induced enteritis in calves.

In conclusion, infection by *S. typhimurium* of ligated ileal loops in calves with Bovine Leukocyte Adhesion Deficiency results in markedly distinct morphologic and immunologic changes compared to normal animals negative for the BLAD defect. The most important differences include essentially the absence of typical *S. typhimurium*-induced neutrophilic enteritis, unique pattern and reduced magnitude of necrosis, and differential gene expression profiles of major neutrophil chemokines and pro-inflammatory cytokines. These differences in BLAD calves are associated with a significantly increased bacterial invasion and reduced fluid accumulation supporting the hypothesis that *S. typhimurium*-induced diarrhea in normal calves is primarily exudative in nature and caused by the massive tissue influx of neutrophils. This new evidence enhances our understanding of the pathogenesis of diarrhea of human and ruminant non-typhoidal salmonellosis.

CHAPTER III

ANALYSIS OF CYTOKINE PROFILES IN *S.* Typhimurium-INFECTED CALVES WITH BOVINE LEUKOCYTE ADHESION DEFICIENCY BY LASER CAPTURE MICRODISSECTION

Introduction

Cytokine and chemokine activation and signaling largely mediated the type of inflammatory response induced by the host-agent interaction during *in vivo Salmonella* infections (31). Studies in bovine ligated ileal loops infected with *Salmonella enterica* serovar Typhimurium (hereafter *S. typhimurium)*, a suitable model for human salmonellosis (189), provide strong evidence that the massive tissue influx of neutrophils, followed by necrosis and diarrhea that characterize *S. typhimurium*-induced enteritis, is driven mainly by activation of pro-inflammatory cytokines and potent neutrophil chemokines (CXC chemokines) activated upon infection of the host (161, 221, 222). In contrast, infection of mice by *S. typhimurium* elicit strikingly distinct chemokine gene expression in the intestine compared to bovine, characterized by preferential activation of mononuclear cell chemoattractants (CC chemokines), which results in the typical mononuclear

enteritis in the absence of necrosis and diarrhea (221). Taking together these studies in bovine and mice indicate that the nature and dynamics of pro-inflammatory cytokine and chemokine activation during infection play a major role in the pathogenesis of *S. typhimurium*-induced diarrhea.

The role of chemokines in the pathogenesis of Salmonellosis has also been investigated by *in vitro* studies, which identified epithelial secretion of IL-8 as a major triggering event in neutrophil recruitment (92). Studies using polarized human intestinal cell lines found that *Salmonella* releases the protein flagellin that binds to toll-like receptor 5 (TLR5) restricted to the basolateral surface of epithelial cells resulting in activation of a signaling pathway leading to IL-8 secretion (65, 66). While migration of neutrophils from the microvasculature through the endothelium to the submucosa and to the basolateral surface of the epithelial monolayer appear to be dependent on IL-8 secretion (119), neutrophil migration across the epithelial barrier into the lumen appears to be driven by a small 1-3 KDa chemoattractant, previously known as known as pathogen-elicited epithelial chemokine (PEEC), recently renamed hepoxilin A_3 (120, 129). Hepoxilin A3 was found to be secreted solely in the apical compartment of polarized monolayer of intestinal epithelial cells in response to *Salmonella* activation of protein kinase C (PKC) (107).

To better understand the dynamics of gene activation and anatomic localization of major pro-inflammatory cytokines and neutrophil CXC chemokines during *S. typhimurium*-induced enteritis, we employed the Laser Capture Microdissection technology (LCM) in the ligated ileal loop model in calves with

bovine leukocyte adhesion deficiency (BLAD). Calves affected by the BLAD condition are born with a single point mutation in the common β2 integrin subunit CD18 resulting in deficient expression of all four classes of β2 integrin (CD11a, b, c, d/CD18) on the surface of leukocytes (132). The defect renders neutrophils incapable to extravasate from blood vessels and reach the extracellular matrix during inflammation (5, 7). In addition to deficient extravasation, BLAD calf neutrophils have marked functional abnormalities including severely decreased adherence, chemotactic movements, phagocytosis, luminol-dependent chemiluminescent response, and O (2-)- producing activities (135). The use of the BLAD calf in this study, which is essentially a model of "neutrophil knockout", was employed to better understand the influences of neutrophilic influx over the cytokine and chemokine activation milieu during *S. typhimurium*-induced enteritis.

Material and Methods

Bacterial strains and growth conditions

Strains of *S. typhimurium* used in this study included the Wild Type strain IR715 (ATCC 14028 wild type *nal*) (178) and the mutant strain ZA21

(Δ*sipAsopABDE2* - ATCC 14028 *nal*) (223). All strains were grown in Luria-Bertani (LB) medium with nalidixic acid antibiotic (50 mg/liter) under agitation (250 rpm) overnight at 37^{o}C; 50 μl of the culture was inoculated into 5ml of fresh LB medium and sub-cultured for additional 4 hours before inoculation.

Animals, surgical procedure, and sampling

BLAD Holstein calves, 5 weeks of age, one male and one female, weighting approximately 45 to 55 Kg were used in these experiments. The two calves were homozygous for the BLAD defect (CD18 -/-) as determined by a PCR-based DNA test combined with restriction enzyme analysis (99, 171). Embryo transfer technology (168) was used to generate the BLAD calves. Embryos were donated the USDA/ARS National Animal Disease Center (NADC) – Ames, IA. The calves were kept clinically healthy before the experiments at the Large Animal Hospital of the College of Veterinary Medicine, Texas A&M University, College Station – TX and negative for *Salmonella spp.* as determined by fecal culture using enrichment in tetrathionate broth (Difco, Detroit, MI). Calves were fed antibiotic-free milk replacer twice a day, water *ad libitum*, and fasted 24 hours prior to experimental surgeries. The ligated ileal loop surgical procedure was employed as previously described (164, 166). Briefly, anesthesia was induced with propofol (Abbot Laboratories, Chigaco, IL) followed by

placement of endotracheal tube and maintenance with isofluorane (Abbot Laboratories, Chigaco, IL) for the duration of the experiment. A laparotomy was performed, the ileum and jejunum were exposed and 16-20 loops, 5 to 8 cm long, were ligated in the ileum and distal jejunum, intercalated with 1-2 cm loops. The loops were injected with 3 ml of either sterile LB broth (control loops) or LB containing approximately 0.75 x 10^9 colony-forming units (cfu) of the *S. typhimurium* strains previously described. Loops were replaced into the abdominal cavity and excised at 1 hour post-infection (HPI). Samples for immunohistochemistry (IHC), quantitative Real-Time PCR (qRTPCR), and Laser Capture Microdissection (LCM) were collected.

Real-time polymerase chain reaction (qRTPCR)

As a source of host RNA, six to eight 6 mm biopsy punches were taken from the intestinal tissue including Peyer's patches. Punches were immediately cleaned to remove debris, minced into small pieces with a sterile scalpel or razor blade, immersed in 4°C 500 μl of TRI-reagent® (Ambion, Foster City, CA) and further homogenized using a tissue grinder. The RNA was extracted according to TRI-reagent manufacturer instructions, the pellet was re-suspended in nuclease-free water (Ambion, Foster City, CA), and contaminating DNA was removed by RNase-free DNase I treatment (Ambion, Foster City, CA)

according to manufacturer's instructions. Samples were stored at -80^{o}C until used. The resultant DNA-free RNA was quantified using a NanoDrop® ND-1000 spectrophotometer (NanoDrop Technologies, Wilmington, DE) and assessment of RNA quality was determined using an Agilent 2100 Bioanalyser (Agilent Technologies, Santa Clara, CA).

Selected RNA samples of adequate quality from each condition was used to determine the gene expression levels of IL-8, GRO-α, IL-1β, and TNF-α by qRTPCR as previously described (221). Briefly, 2 μg of RNA was reverse transcribed at 48 ^{o}C for 30 min with random hexamer primers and Multiscribe Reverse Transcriptase (Applied biosystems, Foster City, CA). The resultant cDNA at concentration of 40 ηg per sample was mixed with 4 SmartMix beads per sample (Cepheid, Sunnyvale, CA), SYBRGreen-I 0.2x (Invitrogen Corporation, Carlsbad, CA) and 500 nM of each primer set (Table 2). The qRTPCR reaction was performed using a Smart Cycler II (Cepheid, Sunnyvale, CA). The quantitative gene expression of each cytokine and chemokine was normalized to the internal control glyceraldehyde-3-phosphate dehydrogenase (GAPDH). The normalized levels of gene expression in infected tissues were calculated relative to uninfected control tissues as previously described (221).

Laser capture microdissection

The same BLAD calves submitted to the previously described experimental surgeries were also used as source of host RNA for LCM. The intestinal samples collected at surgery (1 HPI) were placed in a cryomold containing Optimal Cutting Temperature (OCT) compound and immediately transferred to dry ice followed by storage at -80^{o}C until sectioning. Frozen blocks were trimmed at 8 μm under RNAse-free conditions using the cryostat UltraPro 5000 (Vibratome, St. Louis, MO). Trimmed sections were transferred to a cold adhesive-coated glass slide at 1x adhesive concentration by using the CryoJane® Tape-Transfer system (Instrumedics Inc, St. Louis, MO) according to manufacturer's instruction. Resulting tissue sections were fixed in 70% ethanol, stained by HistoGene LCM frozen section staining kit (Molecular Devices Corporation, Sunnyvale, CA), and subjected to LCM using the PixCell II system (Molecular Devices Corporation, Sunnyvale, CA). Enterocytes of absorptive villi and crypts, plus the entire domed villi were captured onto CapSure Macro LCM caps (Molecular Devices Corporation, Sunnyvale, CA) (18, 43, 44, 49). Domed villi included the lining enterocytes of non-absorptive villi (follicle-associated epithelium) and underlying lamina propria.

LCM RNA isolation, amplification, and gene expression

Approximately 1000 cells were captured for each one of the histologic units, i.e. villi tips, crypts, and domed villi, in each sample. RNA from captured cells was isolated using PicoPure RNA Isolation Kit (Molecular Device Corporation, Sunnyvale, CA) (125). RNA quality and quantity from captured cells was evaluated using an Agilent 2100 Bioanalyser (Agilent Technologies, Santa Clara, CA). RNA samples of appropriate quality were selected and 2.5 ηg per sample was submitted to two rounds of amplification using RiboAmp HS RNA Amplification Kits according to the manufacturer's instructions (Molecular Devices Corporation, Sunnyvale, CA) (218). Gene expression of IL-8, GRO-α, IL-1β, and TNF-α from uninfected controls, WT and MT *S. typhimurium*-infected samples were measured by qRTPCR using 500 nM of each primer set (Table 2), as previously described above.

Table 2- Primer sequences used in qRTPCR to study the gene expression of *S. typhimurium* infected bovine intestine in samples derived form the whole intestinal tissue including mucosa and submucosa (whole tissue) and cells captured by Laser Capture Microdissection (LCM).

Sample type	Target	Primer sequence[a]	Amplicon size (bp)
Whole tissue	GAPDH	TTCTGGCAAAGTGGACATCGT	114
		GCCTTGACTGTGCCGTTGA	
	GRO-α	CACTGCGACCAAACCGAAGT	153
		GTATCAAGAAGCTCGTTCCAT	
	IL-8	TGCTTTTTTGTTTTCGGTTTTTG	71
		AACAGGCACTCGGGAATCCT	
	IL-1β	CCAGCCTGGCAAAAACCAT	201
		CCGGAAATTGGTTCCACAGT	
	TNF-α	GTTCCTCACCCACACCATCAG	283
		GGTAGTCCGGCAGGTTGATC	
LCM	GAPDH	TTCCTGGTACGACAATGAATTT	162
		CAGTGTGGCGGAGATGGGGCACG	
	GRO-α	CACTGTTAATGTAGGGAATGTAT	147
		TGTCCAAGGGATATTTAGATCATTG	
	IL-8	AATCTTGAGACTGTCTTTCC	139
		TAAAGTTTATGTTCGAATACACAA	
	IL-1β	CCAGCCTGGCAAAAACCAT	201
		CCGGAAATTGGTTCCACAGT	
	TNF-α	GTTCCTCACCCACACCATCAG	283
		GGTAGTCCGGCAGGTTGATC	

[a]Sequences for bovine genes were obtained from GenBank. Top row represents forward primers and bottom row shows reverse primers.

Immunohistochemistry

Intestinal samples for immunohistochemistry (IHC) were fixed in neutral 10% buffered formalin, processed according to routine procedures for paraffin embedding, sectioned at 4-5 μm, and submitted to IHC, which was performed using the MACH 2 polymer detection kit (Biocare Medical, Concord, CA) according to manufacter's instructions. For *in situ* detection of *S. typhimurium, Salmonella* O group B antiserum (BD biosciences, San Jose, CA) was used. The primary antibody was substituted with a universal rabbit control (DakoCytomation, Carpinteria, CA) and DAB (3,3'-diaminobenzidine) (DakoCytomation, Carpinteria, CA) was used as the chromogen.

Statistical analysis

The gene expression of cytokines and chemokines were analyzed by calculation of geometric means and standard deviation, followed by the use of a Student's *t* test to determine differences with statistical significance ($p < 0.05$).

Results

The LCM technique

The LCM technique was found to be adequate to generate good quality RNA as accessed by the Agilent bioanalyser (data not shown). The cells captured, approximately 1000 per sample, yielded 4.0 to 53.0 ηg of total RNA. For each sample, 2.5 ηg of RNA generated between 3.2 and 42.0 μg of amplified mRNA used for qRTPCR. Figure 13 shows examples of the histologic sections used during LCM and all three captured histologic units.

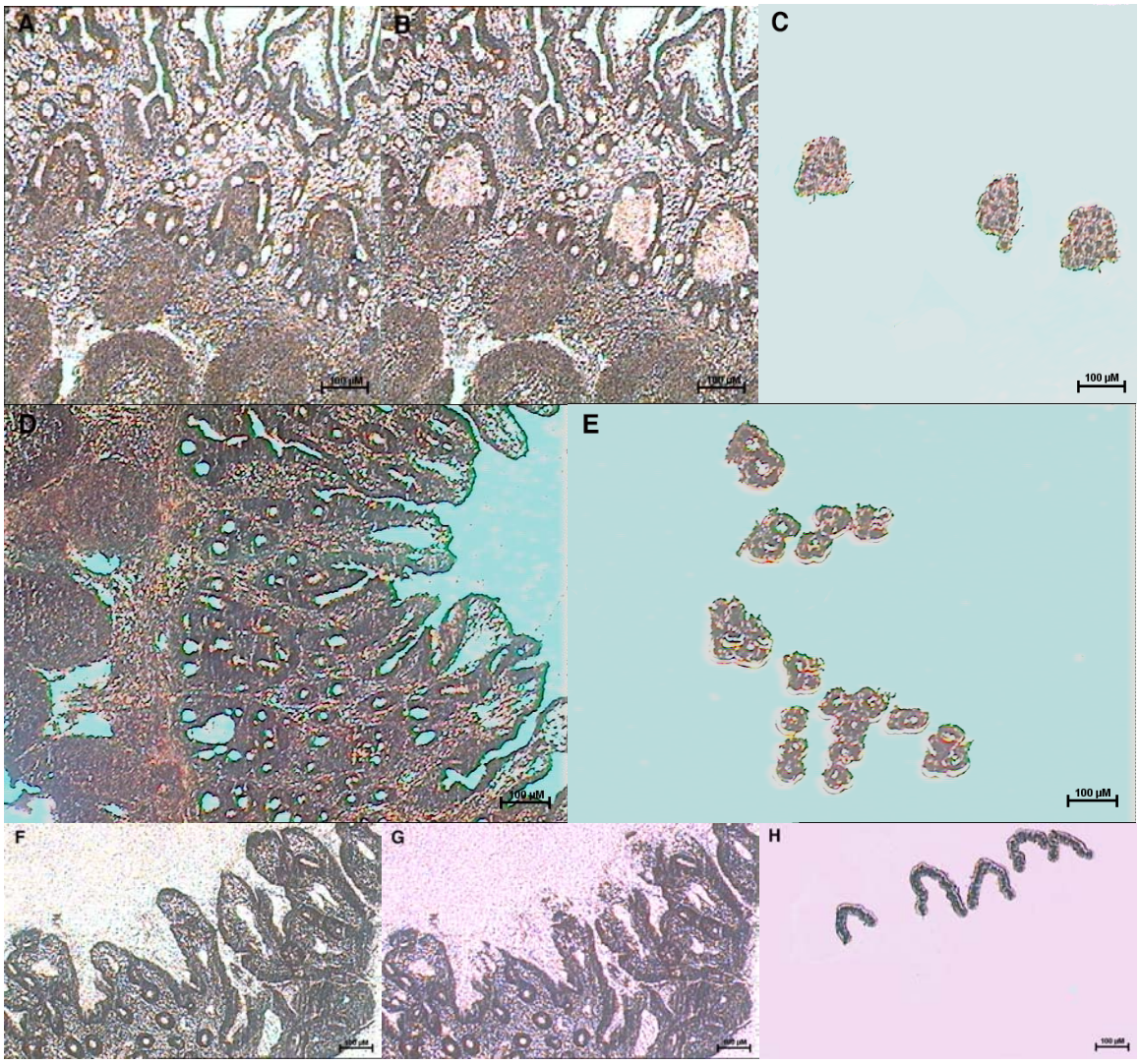

Figure 13: Examples of domed villi (A-C), crypts (D and E), and tips of absorptive villi (F-H) captured by LCM. Histologic fields containing cells of interest were selected (A, D, and F) and cells were captured in CapSure Macro LCM caps (C, E, and H). B and G illustrate missing cells captured after the laser was applied.

Chemokine and cytokine profile in the intestine

For the sake of comparison with the gene expression obtained by the LCM, the expression of the same cytokines (IL-1β & TNF-α) and neutrophil chemokines (IL-8 & GRO-α) at the same time point and same calves as the LCM experiments (1 HPI) was also determined at whole intestinal samples by qRTPCR. This was accomplished using RNA isolated from heterogeneous ileal samples that included the mucosa, submucosa, and Peyer's patches. Results are summarized in Figure 14. At the initial stages of acute infection, represented here by 1 HPI, GRO-α had the highest gene expression levels for both WT and MT-infected samples, followed a mild up-regulation of IL-8 also in both WT and MT-infected tissues. The gene expression of the pro-inflammatory cytokines IL-1β and TNF-α were reduced when compared to the levels attained by the two chemokines, especially GRO-α. In addition, the gene expression of IL-1β & TNF-α in WT and MT-infected samples had similar intensities to each other as opposed to what was detected for IL-8 & GRO-α.

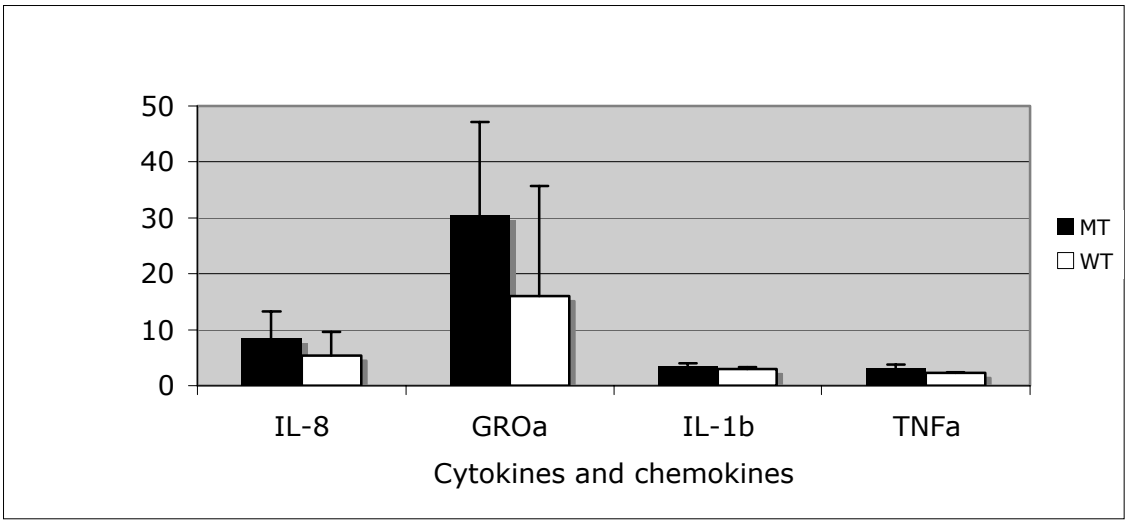

Figure 14: Wild type (WT) and Mutant (MT) *S. typhimurium*-induced cytokine and chemokine gene expression in the ileum of BLAD calves at 1 hour post-infection.

Chemokine and cytokine profile in captured cells (LCM)

Gene expression of all cytokines and chemokines included in this study, except TNF-α, were detected by qRTPCR in all distinct groups of cells captured by LCM (Fig. 15). For all three distinct inflammatory mediators detected, i.e. IL-8, GRO-α, and IL-1β, enterocytes of crypts presented the highest levels of gene expression compared to enterocytes of villi tips and cells of domed villi in WT-infected samples (Fig. 15). The gene expression of all cytokines was predominantly lower in MT-infected samples compared to WT-infected in crypts (Fig. 15). Enterocytes of villi tips and cells of domed villi demonstrated similar levels of gene expression for all cytokines in both WT and MT-infected samples (Fig. 15).

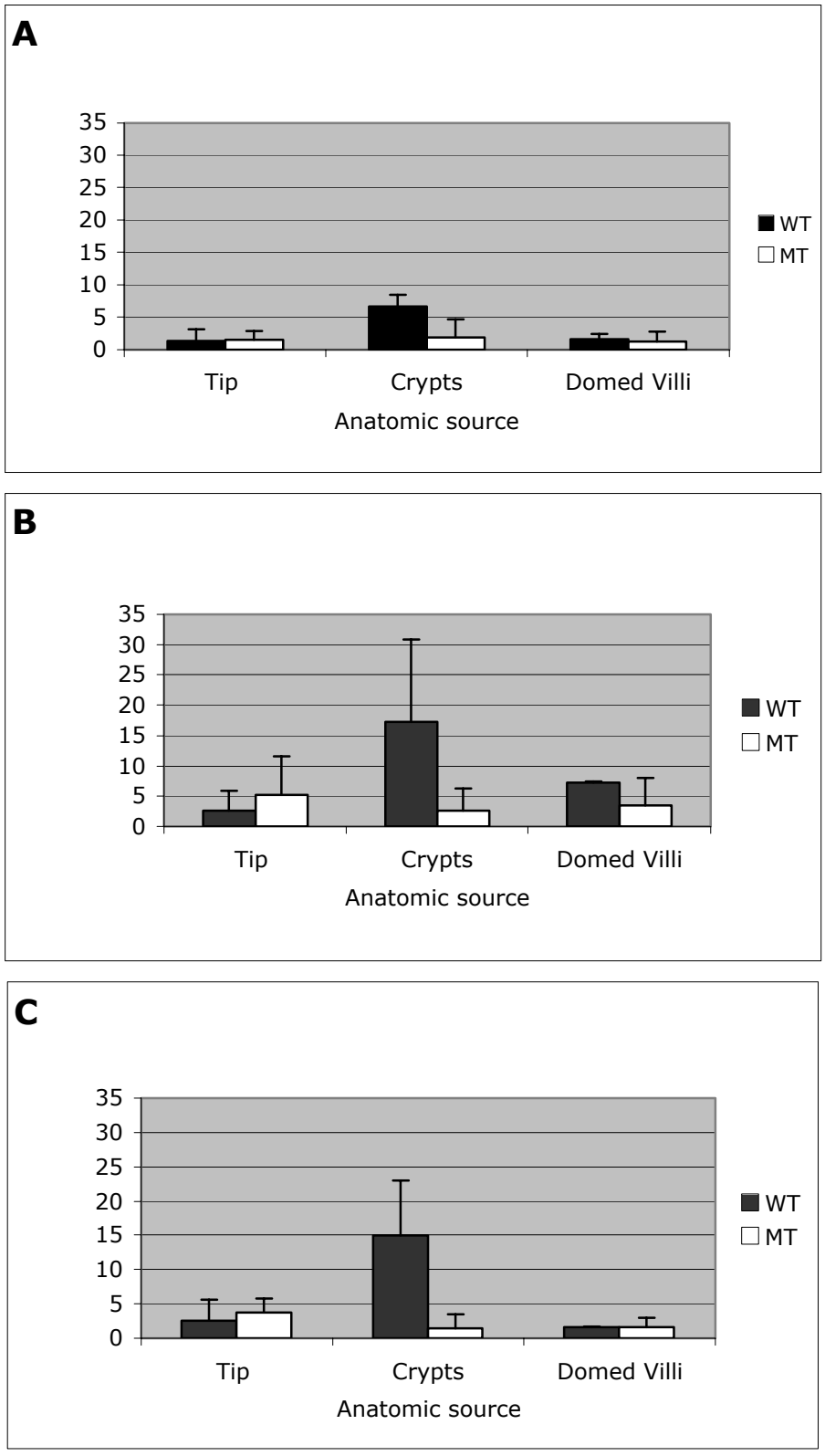

Figure 15: Wild type (WT) and Mutant (MT) *S. typhimurium*-induced IL-8 (A), GRO-α (B), and IL-1β (C) gene expression in villi tips, crypts, and domed villi in the ileum of BLAD calves at 1 hour post-infection.

Immunohistochemistry

The distribution of invading *S. typhimurium* was investigated by IHC at 1 HPI. Our results indicate that WT and MT strains have an equal pattern of invasion in the ileal mucosa. The most common sites of *S. typhimurium* invasion were the basolateral enterocytes of absorptive villi and the follicle-associated epithelium of domed villi (Figure 16), followed by fewer bacteria observed within enterocytes of villi tips. The organism was also infrequently detected in the lamina propria of absorptive villi and domed villi.

Discussion

Infection with *Salmonella* species causes significant immune activation and consequent inflammation often resulting in host damage. While *Salmonella*-induced inflammatory responses contribute to the nature and severity of the immunopathology, the inflammatory infiltrates are also clearly critical for control of infection (31). The ultimate outcome of this competition, which may benefit the host or the bacteria, is highly influenced by the set of cytokines and chemokines produced by the host in response to infection (177). For this reason, understanding of the pathogenesis and dynamics of cytokine and chemokine

activation during infection represents an important step in developing novel therapeutic approaches for *Salmonella* infection.

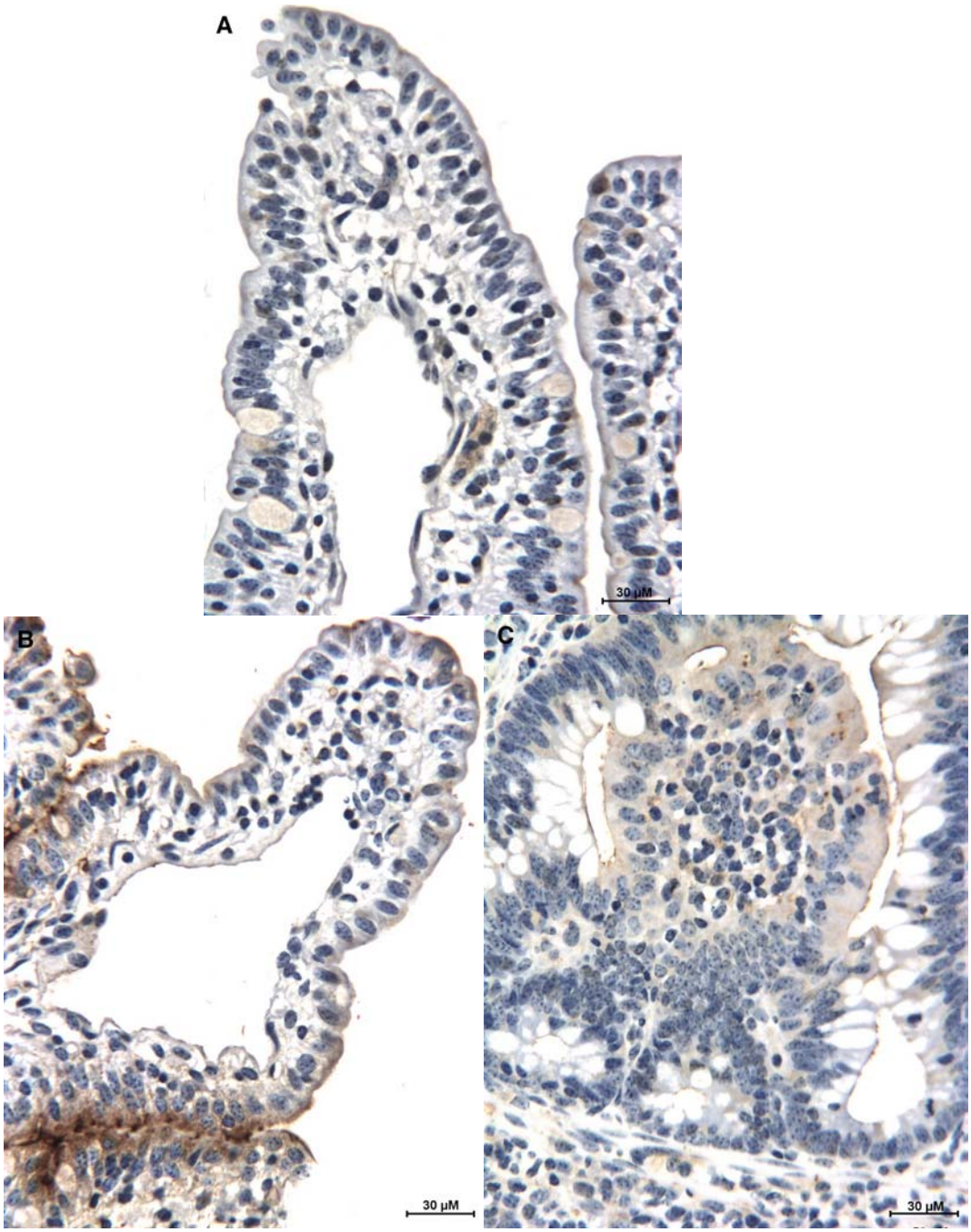

Figure 16: Immunohistochemistry for *Salmonella* O antigen in bovine ligated ileal loops of control uninfected (A) and *S. typhimurium* WT-infected tissues (B and C). Note the preferential distribution of invading bacteria along enterocytes of basolateral villi (B) and follicle-associated epithelium of domed villi (C). 1 hour post-infection. BLAD calf (CD18 -/-).

The gene expression profiles of cytokines and chemokines induced by *Salmonella* infection have been extensively investigated; however, the vast majority of these studies employed *in vitro* cell culture systems or *in vivo* mouse models of infection (41). This type of information in the bovine models of human salmonellosis is proportionally scarce compared to the information derived from cell culture systems and mice. The data generated in our work is innovative, because we used calves with leukocyte adhesion deficiency unable to mount an adequate neutrophilic response against *S. typhimurium* infection, which is considered the hallmark of *Salmonella*-induced enteritis and diarrhea (190). The lack of tissue neutrophils observed in our experimental animals allowed an enhanced analysis and characterization of the innate immune response induced by *Salmonella* infection alone without the influences of the neutrophilic exudate and massive necrosis occurring in the later stages of acute infection in the bovine model. Despite the fact that significant statistical differences were not observed in any comparison between genetic expression levels of cytokine, our data revealed interesting tendencies relevant to the understanding of salmonellosis. The reduced number of calves available for the LCM studies accounts for the lack of statistical significance in our data.

The most interesting finding is our study was the preferential genetic up-regulation of all cytokines detected (IL-8, GRO-α, and IL-1β) in crypts when compared to those in tips and domed villi. Previous *in situ* hybridization studies using regular calves, i.e. negative for the BLAD defect, infected by *S. typhimurium* found that GRO-α transcripts were detected primarily in enterocytes lining the intestinal crypts, at the base of absorptive villi, and in the follicle-associated epithelium of lymphoid nodules with minimal detection in tips of absorptive villi (221). These findings of preferential localization of GRO-α transcripts strongly support our data. The base of absorptive villi was not used in our LCM studies; however, the gene expression profiles of cytokines in these enterocytes are likely to be similar to those in crypt enterocytes, because the yet immature enterocytes lining the base of absorptive villi are continuous and closely related to that of the crypts (219). The enterocytes covering the tips of villi are also continuous with enterocytes lining the base of absorptive villi, but unlike those lining the basolateral surface, the enterocytes of the tips of the villi have the highest degree of maturation as they migrate from crypts (219), presumably accounting for the differences in cytokine gene expression observed between crypts and tips of villi.

The gene expression levels in WT-infected samples detected in the LCM study correlates well with the gene expression observed in the whole intestinal samples derived from the same animals, confirming the highest expression levels for GRO-α followed by IL-8 and IL-1β. However, the IL-1β gene expression in crypts (approximately 15 fold) was markedly elevated to levels above the IL-8 gene expression (approximately 7 fold) in WT-infected samples as opposed to the reverse tendency observed in the data from whole intestinal samples. These data suggest that crypts are likely the principal source for the vast majority of the relatively low expression of IL-1β observed in bovine intestinal samples infected by *S. typhimurium*. The contribution of epithelial cells to IL-1β gene expression induced by *Salmonella* infection was largely unknown before this study, because data available to date focused to report IL-1β up-regulation limited to macrophages (41, 155). *In vitro* studies demonstrated that epithelial cells are a major source of IL-8 gene expression during *Salmonella* infection (42, 97, 118), but the prioritized contribution of crypt enterocytes compared to tips and domed villi found in this work was not previously reported in the literature.

Several studies highlight the importance of TNF-α during salmonellosis indicating that this pro-inflammatory cytokine plays a protective role against *Salmonella* infection (41). Our data on whole intestinal samples support up-regulation of this cytokine in the early stages of acute infection, yet its gene expression levels were relatively low compared to GRO-α and IL-8. Interestingly, this cytokine was not be detected in the LCM studies despite

several attempts of optimization using distinct sets of primer sequences and distinct PCR conditions. Our data suggest that none of the cells evaluated by LCM, including enterocytes of villi tips and crypts, are significant sources of TNF-α gene expression *in vivo* in contrast to *in vitro* studies indicating up-regulation of TNF-α in human intestinal epithelial cell lines infected by *Salmonella* (97). In addition, since tissue influx of neutrophils was not present in the whole intestinal samples, our data suggest that neutrophils were also not a significant source of TNF-α gene expression during infection.

A recent investigation demonstrated that the gene expression of GRO-α and IL-8 in MT-infected samples was significantly reduced compared to that of WT-infected samples in normal calves suggesting that expression of genes *sipAsopABDE2* are necessary for eliciting up-regulation of these two major neutrophil chemokines (221). Data in our BLAD calves from whole intestinal samples support this finding and also indicate that down-regulation of these two chemokines in MT-infected samples are independent of tissue influx of neutrophils.

Previous morphologic studies in bovine ligated ileal loops using normal (CD18 +/+) calves concluded that *S. typhimurium* infect a variety of intestinal cells with no predilection for any specific cell type (164). In contrast, M cells along the follicle-associated epithelium of Peyer's patches have been demonstrated to be the target for *Salmonella* invasion in mice (30, 95). In BLAD calves, our IHC findings partially support the findings in the normal calves; however, bacteria in BLAD calves were predominantly detected in enterocytes of

basolateral villi and follicle-associated epithelium of Peyer's patches when compared with enterocytes forming tips of absorptive villi. This partial discrepancy between normal and BLAD calves regarding the preferential localization of invasion can be attributed to the fact that data in normal calves originated from electron microscopy rather than IHC.

In summary, the LCM technique allowed isolation of high quality RNA derived from specific groups of cells in the heterogeneous and complex intestinal tissue. The cell-specific RNA was then submitted to qRTPCR facilitating determination of precise anatomic localization of gene expression. For the first time in the Salmonella literature, enterocytes of crypts were identified as the major source of cytokines and chemokines involved in the pathogenesis of S. typhimurium-induced enteritis. The essential role of functional *sipAsopABDE2* genes for inducing up-regulation of these inflammatory mediators was confirmed by LCM data.

CHAPTER IV

HOST TEMPORAL GLOBAL GENE EXPRESSION ANALYSIS IN *Salmonella typhimurium*-INFECTED CALVES WITH BOVINE LEUKOCYTE ADHESION DEFICIENCY

Introduction

The pathogenesis of non-typhoidal salmonellosis involves a highly complex interaction between the host and agent (31). Successful intestinal invasion and multiplication of *Salmonella enterica* serovar Typhimurium (hereafter *S. typhimurium),* one of the major etiologic agents of non-typhoidal salmonellosis, depends on a fine balance between expression of bacterial and host genes ultimately favoring disease manifestation (177). To date, most available information on the gene expression profiles involved in the pathogenesis of a successful *S. typhimurium* infection refers to bacterial genes encoding effector proteins that subvert the host defense mechanisms facilitating progression to disease (149). One of the most studied set of these genes, for instance, are the *Salmonella* Pathogenicity Island 1 (SPI-1)-encoded genes *sipAsopABDE2,* which act synergistically to invade host intestinal cells (111) and

trigger the massive tissue influx of neutrophils, considered the hallmark of *S. typhimurium*-induced diarrhea (221). Studies in the calf ligated ileal loop model, a well-established and useful model for non-typhoidal salmonellosis in humans (221), revealed that *S. typhimurium* carrying simultaneous mutations in *sipAsopABDE2* exhibited markedly reduced ability to invade intestinal epithelial cells and markedly attenuated pathogenicity resulting only in mild neutrophilic enteritis and mild diarrhea (161, 201, 222). Another classic example of bacterial genes manipulating the host machinery are the products of the *Salmonella* genes encoded by a second pathogenicity island (SPI-2), which are responsible for intracellular survival, replication, and modification of host cell transport processes (1, 106).

The host genes involved in the pathogenesis of non-typhoidal salmonellosis are beginning to be elucidated. Perhaps one of most important and most studied genetic contributions of the host during intestinal infection is activation of the innate immune recognition against *Salmonella* infection (177). Noteworthy is the expression of Toll-like receptors (TLR) in host cells upon infection, particularly, the expression of TLR5 in the basolateral surface of epithelial cells (23, 65). *In vitro* studies found that invading *Salmonella* secrete flagellin, which is transcytosed from the apical surface of epithelial cells by vesicular transport reaching the basolateral portion and activating TLR5 resulting in changes in host gene expression that leads to secretion of pro-inflammatory mediators (179). Other TLRs, like TLR2 and TLR4, have also been implicated in the pathogenesis of non-typhoidal salmonellosis based mostly on *in vitro* studies

(149), albeit the contribution of TLRs as well as several other host genes in the pathogenesis of non-typhoidal salmonellosis remain to be better characterized using *in vivo* models.

The goal of this study is to improve our knowledge on the genetic contribution of the host during *S. typhimurium* infection by evaluating the global temporal transcription profiles of the bovine host by using microarray technology. The bovine ligated ileal loop model was used here in calves with Bovine Leukocyte Adhesion Deficiency (BLAD). BLAD calves are unable to mount an appropriate innate immune response against bacterial infections because they carry a genetic mutation in the common CD18 subunit of cell surface adhesion molecule β2 integrin, which prevents neutrophils from extravasating into the extravascular space during infection (62, 132, 136). These calves facilitate investigation of the host gene expression in the context of absent or minimal tissue influx of neutrophils during *S. typhimurium* infection.

Materials and Methods

Bacterial strains and growth conditions

The strain of *S. typhimurium* used in this study was the Wild Type

IR715 (ATCC 14028 wild type *nal*) (178). The bacteria were grown in Luria-Bertani (LB) medium with nalidixic acid antibiotic (50 mg/liter) under agitation (250 rpm) overnight at 37^{o}C. Fifty μl of the culture was inoculated into 5ml of fresh LB medium and sub-cultured for additional 4 hours before inoculation.

Animals, surgical procedure, and sampling

A total of three BLAD Holstein calves (hereafter BLAD), 1 to 5 weeks of age, represented by both genders, weighting approximately 35 to 55 Kg were used in these experiments. All BLAD calves were homozygous for the BLAD defect (CD18 -/-) as determined by a PCR-based DNA test combined with restriction enzyme analysis (99, 171). Embryo transfer technology (168) was used to generate all three BLAD calves present in this study. Embryos were donated by the USDA/ARS National Animal Disease Center (NADC) – Ames, IA. The calves were kept clinically healthy before experimental surgeries at the Large Animal Hospital of the College of Veterinary Medicine, Texas A&M University, College Station – TX. All calves were tested negative for *Salmonella spp.* as determined by standard fecal culture using enrichment in tetrathionate broth (Difco, Detroit, MI). Calves were fed milk replacer twice a day, water *ad libitum*, and fasted 24 hours prior to experimental surgeries. The ligated ileal loop surgical procedure was employed as previously described (164, 166). Briefly,

anesthesia was induced with propofol (Abbot Laboratories, Chigaco, IL) followed by placement of endotracheal tube and maintenance with isofluorane (Abbot Laboratories, Chigaco, IL) for the duration of the experiment. A laparotomy was performed, the ileum and distal jejunum were exposed and 16-20 loops, 5 to 8 cm long, were ligated in the ileum and distal jejunum, intercalated with 1-2 cm loops. The loops were injected with 3 ml of either sterile LB broth (control loops) or LB containing approximately 0.75 x 10^9 colony-forming units (cfu) of WT *S. typhimurium*. Loops were replaced into the abdominal cavity and excised at 1, 4, 8, and 12 hours post-infection (HPI). Samples for microarray analysis and quantitative Real-Time PCR (qRTPCR) were collected immediately after loop excision. The microarray data from BLAD were analyzed and compared to the data obtained similarly from four, male, 3-6 week old, Holstein calves negative for the BLAD defect (CD18 +/+) submitted to identical experimental protocols (hereafter Control).

RNA extraction and isolation

As the source of host RNA for the microarray analysis and qRTPCR, six to eight 6 mm biopsy punches were taken from the intestinal wall including mucosa, submucosa, and Peyer's patches. Punches were immediately cleaned to remove debris, minced into small pieces with a sterile scalpel or razor

blade, immersed in 500 μl of TRI-reagent® at 4°C (Ambion, Foster City, CA) and further homogenized using a tissue grinder. The RNA was extracted according to TRI-reagent manufacturer instructions, the pellet was re-suspended in nuclease-free water (Ambion, Foster City, CA), and any contaminating DNA was removed by RNase-free DNase I treatment (Ambion, Foster City, CA) according to manufacturer's instructions. Samples were stored at -80°C until used. The resultant DNA-free RNA was quantified using a NanoDrop® ND-1000 spectrophotometer (NanoDrop Technologies, Wilmington, DE), and assessment of RNA quality was determined using an Agilent 2100 Bioanalyser (Agilent Technologies, Santa Clara, CA).

Preparation of bovine reference RNA

Total RNA was isolated from Madin-Darby bovine kidney (MDBK) and bovine B lymphocyte (BL-3) cell lines (American Type Culture Collection, Manassas, VA) as well as from the cerebral cortex and cerebellum collected from control surgery calves immediately after surgery following euthanasia. Cell lines were grown in 150 cm^2 cell culture flasks with Eagle's minimum essential medium (E-MEM) (ATCC) supplemented with 10% HI-FBS. The cerebral and cerebellar tissues were immediately homogenized in 4°C Tri-reagent® (Ambion, Austin, TX), the RNA was extracted, and any contaminting DNA was removed as

previously described under RNA extraction and isolation. RNA concentration and quality from each sample were determined using a NanoDrop® ND-1000 spectrophotometer and an Agilent 2100 Bioanalyser respectively, before and after pooling the samples. Total RNA isolated from three samples was pooled together in equal amounts, aliquoted, and stored at -80ºC until used.

Construction of bovine cDNA microarrays and annotation

Selected unique 70-mers oligonucleotide set representing 13,257 cattle open reading frames (ORFs) were obtained from normalized and subtracted cattle placenta and spleen cDNA libraries based upon the earlier bovine cDNA array platform GPL2864 (46) and subtracted cDNA libraries created from embryonic (day 36 and day 64) and extra-embryonic (day 14 to 25) tissues (NCBI libraries 15993, 15993, and 17188). Positive controls included the genes β-actin (*ACTB*), glyceraldehyde-3-phosphate dehydrogenase (*GAPDH*), and hypoxanthine phosphoribosyltransferase (*HPRT*). Exogenous spiking controls included the soybean genes chlorophyll a-b binding protein (*CAB*), rubisco small chain 1 (*RBS1*), and major latex protein (*MSG*). Negative controls consisted of Cot1 DNA, genomic DNA, spotting buffer, poly-A oligonucleotides, and water. All 70-mer oligos were printed in duplicates on aminosilane-coated glass slides in 150 mM phosphate buffer at 20 uM concentration, at the W. M.

Keck Center (University of Illinois at Urbana-Champaign). The oligos were annotated based on the most currently available GenBank accession number.

Microarray sample preparation and slide hybridization

The washing, labeling, and hybridization procedures were performed as previously described (46). In summary, RNA-derived cDNA from all seven calf experimental samples (three BLAD and four control calves), including infected and control uninfected loops (LB broth), were co-hybridized against cDNA generated from the bovine reference RNA sample followed by hybridization to the previously described custom 13K bovine ESTs, –70mer, oligoarray. High quality RNA derived from all experimental loops was reverse transcribed to cDNA using Superscript III reverse transcriptase (Invitrogen, Carlsbad, CA) and labeled with amino-allyl-UTP (Ambion, Austin, TX). Cy3 and Cy5 dye esters were covalently linked to the amino-allyl group by incubating the resultant amino-allyl-labeled cDNA with the dye esters in 0.1M sodium carbonate buffer. Prior to hybridization, the microarrays were denatured by boiling, UV cross-linked, and immersed in prehybridization buffer [5X sodium chloride, sodium citrate buffer (SSC), 0.1% sodium dodecyl sulfate (SDS) (Ambion, Austin, TX) and 1% bovine serum albumin (BSA)] at 42ºC for a minimum of 45 min followed by four washes in RNase-, DNase-free, distilled water; immersed in

100% isopropanol for 10 seconds, and dried by centrifugation. Slides were hybridized at 42ºC for approximately 40 hours in a dark humid chamber (Corning, Corning, NY) and washed for 5-10 min at 42ºC with low stringency buffer [1 X SSC, 0.2% SDS] followed by two 5-10 min washes in a higher stringency buffer [0.1 X SSC, 0.2% SDS and 0.1 X SSC] at room temperature with agitation.

Acquisition and analysis of microarray data

Immediately after hybridization and washing, the slides were scanned using a commercial laser scanner (GenePix 4100; Axon Instruments Inc., Foster City, CA). The spots representing genes on the arrays were adjusted for background and normalized to internal controls using image analysis software (GenePixPro 4.0; Axon Instruments Inc.). Spots with fluorescent signal values below background were disregarded in all analyses. All host signals were normalized against bovine reference RNA signals. The resulting data were analyzed using Seralogix™'s suite of gene expression analysis and modeling tools (www.seralogix.com). Genes were designated to have significant differential expression (up- or down-regulation) based on Seralogix's Bayesian z-score method. In this method, genes are ranked and ordered according to their expression magnitudes. In addition, gene variance is computed using a Bayesian predicted variance value. The Bayesian variance is determined by using a sliding

window algorithm that averages 50 variances directly on the ascending and descending ordered sides of each gene of interest. This method is used to smooth the variances across the dynamic range of intensity values. Genes with statistically significant differential expression were determined with the Bayesian z-test ($p \leq 0.025$). Identification of Biosignature Dynamic Bayesian Network (DBN) modeling, mechanistic gene discovery, and pattern and pathways of recognition were determined by advanced computational tools developed by Seralogix™. Biosignature Analysis Framework developed by Seralogix™ is comprised of an integrated suite of software tools (XManager, XConsole & XBuilder) and relational database storage specialized for management and analysis of biosignature data. The Seralogix™ analysis defines mechanistic as the genes responsible for the temporal pattern within their DBN models. In other words, they are the principal genes that have the most influence in making the DBN of a certain condition, in this case BLAD, different from control conditions (control). Our analysis focused primarily in the mechanistic genes differentially expressed in samples from WT-infected BLAD versus WT-infected control calves (Appendix C) and less on the individual genes identified in WT-infected control animals versus uninfected samples (LB broth) from the same animals (Appendix A) or WT-infected BLAD animals versus uninfected samples (LB broth) from the same animals (Appendix B).

Validation of microarray results

Four randomly selected bovine genes with differential expression on microarray analysis common to both BLAD and control animals were analyzed by qRTPCR. Quantitative gene expression was determined using an Applied Biosystems 5700 DNA Sequence detection system (Applied Biosystems, Foster City, CA). RNA from all experimental loops was reverse transcribed to cDNA by adding 2 μg of total RNA to a 100 µl reaction containing 2.5 µM of random hexamers and reagents from the reverse transcription kit (Applied Biosystems, Foster City, CA). The thermal cycle parameters used for reverse transcription were 10 minutes at 25^{o}C, followed by 30 min at 48^{o}C, and finalizing with 5 min at 95^{o}C. The final working solution of cDNA was diluted to generate the concentration of 2 ηg per 10 μl sample. Diluted cDNAs were stored at -80°C until used. qRTPCR was performed with SYBR Green PCR Master Mix (Applied Biosystems, Foster City, CA). All primers were designed by Primer Express Software (Applied Biosystems, Foster City, CA) and synthesized by Sigma-Genosys (The Woodlands, TX). The list of primers used in this study is provided in Table 3.

Analysis of qRTPCR data

Analysis of the qRTPCR data was performed with the 2-$\Delta\Delta$Ct method as previously described (108). The gene *GAPDH* was used as the control housekeeping gene. According to the 2-$\Delta\Delta$Ct method, the cycle number was determined as the cycle at which fluorescence crossed a threshold above background (Ct). The resulting Ct value was recorded for each sample for genes of interest. The Delta Ct value (ΔCt) for each gene of interest was obtained by subtracting their Ct value from their respective housekeeping gene Ct value (*GAPDH*). This was followed by determination of the $\Delta\Delta$Ct by subtracting the resultant ΔCt for the control samples from the ΔCt obtained for the infected samples. The gene expression fold change in infected tissues compared to uninfected control was calculated by converting $\Delta\Delta$Ct into 2-$\Delta\Delta$Ct. A negative control (water) and an RNA sample without reverse transcriptase to determine genomic DNA contamination were included as controls during cDNA quantization for each primer pair used. Since the Seralogix™ microarray analysis considered genes differentially expressed based on a z-score and not on a fold-change, the microarray data were considered valid if the fold change of each gene tested by qRTPCR was expressed in the same direction, i.e. up or down-regulated, as determined by the microarray analysis.

Table 3- Primer sequences used in qRTPCR to study the gene expression of *S. typhimurium*-infected bovine ileal loops.

GenBank accession #	Gene symbol	Gene name	Primer sequence[a]
BM_001034034	*GAPDH*	Glyceraldehide-3-phosphate dehydrogenase	TTCTGGCAAAGTGGACATCGT GCCTTGACTGTGCCGTTGA
NM_001001175	*Apoc3*	Apolipoprotein C3	GCACCAAGACCGCCAA GCAGATTCCCAGAAGTCAGTGAA
NM_182786	*FOS*	v-fos FBJ murine osteosarcoma viral oncogene homolog	ATCTGCTGAAGGAGAAGGAAAAAC TGAGGAGTGGCAGGGTGAAG
NM_174147	*PLAU*	plasminogen activator, urokinase	TGAACGGAGGAAAATGTGTAACC TCAGAAGGACGGTGGGAGAG
NM_174576	*PIK3R2*	phosphoinositide-3-kinase, regulatory subunit 2 (p85 beta)	GCTCCTCTACCCAGTGTCCAAGT ACGCTGTCCTCCTTGACGAT

[a]Sequences for bovine genes were obtained from GenBank. Top row represents forward primers and bottom row shows reverse primers.

Results

Transcriptional profile of bovine host intestinal loops inoculated with S. Typhimurium

The general host gene expression response

Samples of distal small intestine (ileum and distal jejunum) including Peyer's patches inoculated with LB broth (uninfected loops) and *S. typhimurium* (WT), from three distinct BLAD (CD18 -/-) and four distinct control calves (CD18 +/+) collected a 1, 4, 8 and 12 HPI (n = 56) were used as the source of host RNA for the microarray analysis and qRTPCR for validation of microarray data. The RNA was indirectly labeled and co-hybridized against bovine reference RNA on a custom 13K bovine-specific oligoarray. Experimental RNA samples of adequate quality from BLAD and control animals were selected based on the following bioanalyzer parameters: RNA integrity number (RIN) > 5.0 and 28S/18S ratio > 1.1. The bioanalyzer parameters for the reference RNA were RIN = 9.7 and 28S/18S ratio = 2.1. The percentage of microarray spots having a signal to noise ratio (SNR) higher than three above background (SNR > 3) was variable among arrays. A minimum of 40%, 60%, and 46% of spots had a SNR > 3 in experimental samples (Cy3 channel; laser excitation = 532), reference

samples (Cy5 channel; laser excitation = 635), and combined samples (Cy3-Cy5 channels), respectively.

The number of genes identified as differentially expressed (z-score $p \leq 0.025$) by the microarray analysis varied substantially between the two distinct treatment groups used, i.e. BLAD and control calves (Table 4). When compared to uninfected loops (LB broth), samples from BLAD calves inoculated with WT *S. typhimurium* had a total of 1,504 uniquely differentially expressed genes compared to 673 uniquely differentially expressed genes detected in S. typhimurium-infected samples from control calves ($p \leq 0.025$) (Table 4). Analysis of significant gene expression across all time points taking in consideration identical genes expressed at more than one time point revealed that 83.71% of the total gene appearances had up-regulation in BLAD contrasted with 74.32% of up-regulation appearances in control calves (Table 4). The temporal pattern of gene expression had remarkable differences. While the peak of gene expression in BLAD calves occurred at 4 HPI followed by a progressive reduction in the number of differentially expressed genes on late time points, control calves had an earlier peak of gene expression at 1 HPI followed by a marked reduction at 4HPI and *de novo* high expression profiles at 8 and 12 HPI (Figure 16).

Table 4- Summary of differentially expressed genes at each time point in *S. typhimurium*-infected bovine ligated ileal loops from BLAD and control calves compared to uninfected control loops (LB broth).

Condition	Total genes changed[a]	Total up and down-regulated[b]	Time post-inoculation			
			1	4	8	12
BLAD	1504	1445	43	740	375	287
		222	21	19	22	160
Control	673	660	168	43	220	229
		228	136	7	30	55
Genes common across the 2 conditions			11	9	30	80

[a]Total genes with significantly different expression reflect the total number of genes that were uniquely expressed across all time points without taking into consideration expression of a gene in more than one time point.

[b]For each treatment group, the top row represents significantly up-regulated genes and the bottom row denotes the significantly down-regulated genes ($p \leq 0.025$). Total numbers of up or down-regulated genes include identical genes expressed at more than one time point.

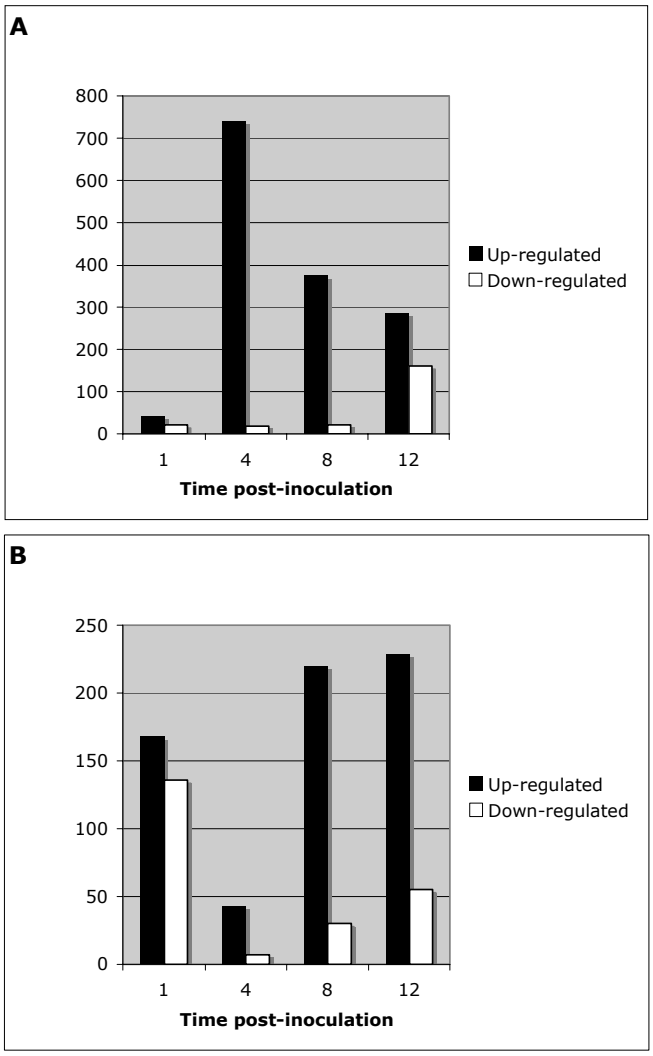

Figure 16: Temporal profile of differentially expressed genes ($p \leq 0.025$) in *S. typhimurium*-infected bovine ligated ileal loops from BLAD (A) and control calves (B) compared to uninfected control loop (LB broth).

The Seralogix™ statistical methods used in the analysis of our microarray data identified the most significantly activated pathways across all time points ranked by z-score. The list of the top 20 scoring pathways identified for *S. typhimurium*-infected BLAD and control calves compared to loops of uninfected control calves (LB broth) had striking differences between the two

treatment groups (Table 5). While some of most studied pathways in *Salmonella* infections including regulation of actin cytoskeleton (73, 145, 156), Toll-like receptor (TLR) signaling pathway (37, 64), and apoptosis (72, 103), were among the top activated in Control, the list of top scoring pathways in BLAD was dominated by a vast majority of genes associated with metabolic pathways important for normal cell metabolism (Table 5).

Table 5- Top 20 scoring cellular pathways activated in *S. typhimurium*-infected bovine ligated ileal loops from BLAD and control calves compared to uninfected control loops (LB broth).

Rank[a]	CONTROL (CD18 +/+)	BLAD (CD18 -/-)
1	Oxidative phosphorylation	Cyanoamino acid metabolism
2	Cytokine-cytokine receptor interaction	Cysteine metabolism
3	Toll-like receptor signaling pathway	Taurine and hypotaurine metabolism
4	MAPK signaling pathway	Maturity onset diabetes of the young
5	Apoptosis	Ethylbenzene degradation
6	Jak-STAT signaling pathway	Alkaloid biosynthesis I
7	Leukocyte transendothelial migration	CD40L Signaling Pathway
8	Epithelial cell signaling in Helicobacter pylori infection	Glycolysis / Gluconeogenesis
9	Propanoate metabolism	Stilbene, coumarine and lignin biosynthesis
10	Type I diabetes mellitus	Urea cycle and metabolism of amino groups
11	Natural killer cell mediated cytotoxicity	Linoleic acid metabolism
12	Dichlorobenzoate degradation	Reductive carboxylate cycle (CO2 fixation)
13	Long-term depression	Phenylalanine, tyrosine and tryptophan biosynthesis
14	Citrate cycle (TCA cycle)	C21-Steroid hormone metabolism
15	Cysteine metabolism	Gamma-Hexachlorocyclohexane degradation
16	T cell receptor signaling pathway	Biotin metabolism
17	TGF-beta signaling pathway	Prion disease
18	Gap junction	Lysine biosynthesis
19	Long-term potentiation	Glycosylphosphatidylinositol (GPI)-anchor biosynthesis
20	Regulation of actin cytoskeleton	Porphyrin and chlorophyll metabolism

[a] Pathways listed from the highest to the lowest z-score value.

Inflammation and immune response

Comparative analysis of the global gene expression between BLAD and control treatment groups at the first stages of acute infection revealed evidence of an early activation of inflammatory response in control animals. At 1 and 4 HPI, samples from control but not from BLAD calves (Appendices A & B) had up-regulation of the major pro-inflammatory gene *PTGS2* (prostaglandin-endoperoxide synthase 2). The protein encoded by this gene, also known as Cyclooxygenase-2, is a key enzyme in prostanoid biosynthesis and generation of other mediators that initiate inflammation (93). Regardless of this strong evidence of early inflammatory signaling initiation in control animals, our data provided evidence that endothelial transmigration of leukocytes was possibly impaired at the earliest stage of infection (1 HPI) in BLAD animals since our analysis revealed that down-regulation of the mechanistic gene *ICAM1* (intercellular adhesion molecule-1) (Appendix C) and down-regulation of *VCAM* (vascular adhesion molecule) (Appendices A & B) in samples from control when compared to those from BLAD calves. The proteins encoded by these two genes are endothelial adhesion molecules activated during leukocyte transmigration in acute inflammation and are required for extravasation of leukocytes into the surrounding tissue (28). In addition to inflammation, the cell mediated immune response at 1 HPI showed evidence of impairment in samples from control compared to those from BLAD animals, characterized by down-regulation of the

genes *BoLA-DRB3* (major histocompatibility complex, class II, beta chain) and *CD3D* (CD3d molecule, delta) (Appendices A & B). The protein encoded by *BoLA-DRB3* (MHC class II) is required for presentation of intracellularly processed antigens to CD4+ helper T cells during induction of cellular immunity (116). The *CD3D* gene encodes a structural component that forms part of the CD3 molecule, a T-cell receptor (TCR) accessory protein (126). TCRs are transmembrane proteins expressed in lymphocytes that recognize and bind to MHC-presented antigens during activation of the cellular immune response (126). Also at 1 HPI, samples from control but not from BLAD calves had down-regulation of the gene *CD79a* (Appendices A & B). This gene encodes a structural component of the B-cell receptor (BCR), which generates signals that mediate the humoral immune response triggered by antigen recognition (13).

Toll-like receptor signaling pathway

Unlike the earliest stage of acute infection at 1 HPI, our data showed that the majority of inflammation-associated genes were differentially expressed beginning at 4 HPI. Perhaps, the most important of these genes when considering the current literature relevant to salmonellosis are those encoding TLRs. The most studied TLRs in *Salmonella* infections are TLR2, TLR4, and TLR5, which are activated by bacterial lipoproteins, lipopolysaccharide (LPS),

and flagellin, respectively (64). TLR4 signaling in mice plays a important role in the host defense against *Salmonella* infection by controlling the bacterial loads in mesenteric lymph nodes (208). Infection of human macrophages by *S. typhimurium* activates *TLR4* resulting in CXC chemokine production, which is the triggering factor leading to the massive tissue influx of neutrophils characteristic of non-typhoidal salmonellosis (141, 155). Our data demonstrated up-regulation of *TLR4* in both treatment groups and this expression coincided with the peak of gene expression in BLAD calves at 4 HPI and the two late peaks of gene expression in control calves at 8 and 12 HPI (Appendices A and B). This up-regulation of *TLR4* in the late stages of acute infection in control was also supported in our analysis by late up-regulation of other directly related downstream genes as part of the TLR4-signaling pathway including *NFKBIA* and *FOS* (Appendix A). Although significant up-regulation of *TLR4* was not observed after 4 HPI in BLAD calves, our data showed significant up-regulation of *NFKBIA* and *FOS* at the later time points at 8 and 12 HPI (Appendix B), indicating that TLR signaling pathway maintains an activated state in BLAD calves in the later stages of acute response and that this activation may be independent of TLR4 activation.

In addition to TLR-associated genes, other inflammatory genes were consistently up-regulated in samples from control animals at or after 4 HPI including *SELP* (P-selectin) and *Cebpd* (CCAAT/enhancer binding protein) (Appendix A), as well as the two mechanistic genes *ICAM-1* and *TNFRSF1A* (tumor necrosis factor receptor superfamily, member 1A) (Appendix C). Similarly

to ICAM-1 and VCAM, P-selectin is an endothelial adhesion molecule that facilitates endothelial transmigration of leukocytes during acute inflammation (28). The gene *Cebpd* encodes a transcription factor that results in production of pro-inflammatory mediators by possibly activating COX-2 transcription (27) and *TNFRSF1A* encodes an extracellular domain of the TNF receptor (153). The TNF receptor is commonly activated during inflammatory conditions and is important to orchestrate an adequate cellular response (153). None of these inflammation-associated genes were up-regulated in samples from BLAD animals at any time point (Appendices B and C).

Cytokine profile

The profile of cytokine activation during *Salmonella*-induced enteritis has been extensively investigated; however, the global gene expression profile in *S. typhimurium*-infected intestine using an *in vivo* model of non-typhoidal salmonellosis has not been characterized (41). Our mechanistic gene data comparing WT-infected samples from BLAD versus control calves had consistent up-regulation of typical *Salmonella*-infection associated pro-inflammatory cytokine genes such as *IL-1β* and *IL-6* across all time points in control animals (Appendix C). Interestingly, BLAD animals also had a similar temporal pattern of pro-inflammatory cytokine gene expression beginning at 4

HPI with up-regulation of the cytokine genes *IL-1β* and *IL-6* (Appendix C). Cytokine genes whose products exhibit primary chemotactic activity for monocytes but not for neutrophils such as the chemokine genes *CCL2* (encodes monocyte chemoattractant protein-1/MCP-1) and *CCL8* (encodes monocyte chemoattractant protein 2/MCP-2) (12) were persistently up-regulated across all time points in control calves (Appendix C). These chemokine genes were generally up-regulated in BLAD animals as well except at 8 HPI, when both genes were down-regulated (Appendix C).

Apoptosis

Induction of apoptosis has been previously implicated in the pathogenesis of *Salmonella* infections (82, 103). The global expression of apoptosis-associated genes in our samples had distinct gene expression profiles in control as compared to BLAD animals. While the results of gene expression in samples from control calves had a final balance between pro- and anti-apoptotic stimuli, the few apoptosis-associated genes differentially expressed in samples from BLAD animals were dominated by pro-apoptotic stimuli (Table 6).

Table 6- Apoptosis-associated genes differentially expressed in *S. typhimurium*-infected bovine ligated ileal loops from BLAD and Control calves compared to uninfected control loop (LB broth).

Condition	Symbol	Gene Name	Expression[a]	Function	Ref.
Control	AKT1	v-akt murine thymoma viral oncogene homolog 1	Down	anti-apoptotic	(19)
	MGC133975	similar to BCL2/adenovirus E1B 19kD interacting protein 1 isoform BNIP1-c	Down	anti-apoptotic	(140)
	cFLAR	CASP8 and FADD-like apoptosis regulator	Up	anti-apoptotic	(173)
	BCL2A1	BCL2-related protein A1	Up	anti-apoptotic	(209)
	MGC139459	similar to RTP801	Up	anti-apoptotic	(170)
	LOC512355	similar to TNF receptor-associated factor 2	Up	anti-apoptotic	(104)
	LOC522886	similar to periplakin	Up	anti-apoptotic	(194)
	CASP4	caspase 4	Up	pro-apoptotic	(204)
	LOC517192	similar to jun D proto-oncogene	Up	pro-apoptotic	(83)
BLAD	AKT1	v-akt murine thymoma viral oncogene homolog 1	Up	anti-apoptotic	(19)
	MGC133975	similar to BCL2/adenovirus E1B 19kD interacting protein 1 isoform BNIP1-c	Up	anti-apoptotic	(140)
	CASP6	Caspase 6	Down	Pro-apoptotic	(209)

[a] Gene expression was variable among distinct time points but with no preference for any time point.

Intracellular defense against infection

Phagocytic cells play a crucial role in host resistance to *Salmonella* following intestinal invasion (50, 198, 199). Immediately following phagocytosis, the intracellular NADPH oxidase system in phagocytes produces highly toxic reactive oxygen and nitrogen species (ROS and NOS) that control infection by promoting *Salmonella* killing (198). Although essential for intracellular defense against *Salmonella,* elevated levels of ROS AND NOS can cause severe damage to DNA, protein, and lipids in phagocytes, as well as necrosis of surrounding tissue as a result of leakage during phagocytosis (16, 151). However, cells have evoked mechanisms of defense against oxidative and nitrosative damage represented by the antioxidants (115). Analysis of differentially expressed genes associated with the intracellular oxidative and nitrosative systems in our samples from control animals had predominantly up-regulation of antioxidant genes including *SOD2* (superoxide dismutase 2) (Appendixes A and C), *TXNRD1* (thioredoxin reductase), and *ARG2* (arginase, type II) (Appendix A). The gene *SOD2*, whose product is important to protect macrophages from oxidative stress during microbial infections (151), was up-regulated at all time points with progressively higher fold change towards later time points reaching up to 15 fold-change compared to uninfected samples (LB broth) at 12 HPI (data not shown).

The genes *TXNRD1* and *ARG2* were both up-regulated in the late stages of acute infection (Appendix A). *TXNRD1* encodes a oxidoreductase that protects against oxidative stress especially in vascular endothelial cells (186) and the product of gene *ARG2* has been shown to play an important role in limiting nitric oxide production in bovine (29). In samples from BLAD calves, three genes associated with the oxidase and nitrosative systems were identified with *SOD2* being the only gene in common with samples from control animals. Besides *SOD2,* a second antioxidant-associated gene, *NQO1* (NAD(P)H dehydrogenase, quinone 1) was up-regulated (Appendixes B and C). Up-regulation of *SOD2* was observed at 4 and 12 HPI with a lower fold-change increase compared to control animals (data not shown) while up-regulation of *NQO1* was observed at 4 and 8 HPI. The product of *NQO1* is a cytoprotective enzyme that promotes detoxification of ROS (9). The third and last gene, *CYP11A1*, encodes a member of the cytochrome P450 family (cytochrome P450, family 11, subfamily A, polypeptide 1) which was up-regulated at 4 HPI (Appendix B). The cytochrome P450 proteins are monooxygenases, which catalyze many reactions involved in drug metabolism and synthesis of cholesterol, but also are well-known sources of mitochondrial ROS production (38). In addition, BLAD but not control animals, had down-regulation of the anti-inflammatory interleukin-10 gene (*IL10*) at 12 HPI (Appendix B).

IL-10 exerts its anti-inflammatory properties by down-regulating neutrophil functions, especially reactive oxygen species (ROS) production via NADPH oxidase (35). Collectively, the data from BLAD animals indicate a balance between genes involved in production of ROS and NOS potentially deleterious to the host and genes with anti-oxidant protective functions.

Validation of microarray gene expression results by qRTPCR

The cDNA used on qRTPCR to validate the microarray results was synthesized from the same RNA samples used for microarray hybridization. Analysis of gene expression in all tested genes at all time points had fold changes altered in the same direction in microarray and qRTPCR analyses in samples from both BLAD (Fig. 17) and control calves (Fig. 18).

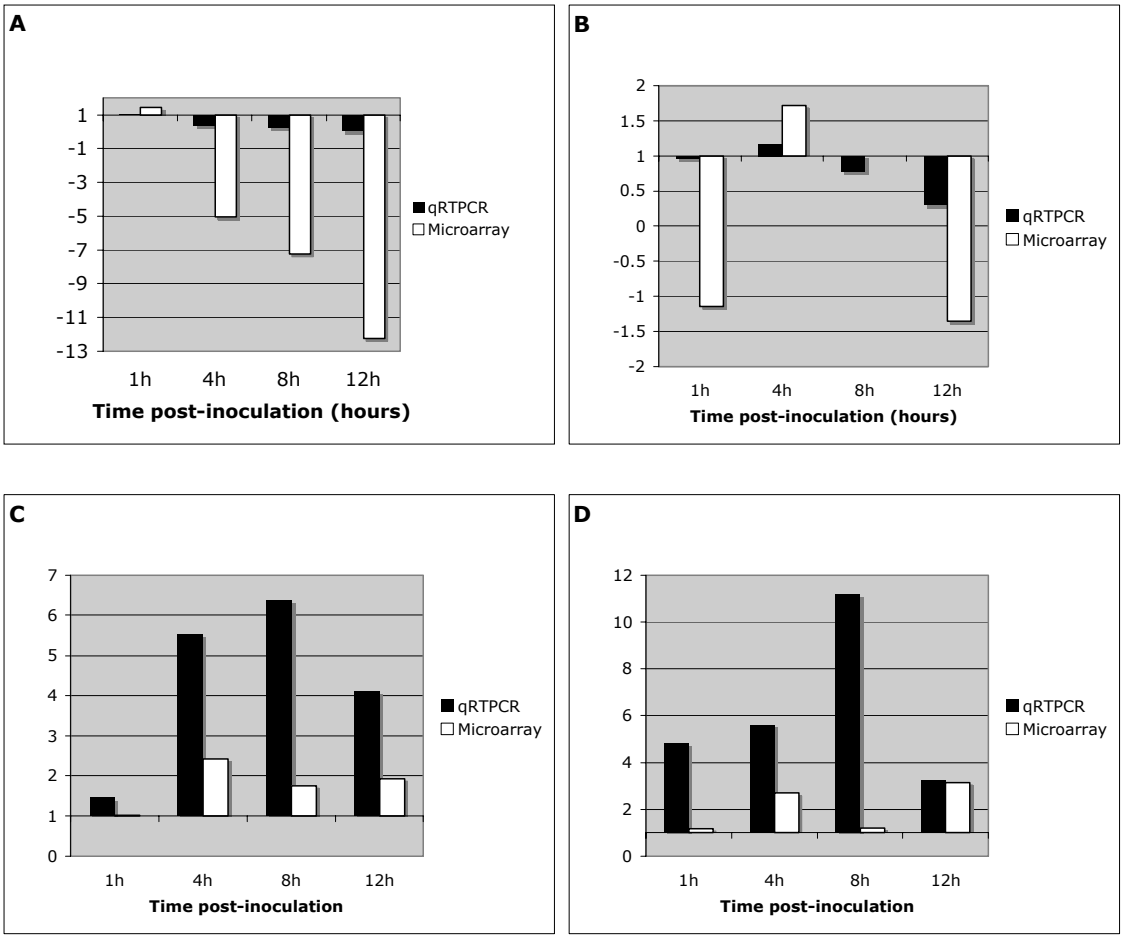

Figure 17: Validation of bovine microarray results by qRTPCR in samples from BLAD calves. Four randomly selected genes are depicted that were differentially expressed as revealed by microarray analysis of *S. typhimurium*-infected bovine ligated ileal loops compared to uninfected control loops (LB broth). A = Apolipoprotein C3 (*Apoc3*); B = phosphoinositide-3-kinase, regulatory subunit 2 (*PIK3R2*); C = Plasminogen, urokinase (*Plau*); D = v-fos FBJ murine osteosarcoma viral oncogene homolog (*FOS*).

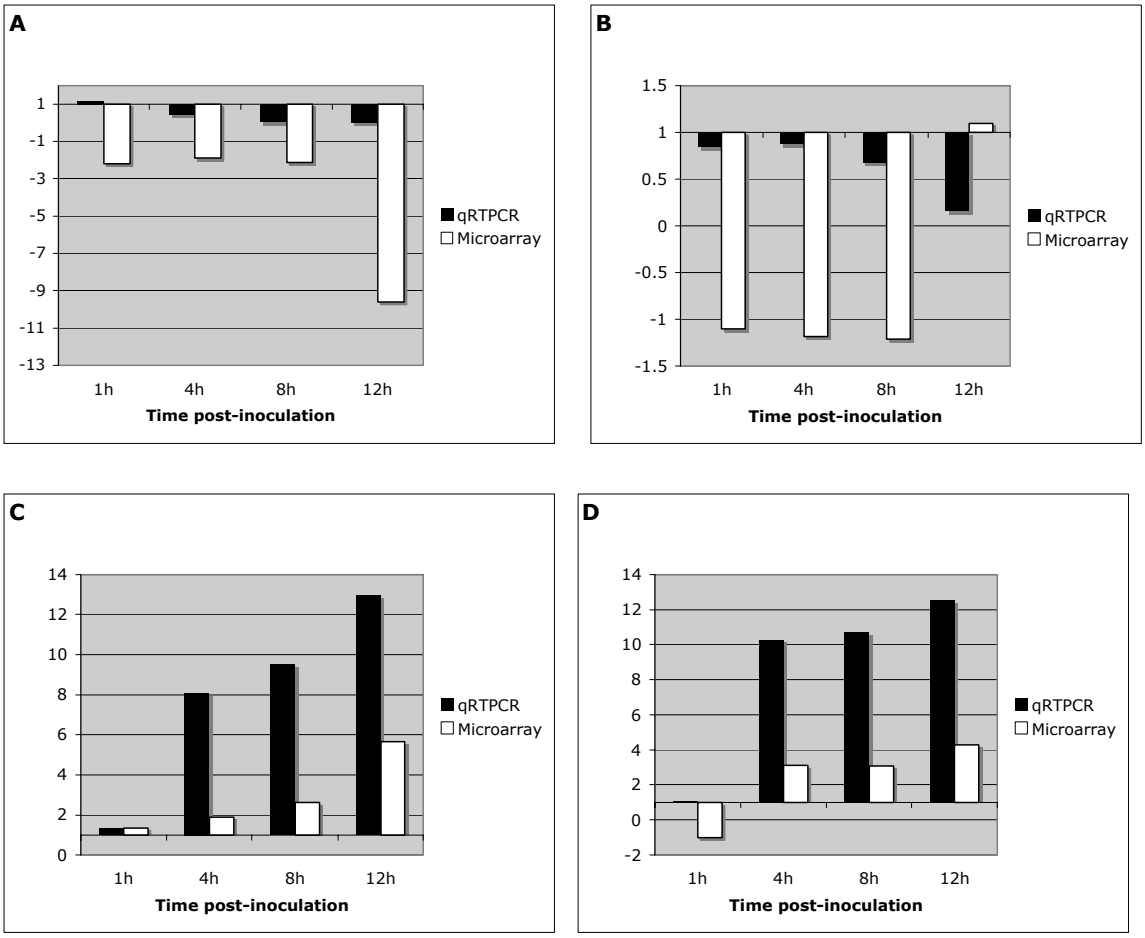

Figure 18: Validation of bovine microarray results by qRTPCR in samples from control calves. Four randomly selected genes are depicted that were differentially expressed as revealed by microarray analysis of *S. typhimurium*-infected bovine ligated ileal loops compared to uninfected control loops (LB broth). A = Apolipoprotein C3 (*Apoc3*); B = phosphoinositide-3-kinase, regulatory subunit 2 (*PIK3R2*); C = Plasminogen, urokinase (*Plau*); D = v-fos FBJ murine osteosarcoma viral oncogene homolog (*FOS*).

Discussion

A massive tissue influx of neutrophils is the hallmark of *S. typhimurium*-induced enteritis and diarrhea in humans and in the bovine model of non-typhoidal salmonellosis (190). The objective of this study was to identify the influence of the neutrophilic inflammation during the temporal global gene expression profiles after intestinal infection by *S. typhimurium*. For this purpose, we employed microarray technology in the well-accepted bovine ligated ileal loop model in calves with confirmed genetic deficiency of neutrophil extravasation, i.e. CD18 -/-, BLAD calves. The Seralogix™ microarray analysis performed on data from BLAD samples were compared to the results from control animals (CD18 +/+) submitted to similar experimental protocols. The current availability of bovine-specific microarrays introduced a new and powerful method capable of significantly raising our understanding on disease pathogenesis in cattle, which was previously limited by the lack of availability of tools to analyze both the host and pathogen responses (212). In addition, DNA microarray analysis of host gene expression allows fundamental questions to be addressed about the basis of host defense and microbial virulence (113), and perhaps most importantly, identification of potential biomarkers that could be used for future therapeutic purposes (69).

Analysis of the general picture obtained from the Seralogix™ analysis of microarray data identified remarkable differences in gene expression between the two animal treatment groups. The marked contrast between total number of uniquely expressed genes in BLAD versus control (1,504 vs. 673) confirmed that the neutrophilic inflammation greatly influences the host gene expression; therefore, suggesting that tissue influx of neutrophils largely dictates the genetic host response. More importantly, our data also revealed that the temporal gene expression during the acute host response to infection is also markedly altered by the neutrophilic influx. While infection in control animals resulted in a initial peak of gene expression (1 HPI) followed by a short silent period (4 HPI) that preceded a return of gene expression peaks (8 and12 HPI), the BLAD data indicated a reduced initial activation of gene expression followed by a later peak at 4 HPI and a progressive decrease during the late stages of acute infection (8 and 12 HPI). These data suggest that the influence of neutrophil influx over the host gene expression begins as early as 1 HPI, despite the fact that influx of neutrophils at that stage is still mild (164).

The period of silent gene expression in control animals coinciding with the peak gene expression in BLAD animals at 4 HPI suggests that the marked influx of neutrophils observed in infected genetically normal calves at this stage (161, 164), prevent bacteria from triggering massive gene expression as seen in BLAD calves. Previous studies have shown that number of invading bacteria in the intestinal mucosa do not reduce over time during this stage of enteritis in calves (223); therefore, it is unlikely that neutrophils prevent this peak

of *Salmonella*-induced host gene expression by controlling the tissue burden of bacteria. An alternative explanation suggested by our data is that phagocytosis of significant numbers of *Salmonella* by infiltrating neutrophils may prevent bacterial activation of gene expression in other host cells such as epithelial cells and macrophages, which are known to play major roles in gene activation during infection (51, 158). Significant phagocytosis of *S. typhimurium* by neutrophils during this stage of infection has been previously documented by electron microscopy studies (164).

The importance of neutrophils in the pathogenesis of host gene activation is emphasized in our data by the marked differences between top-scoring pathways activated throughout the course of infection between control and BLAD animals. The vast majority of top scoring pathways observed in control animals came as no surprise since they indeed represent the major fields of study in *Salmonella* research. The current data available on most of these pathways, which are mainly represented by inflammatory and immune response as well as cell signaling, have been the focus of numerous literature reviews (21, 31, 149, 177). Although most of these top-scoring pathways from control animals were also represented to some degree in BLAD calf samples, the statistical methods used by the Seralogix™ analysis identified the majority were other top scoring unrelated metabolic pathways in BLAD calves, reinforcing the concept that infiltrating neutrophils during *Salmonella*-induced enteritis results in direct and indirect manipulation of the host genetic expression machinery.

The inflammatory lesions that characterize *Salmonella* enteritis result from the triggering of host innate immune responses by the invading pathogen (177). The literature available to date suggests that neutrophilic inflammation in non-typhoidal salmonellosis is likely triggered by the combination of two main events, which are direct activation of pro-inflammatory cytokine genes in the host by effectors proteins secreted by the *Salmonella* pathogenicity island-1 (SPI-1) encoded Type 3 Secretion system (TTSS-1); and indirect activation of innate pathways of inflammation through activation of the pathogen recognition receptor TLR5 by biding of *Salmonella*-produced and secreted flagellin, which is a type of pathogen-associated molecular pattern (PAMP) (79, 190). It is important to note; however, that while the vast majority of evidence supporting the direct activation hypothesis described above are based on *in vivo* models of non-typhoidal salmonellosis such as the bovine (8, 187, 188, 203, 206, 223) and the streptomycin pretreated mice (14, 76), evidence supporting the indirect activation hypothesis via TLR5 is based entirely on *in vitro* studies using human epithelial cells lines, particularly the colonic cell line T84 (65, 66, 88, 179, 183, 220). The microarray data in control animals confirmed the *in vivo* activation of the TLR system (*TLR4*) and downstream genes associated with the TLR pathway (*NFKBIA* & *FOS*) beginning at 4 HPI; however, this activation was not detected in the earliest stage of infection at 1 HPI. Since our data in samples from control animals had evidence of inflammatory gene activation at this time point (*PTGS2*) in the absence of significant TLR gene activation, we suggest that the first morphologic signs of mild neutrophilic inflammation observed in infected

genetically normal calves at 1 HPI is mediated by a TLR-independent mechanism, i.e. most likely via direct activation of pro-inflammatory cytokines by the invading *S. typhimurium*. Interestingly, data from BLAD calves showed activation of the TLR pathway at 4 HPI (*TLR4*) plus the same related downstream genes in later time points (*NFKBIA* and *FOS*) agreeing with the data in samples from control animals; however, no evidence of inflammatory gene activation was detected in BLAD at 1 HPI. Collectively, these observations in BLAD and control animals suggest that the activation of the TLR pathway in *S. typhimurium*-induced enteritis is primarily induced by secreted flagellin and independent of neutrophilic influx. In contrast, the early inflammatory gene activation, which appears to be TLR-independent according to our data, is influenced in some manner by the mild tissue influx of neutrophils observed at that stage.

Sequestration and migration of neutrophils in response to acute inflammation involve sequential steps, including adhesion and transmigration through the vascular wall into interstitial tissues (39). Adhesion and transmigration of neutrophils are largely mediated by endothelial adhesions molecules of the immunoglobulin superfamily, which bind to various integrins present on the leukocyte cell surfaces (152). Data from control animals which had down-regulation of major endothelial adhesion molecule genes (*ICAM1* & *VCAM*) at 1 HPI may explain the mild neutrophilic enteritis seen in *S. typhimurium*-infected bovine ligated ileal loops in this early stage (164). In addition, these data may alternatively suggest that this down-regulation may

represent a host mechanism of negative feedback as an attempt to control exaggerated extravasation of neutrophils and propagation of inflammation, potentially deleterious to the host. The latter suggested hypothesis is also supported by our findings that BLAD animals with their characteristic absence of neutrophilic inflammation did not have down-regulation of these endothelial adhesion molecules at any time point.

Most studies investigating the host immunity to *Salmonella* infections focus in the innate immune response (innate immunity) (1, 17, 177, 211) with only a few manuscripts studying the cell and antibody-mediated immune responses, i.e. the adaptive or acquired immunity (185, 195). T lymphocytes have a central role in controlling and clearing infection by intracellular pathogens through cytokine production (195). In order to become capable of producing cytokines, T lymphocytes need to be activated by interaction with professional antigen-processing cells, typically dendritic cells (DCs), that initiate adaptive immunity against bacteria (185). *In vivo* studies in mice infected with *S. typhimurium* (model of typhoidal salmonellosis) and *in vitro* studies using murine DCs have found that virulent (WT) *S. typhimurium* prevent antigen presentation to T cells, thus escaping acquired immunity suggested to be mediated by effector proteins encoded within the *Salmonella* pathogenicity island 2 (SPI-2) (185). A recent study suggested that *S. typhimurium* have a direct, contact-dependent inhibitory defect in T cells, even in the absence of DC stimulation (195). Although the outcome of *S. typhimurium* infection in the murine model (typhoidal salmonellosis) is distinct from the bovine model (non-typhoidal

salmonellosis) (221), our data from samples of control animals provided evidence of impaired acquired immune response due to down-regulation of *BoLA-DRB3* (MHC-II, *β chain), CD3E*, and *CD79a* at 1 HPI, suggesting that *S. typhimurium* retain their ability to prevent T cell activation in the bovine model of typhoidal salmonellosis. BLAD animals did not have any significant expression of these immunity-related genes at the same point (1 HPI). In addition, none of the several pro-inflammatory genes identified at later time points in control animals, other than the ones associated the TLR-pathway, were differentially expressed in BLAD calves, including genes that encode the proteins P-selectin, TNF receptor, and COX-2, reinforcing the notion that inflammatory gene activation in BLAD were mostly limited to TLR pathway activation. The significance of these findings translates into a concept that tissue influx of neutrophils dramatically influences and manipulates the host pro-inflammatory gene repertoire, except TLR pathway-associated genes, which appear to be essentially under the influence of invading *Salmonella*.

Maintenance, progression, and propagation of intestinal inflammatory changes that follow *S. typhimurium* invasion is essentially orchestrated by the profiles of expression of cytokines and chemokines produced by the genes of the host, regardless of whether it was initiated through direct host gene activation by bacterial effector proteins and/or indirectly through TLR pathway activation (31, 177). Therefore, accurate identification of the pro-inflammatory cytokine profile genes during infection is critical for understanding the pathogenesis of salmonellosis and for future therapeutic interventions. Our

microarray data had many similarities of cytokine and chemokine mechanistic gene expression profiles between control and BLAD animals. Up-regulation of the major pro-inflammatory cytokines genes (*IL-1β* and *IL-6*) and chemokine genes (*CCL2 and CCL8*) were detected in both animal treatment groups. The cytokine gene expression in BLAD animals was delayed beginning at 4 HPI compared to control calves; however, this delay was not observed for chemokines. These results suggest that the presence of tissue neutrophils is not required for expression of major pro-inflammatory cytokines and chemokines throughout most of the course of acute infection, yet tissue neutrophils may act as positive regulators of cytokine gene expression in the earliest stage of infection (1 HPI), or alternatively, they may actually be a source for the cytokine gene expression at this stage. Although the inflammatory infiltrates that characterize *S. typhimurium*-induced enteritis in calves and humans are composed primarily of neutrophils (164, 223), our data found that both BLAD and control animals have the appropriate stimulus for tissue recruitment of macrophages via up-regulation of two major monocyte/macrophage chemoattractant genes, *CCL2* and *CCL8*, which encode MCP-1 and MCP-2 respectively. It is important to note that BLAD animals in response to intestinal bacterial infections typically develop lesions composed predominantly of macrophages and fewer lymphocytes and plasma cells, therefore, despite the fact all leukocytes express β2 integrins on their surface, these cell types are considered to have alternate ways to extravasate and reach the tissue extracellular matrix in BLAD calves (5, 98, 197).

Induction of apoptosis has been recognized as an important mechanism by which *Salmonella* successfully escape from the host cells and re-infect new cells propagating the infection (103). Studies on cell lines and murine macrophages have shown that the SPI-1 effector SipB activates caspase-1 in macrophages, releasing IL-1β and IL-18 and inducing rapid cell death by a mechanism that has features of both apoptosis and necrosis (82, 109). *In vitro* experiments using bovine macrophages found that *S. typhimurium* can induce apoptotic cell death by an early sipB-mediated and delayed sipB-independent mechanisms (162); however, experiments using *in situ* detection of apoptosis in bovine ligated ileal loops infected by *S. typhimurium* showed that apoptosis was not significant in the early stages of acute infection (163). Compared to macrophages, apoptosis in epithelial cells infected by *Salmonella* appear to be delayed or inhibited (103). Data in our samples from control animals had differential expression of several genes directly or indirectly associated with the apoptotic pathway resulting in a final balance between pro- and anti-apoptotic stimuli. In contrast, differential gene expression of apoptosis-associated genes in samples from BLAD animals was limited to three genes only, all of which favor anti-apoptotic stimuli. Two of these genes, whose products are the anti-apoptotic enzyme Akt1 and a protein with functions similar to Bcl-2, were common to both animal groups and found to be up-regulated in BLAD and down-regulated in control samples. Akt1 is a serine/threonine protein kinase that functions as a critical regulator of cell survival by inhibiting apoptosis (175) and members of the anti-apoptotic Bcl-2 family function by interacting with and antagonizing pro-

apoptotic family members (25). These results suggest that intestinal *S. typhimurium* infection *per se*, i.e. in the absence of significant neutrophilic enteritis, induces host gene expression that favors inhibition of apoptosis. In addition, based on the data from control animals, it is tempting to speculate that infiltrating tissue neutrophils can potentially represent the key event that triggers host apoptosis during *S. typhimurium* induced enteritis. This hypothesis is supported by the previous study using *S. typhimurium*-infected bovine ligated ileal loops showing that apoptosis was significantly detected *in situ* only at the last stages of infection when neutrophilic inflammation was severe.

The importance of phagocytic cells in controlling *S. typhimurium* infection in mice has been characterized in several experiments using the murine model of typhoid fever (198). Accordingly, oxidative damage by neutrophils and macrophages is essential for resistance against the early phase of infection, whereas nitrosative stress secondary to the action of inducible nitric oxide synthase (iNOS) plays a role in host resistance in the later phase of infection (36, 117, 169). More importantly, oxygen radicals can have pathological effects in salmonellosis also have been associated with increased lipid peroxidation and cell death of enterocytes in rats (122). Predominant up-regulation of antioxidants from control animals (*Sod2*, *TXNR1*, & *ARG2*) suggests that activation of the oxidative and nitrosative stress in phagocytic cells during *S. typhimurium*-induced enteritis in calves is highly controlled, therefore, also suggesting that tissue damage that accompanies enteritis in this model cannot be attributed mainly to the damaging effects of ROS/NOS. Samples from BLAD animals had similar

responses, i.e. antioxidant-controlled activation of oxidative and nitrosative stress. The only gene associated with oxidative stress common to both animal groups was the major antioxidant enzyme gene *SOD2*, whereas the genes *TXNRD1* and *AGD2* were unique to control animals, while *NQO1* and CYP11A1 genes were unique to BLAD animals. BLAD calves do not typically have significant numbers of tissue neutrophils, yet macrophages are able to extravasate and infiltrate the adjacent tissue during inflammation. This discrepancy of infiltrating inflammatory cell type and the oxidative stress-associated gene types between control and BLAD may simply reflect the predominance of different cell types in each animal treatment group. Therefore, the oxidative genes detected in BLAD calves are most likely derived from macrophages, whereas the genes from control animals likely represent a pool between a predominance of neutrophils and significantly fewer macrophages.

In conclusion, *S. typhimurium* infection of ligated ileal loops in calves with Bovine Leukocyte Adhesion Deficiency results in markedly distinct global and temporal gene expression profiles compared to the gene expression profiles observed in genetically normal calves. Our results confirmed that the massive tissue influx of neutrophils, the hallmark of *Salmonella*-induced enteritis in non-typhoidal salmonellosis, is not only a morphologic outcome of infection but also greatly influences and regulates the host gene expression profile.

Major differences in gene expression on prioritized areas of salmonella research including inflammation and immune response, Toll-like receptor signaling pathway, cytokine profiles, apoptosis, and intracellular defense against infection were detected by microarray analysis and their significance for understanding the pathogenesis of salmonellosis is discussed extensively. It is important to keep in mind, when analyzing the results present in this work, that many differentially expressed genes may partially reflect the gene expression of neutrophils especially in the later stages of infection, given the massive number of tissue neutrophils present in infected normal calves and absent in BLAD calves. Nevertheless, the results produced by these experiments provide essentially more detailed information as the basis for new concepts regarding the host global gene expression using an *in vivo* model for the molecular pathogenesis of non-typhoidal human salmonellosis.

CHAPTER V

CONCLUSIONS

Massive tissue influx of neutrophils is the hallmark of *Salmonella typhimurium*-induced enteritis in calves and humans. Yet, the *in vivo* role of neutrophils in the pathogenesis of *Salmonella*-induced enteritis and diarrhea remains incompletely understood. The overall goal of this investigation was to establish a functional and informative model to evaluate the contribution of neutrophils in the molecular pathogenesis of non-typhoidal ruminant and human salmonellosis. To accomplish this goal, we employed the ligated ileal loop model in calves with the naturally-occurring Bovine Leukocyte Adhesion Deficiency (BLAD) mutation. Neutrophils from BLAD calves are unable to extravasate and infiltrate the tissue matrix as a normal host response to intestinal infection, because these calves carry a genetic mutation in the CD18 molecule of the β2 integrin family of leukocyte adhesion molecules.

In Chapter II, a detailed description of the intestinal morphologic lesions associated with *S. typhimurium* infection in BLAD animals was accomplished as the basis for comparing our findings with previously published studies using genetically normal calves negative for the BLAD mutation. The conclusions of our findings was that the massive tissue influx of neutrophils

following ileal infection in normal calves is a major contributing factor in morphological pathogenesis of the severe pathologic lesions that occur in the acute stage of the enteritis, including the massive superficial enteric necrosis. Also in the same chapter, infected ileal samples from BLAD calves were compared to normal calves and evaluated for fluid accumulation, bacterial invasion, and cytokine profiles. Analysis of our data revealed that the tissue influx of neutrophils and its accompanying tissue damage is strongly associated with the degree of luminal fluid accumulation and diarrhea. These data confirm the prevailing hypothesis that the *Salmonella*-associated diarrhea is primarily caused by a exudative inflammatory mechanism due to loss of mucosal integrity rather than by secretory mechanisms involving chloride secretion. We also found that the presence of tissue neutrophils also aid in the control of bacterial invasion, providing evidence that not only macrophages but also infiltrating neutrophils phagocytose and eliminate invading bacteria as part of the first line of host defense. Analysis of our cytokine profile data clearly demonstrated that the massive influx of neutrophils in the acute infection, especially at the late phase, is mainly driven by the chemokine GRO-α and to a lesser extent by IL-8. We also found the IL-8 can be highly expressed in the absence of neutrophil influx suggesting that infiltrating neutrophils are not significant sources of IL-8 gene expression. Our data also revealed that the influx of neutrophils likely plays a minor role in the expression of the pro-inflammatory cytokines IL-1β and TNF-α, although a tendency for lower expression of IL-1β in the absence of tissue neutrophils was found.

In Chapter III, we applied the Laser Capture Microdissection (LCM) technique to analyze BLAD ileal samples to better characterize the *in situ* localization of gene expression of the cytokines investigated in Chapter II. We showed that enterocytes of crypts, villi tips, and cells that form the domed villi overlying Peyer's patches, including the follicle-associated epithelium, are important sources of gene expression for IL-8, GRO-α, and IL-1β, but not TNF-α. Interestingly, all three detected cytokines were predominantly expressed in enterocytes of crypts. Also in the same Chapter, we investigated the pattern of *S. typhimurium* invasion in ileal loops from BLAD animals by using immunohistochemistry for *Salmonella* O antigen. Our results showed that *S. typhimurium,* in the absence of neutrophil influx, invade the tips of absorptive villi, follicle-associated epithelium of domed villi, and especially enterocytes lining basolateral villi.

Finally, in Chapter IV, we investigated the global temporal gene expression profiles of BLAD ileal tissues compared to normal calves by microarray technology using a custom 13K bovine-specific oligoarray. Analysis of microarray data was performed using the suite of gene expression analysis and modeling tools developed by Seralogix™. Analysis of our data revealed that intestinal infection is initially associated with pro-inflammatory gene expression, which is positively regulated by the mild influx of neutrophils seen at this early stage, yet is independent of Toll-like receptor (TLR) activation. After this initial stage, the TLR is activated along with several other pro-inflammatory genes. Interestingly, unlike the inflammatory genes, the TLR pathway was consistently

activated in BLAD indicating that TLR activation is not under influence of neutrophil influx, but instead, is triggered exclusively by bacterial invasion. In contrast, expression of inflammatory genes other than TLR-associated genes throughout the course of acute infection was highly dependent on the presence of neutrophils. Our data also indicated that this activation of inflammatory genes and the presence of tissue neutrophils in the initial stages of infection led to changes in gene expression the escape escaping of bacteria from innate and acquired immune systems, as demonstrated by down-regulation of genes that promote leukocyte endothelial transmigration and acquired immunity. Also, these data provided evidence that neutrophil influx is required for pro-inflammatory cytokine gene expression in the initial stages, whether by directing the expression of genes or by inducing their up-regulation in other cell types. Although neutrophils represent the vast majority of inflammatory cells during *Salmonella*-induced enteritis, our data indicated that up-regulation of major macrophage chemoattractants, which was independent of neutrophil influx. As an attempt to better characterize the cause for the tissue damage that occurs during the acute infection, we also analyzed the profile of apoptosis and oxidative stress-associated genes. Our microarray data on regulated cell death showed that *S. typhimurium,* in the absence of neutrophil influx predominantly induce gene changes that favor anti-apoptotic stimuli but the presence of neutrophils appeared to trigger apoptosis. Analysis of our data showed that activation of oxidative and nitrosative stress in both animal groups were markedly controlled

by the up-regulation of antioxidant genes regardless of the presence or absence of neutrophil influx.

In conclusion, the data presented in these *in vivo* experiments indicated that tissue influx of neutrophils that characterizes the enteritis in non-typhoidal ruminant and human salmonellosis represent significantly more than just a morphologic hallmark of the disease. We found that neutrophils greatly contribute to tissue damage and diarrhea, help to control bacterial invasion, and greatly influence and modulate host gene expression resulting in activation, maintenance, and propagation of a pro-inflammatory phenotype. While *in vitro* studies in polarized and non-polarized cells cultures have introduced indisputably valuable information on the pathogenesis of non-typhoidal salmonellosis, our investigations have clearly demonstrated that a function-based *in vivo* model capable of mounting an adequate neutrophilic response to infection is essential to understand the highly complex network of events that culminate in enteritis, tissue damage, and diarrhea. The results of these investigations will enhance our knowledge on the intertwined relationship of morphological and molecular pathogenesis of this important world wide enteric disease and most importantly provide information that can be used to reveal potential gene targets for novel therapeutic approaches.

REFERENCES

1. **Abrahams, G. L., and M. Hensel.** 2006. Manipulating cellular transport and immune responses: dynamic interactions between intracellular Salmonella enterica and its host cells. Cell Microbiol **8:**728-737.
2. **Ackermann, M. R., K. A. Brogden, A. F. Florance, and M. E. Kehrli, Jr.** 1999. Induction of CD18-mediated passage of neutrophils by Pasteurella haemolytica in pulmonary bronchi and bronchioles. Infect Immun **67:**659-663.
3. **Ackermann, M. R., M. E. Kehrli, Jr., and K. A. Brogden.** 1996. Passage of CD18- and CD18+ bovine neutrophils into pulmonary alveoli during acute Pasteurella haemolytica pneumonia. Vet Pathol **33:**639-646.
4. **Ackermann, M. R., M. E. Kehrli, Jr., H. K. Hawkins, J. L. Amenson, and J. E. Gallagher.** 1993. Identification of beta 2 integrins in bovine neutrophils by scanning electron microscopy in the backscatter mode and transmission electron microscopy. Vet Pathol **30:**296-298.
5. **Ackermann, M. R., M. E. Kehrli, Jr., J. A. Laufer, and L. T. Nusz.** 1996. Alimentary and respiratory tract lesions in eight medically fragile Holstein cattle with bovine leukocyte adhesion deficiency (BLAD). Vet Pathol **33:**273-281.
6. **Ackermann, M. R., M. E. Kehrli, Jr., and D. C. Morfitt.** 1993. Ventral dermatitis and vasculitis in a calf with bovine leukocyte adhesion deficiency. J Am Vet Med Assoc **202:**413-415.

7. **Agerholm, J. S., H. Houe, C. B. Jorgensen, and A. Basse.** 1993. Bovine leukocyte adhesion deficiency in Danish Holstein-Friesian cattle. II. Patho-anatomical description of affected calves. Acta Vet Scand **34:**237-243.

8. **Ahmer, B. M., J. van Reeuwijk, P. R. Watson, T. S. Wallis, and F. Heffron.** 1999. Salmonella SirA is a global regulator of genes mediating enteropathogenesis. Mol Microbiol **31:**971-982.

9. **Aleksunes, L. M., M. Goedken, and J. E. Manautou.** 2006. Up-regulation of NAD(P)H quinone oxidoreductase 1 during human liver injury. World J Gastroenterol **12:**1937-1940.

10. **Andrews-Polymenis, H. L., W. Rabsch, S. Porwollik, M. McClelland, C. Rosetti, L. G. Adams, and A. J. Baumler.** 2004. Host restriction of Salmonella enterica serotype Typhimurium pigeon isolates does not correlate with loss of discrete genes. J Bacteriol **186:**2619-2628.

11. **Arnaout, M. A.** 1990. Structure and function of the leukocyte adhesion molecules CD11/CD18. Blood **75:**1037-1050.

12. **Baggiolini, M., P. Loetscher, and B. Moser.** 1995. Interleukin-8 and the chemokine family. Int J Immunopharmacol **17:**103-108.

13. **Bankovich, A. J., S. Raunser, Z. S. Juo, T. Walz, M. M. Davis, and K. C. Garcia.** 2007. Structural insight into pre-B cell receptor function. Science **316:**291-294.

14. **Barthel, M., S. Hapfelmeier, L. Quintanilla-Martinez, M. Kremer, M. Rohde, M. Hogardt, K. Pfeffer, H. Russmann, and W. D. Hardt.** 2003.

Pretreatment of mice with streptomycin provides a Salmonella enterica serovar Typhimurium colitis model that allows analysis of both pathogen and host. Infect Immun **71:**2839-2858.

15. **Baumler, A. J., R. M. Tsolis, T. A. Ficht, and L. G. Adams.** 1998. Evolution of host adaptation in Salmonella enterica. Infect Immun **66:**4579-4587.

16. **Bergamini, C. M., S. Gambetti, A. Dondi, and C. Cervellati.** 2004. Oxygen, reactive oxygen species and tissue damage. Curr Pharm Des **10:**1611-1626.

17. **Biedzka-Sarek, M., and M. El Skurnik.** 2006. How to outwit the enemy: dendritic cells face Salmonella. Apmis **114:**589-600.

18. **Bonner, R. F., M. Emmert-Buck, K. Cole, T. Pohida, R. Chuaqui, S. Goldstein, and L. A. Liotta.** 1997. Laser capture microdissection: molecular analysis of tissue. Science **278:**1481,1483.

19. **Bortul, R., P. L. Tazzari, A. Cappellini, G. Tabellini, A. M. Billi, R. Bareggi, L. Manzoli, L. Cocco, and A. M. Martelli.** 2003. Constitutively active Akt1 protects HL60 leukemia cells from TRAIL-induced apoptosis through a mechanism involving NF-kappaB activation and cFLIP(L) up-regulation. Leukemia **17:**379-389.

20. **Boyen, F., F. Pasmans, F. Van Immerseel, E. Morgan, C. Adriaensen, J. P. Hernalsteens, A. Decostere, R. Ducatelle, and F. Haesebrouck.** 2006. Salmonella Typhimurium SPI-1 genes promote intestinal but not tonsillar colonization in pigs. Microbes Infect **8:**2899-2907.

21. **Boyle, E. C., J. L. Bishop, G. A. Grassl, and B. B. Finlay.** 2007. Salmonella: from pathogenesis to therapeutics. J Bacteriol **189:**1489-1495.

22. **Brenner, F. W., R. G. Villar, F. J. Angulo, R. Tauxe, and B. Swaminathan.** 2000. Salmonella nomenclature. J Clin Microbiol **38:**2465-2467.

23. **Cario, E., and D. K. Podolsky.** 2000. Differential alteration in intestinal epithelial cell expression of toll-like receptor 3 (TLR3) and TLR4 in inflammatory bowel disease. Infect Immun **68:**7010-7017.

24. **CDC.** 2005. Salmonella surveillance: annual summary, 2004. Atlanta, GA: US Department of Health and Human services, CDC.

25. **Chan, S. L., and V. C. Yu.** 2004. Proteins of the bcl-2 family in apoptosis signalling: from mechanistic insights to therapeutic opportunities. Clin Exp Pharmacol Physiol **31:**119-128.

26. **Cheminay, C., D. Chakravortty, and M. Hensel.** 2004. Role of neutrophils in murine salmonellosis. Infect Immun **72:**468-477.

27. **Chen, J. J., W. C. Huang, and C. C. Chen.** 2005. Transcriptional regulation of cyclooxygenase-2 in response to proteasome inhibitors involves reactive oxygen species-mediated signaling pathway and recruitment of CCAAT/enhancer-binding protein delta and CREB-binding protein. Mol Biol Cell **16:**5579-5591.

28. **Chen, Y. H., S. J. Lin, Y. L. Chen, P. L. Liu, and J. W. Chen.** 2006. Anti-inflammatory effects of different drugs/agents with antioxidant property on

endothelial expression of adhesion molecules. Cardiovasc Hematol Disord Drug Targets **6:**279-304.

29. **Chicoine, L. G., M. L. Paffett, T. L. Young, and L. D. Nelin.** 2004. Arginase inhibition increases nitric oxide production in bovine pulmonary arterial endothelial cells. Am J Physiol Lung Cell Mol Physiol **287:**L60-68.

30. **Clark, M. A., M. A. Jepson, N. L. Simmons, and B. H. Hirst.** 1994. Preferential interaction of Salmonella typhimurium with mouse Peyer's patch M cells. Res Microbiol **145:**543-552.

31. **Coburn, B., G. A. Grassl, and B. B. Finlay.** 2007. Salmonella, the host and disease: a brief review. Immunol Cell Biol **85:**112-118.

32. **Coombes, B. K., B. A. Coburn, A. A. Potter, S. Gomis, K. Mirakhur, Y. Li, and B. B. Finlay.** 2005. Analysis of the contribution of Salmonella pathogenicity islands 1 and 2 to enteric disease progression using a novel bovine ileal loop model and a murine model of infectious enterocolitis. Infect Immun **73:**7161-7169.

33. **Cox, E., J. Mast, N. MacHugh, B. Schwenger, and B. M. Goddeeris.** 1997. Expression of beta 2 integrins on blood leukocytes of cows with or without bovine leukocyte adhesion deficiency. Vet Immunol Immunopathol **58:**249-263.

34. **Crump, J. A., S. P. Luby, and E. D. Mintz.** 2004. The global burden of typhoid fever. Bull World Health Organ **82:**346-353.

35. **Dang, P. M., C. Elbim, J. C. Marie, M. Chiandotto, M. A. Gougerot-Pocidalo, and J. El-Benna.** 2006. Anti-inflammatory effect of interleukin-

10 on human neutrophil respiratory burst involves inhibition of GM-CSF-induced p47PHOX phosphorylation through a decrease in ERK1/2 activity. Faseb J **20:**1504-1506.

36. **De Groote, M. A., U. A. Ochsner, M. U. Shiloh, C. Nathan, J. M. McCord, M. C. Dinauer, S. J. Libby, A. Vazquez-Torres, Y. Xu, and F. C. Fang.** 1997. Periplasmic superoxide dismutase protects Salmonella from products of phagocyte NADPH-oxidase and nitric oxide synthase. Proc Natl Acad Sci U S A **94:**13997-14001.

37. **Delbridge, L. M., and M. X. O'Riordan.** 2007. Innate recognition of intracellular bacteria. Curr Opin Immunol **19:**10-16.

38. **Derouet-Humbert, E., K. Roemer, and M. Bureik.** 2005. Adrenodoxin (Adx) and CYP11A1 (P450scc) induce apoptosis by the generation of reactive oxygen species in mitochondria. Biol Chem **386:**453-461.

39. **Downey, G. P., L. Fialkow, and T. Fukushima.** 1995. Initial interaction of leukocytes within the microvasculature: deformability, adhesion, and transmigration. New Horiz **3:**219-228.

40. **Eckmann, L., J. Fierer, and M. F. Kagnoff.** 1996. Genetically resistant (Ityr) and susceptible (Itys) congenic mouse strains show similar cytokine responses following infection with Salmonella dublin. J Immunol **156:**2894-2900.

41. **Eckmann, L., and M. F. Kagnoff.** 2001. Cytokines in host defense against Salmonella. Microbes Infect **3:**1191-1200.

42. **Eckmann, L., M. F. Kagnoff, and J. Fierer.** 1993. Epithelial cells secrete the chemokine interleukin-8 in response to bacterial entry. Infect Immun **61:**4569-4574.

43. **Emmert-Buck, M. R., R. F. Bonner, P. D. Smith, R. F. Chuaqui, Z. Zhuang, S. R. Goldstein, R. A. Weiss, and L. A. Liotta.** 1996. Laser capture microdissection. Science **274:**998-1001.

44. **Espina, V., J. Milia, G. Wu, S. Cowherd, and L. A. Liotta.** 2006. Laser capture microdissection. Methods Mol Biol **319:**213-229.

45. **Everest, P., J. Ketley, S. Hardy, G. Douce, S. Khan, J. Shea, D. Holden, D. Maskell, and G. Dougan.** 1999. Evaluation of Salmonella typhimurium mutants in a model of experimental gastroenteritis. Infect Immun **67:**2815-2821.

46. **Everts, R. E., M. R. Band, Z. L. Liu, C. G. Kumar, L. Liu, J. J. Loor, R. Oliveira, and H. A. Lewin.** 2005. A 7872 cDNA microarray and its use in bovine functional genomics. Vet Immunol Immunopathol **105:**235-245.

47. **Forshell, L. P., and M. Wierup.** 2006. Salmonella contamination: a significant challenge to the global marketing of animal food products. Rev Sci Tech **25:**541-554.

48. **Fegan, N., P. Vanderlinde, G. Higgs, and P. Desmarchelier.** 2004. Quantification and prevalence of Salmonella in beef cattle presenting at slaughter. J Appl Microbiol **97:**892-898.

49. **Fend, F., and M. Raffeld.** 2000. Laser capture microdissection in pathology. J Clin Pathol **53:**666-672.

50. **Fields, P. I., E. A. Groisman, and F. Heffron.** 1989. A Salmonella locus that controls resistance to microbicidal proteins from phagocytic cells. Science **243:**1059-1062.

51. **Finlay, B. B., and J. H. Brumell.** 2000. Salmonella interactions with host cells: in vitro to in vivo. Philos Trans R Soc Lond B Biol Sci **355:**623-631.

52. **Francis, C. L., T. A. Ryan, B. D. Jones, S. J. Smith, and S. Falkow.** 1993. Ruffles induced by Salmonella and other stimuli direct macropinocytosis of bacteria. Nature **364:**639-642.

53. **Freeman, J. A., M. E. Ohl, and S. I. Miller.** 2003. The Salmonella enterica serovar typhimurium translocated effectors SseJ and SifB are targeted to the Salmonella-containing vacuole. Infect Immun **71:**418-427.

54. **Frost, A. J., A. P. Bland, and T. S. Wallis.** 1997. The early dynamic response of the calf ileal epithelium to Salmonella typhimurium. Vet Pathol **34:**369-386.

55. **Gahmberg, C. G.** 1997. Leukocyte adhesion: CD11/CD18 integrins and intercellular adhesion molecules. Curr Opin Cell Biol **9:**643-650.

56. **Galan, J. E.** 1999. Interaction of Salmonella with host cells through the centisome 63 type III secretion system. Curr Opin Microbiol **2:**46-50.

57. **Galan, J. E.** 2001. Salmonella interactions with host cells: type III secretion at work. Annu Rev Cell Dev Biol **17:**53-86.

58. **Galan, J. E., and H. Wolf-Watz.** 2006. Protein delivery into eukaryotic cells by type III secretion machines. Nature **444:**567-573.

59. **Galanis, E., D. M. Lo Fo Wong, M. E. Patrick, N. Binsztein, A. Cieslik, T. Chalermchikit, A. Aidara-Kane, A. Ellis, F. J. Angulo, and H. C. Wegener.** 2006. Web-based surveillance and global Salmonella distribution, 2000-2002. Emerg Infect Dis **12:**381-388.

60. **Galyov, E. E., M. W. Wood, R. Rosqvist, P. B. Mullan, P. R. Watson, S. Hedges, and T. S. Wallis.** 1997. A secreted effector protein of Salmonella dublin is translocated into eukaryotic cells and mediates inflammation and fluid secretion in infected ileal mucosa. Mol Microbiol **25:**903-912.

61. **Garcia-del Portillo, F., and B. B. Finlay.** 1994. Salmonella invasion of nonphagocytic cells induces formation of macropinosomes in the host cell. Infect Immun **62:**4641-4645.

62. **Gerardi, A. S.** 1996. Bovine leukocyte adhesion deficiency: a brief overview of a modern disease and its implications. Acta Vet Hung **44:**1-8.

63. **Gerner-Smidt, P., and J. M. Whichard.** 2007. Foodborne disease trends and reports. Foodborne Pathog Dis **4:**1-4.

64. **Gerold, G., A. Zychlinsky, and J. L. de Diego.** 2007. What is the role of toll-like receptors in bacterial infections? Semin Immunol **19:**41-47.

65. **Gewirtz, A. T., T. A. Navas, S. Lyons, P. J. Godowski, and J. L. Madara.** 2001. Cutting edge: bacterial flagellin activates basolaterally expressed TLR5 to induce epithelial proinflammatory gene expression. J Immunol **167:**1882-1885.

66. **Gewirtz, A. T., P. O. Simon, Jr., C. K. Schmitt, L. J. Taylor, C. H. Hagedorn, A. D. O'Brien, A. S. Neish, and J. L. Madara.** 2001.

Salmonella typhimurium translocates flagellin across intestinal epithelia, inducing a proinflammatory response. J Clin Invest **107:**99-109.

67. **Giannella, R. A., S. B. Formal, G. J. Dammin, and H. Collins.** 1973. Pathogenesis of salmonellosis. Studies of fluid secretion, mucosal invasion, and morphologic reaction in the rabbit ileum. J Clin Invest **52:**441-453.

68. **Gilbert, R. O., W. C. Rebhun, C. A. Kim, M. E. Kehrli, Jr., D. E. Shuster, and M. R. Ackermann.** 1993. Clinical manifestations of leukocyte adhesion deficiency in cattle: 14 cases (1977-1991). J Am Vet Med Assoc **202:**445-449.

69. **Giltnane, J. M., and D. L. Rimm.** 2004. Technology insight: Identification of biomarkers with tissue microarray technology. Nat Clin Pract Oncol **1:**104-111.

70. **Gopinath, R. S., A. P. Ambagala, T. C. Ambagala, W. Liu, and S. Srikumaran.** 2006. Molecular cloning and characterization of cDNA encoding CD11b of cattle. Vet Immunol Immunopathol **110:**349-355.

71. **Gu, Y. C., T. R. Bauer, Jr., M. R. Ackermann, C. W. Smith, M. E. Kehrli, Jr., M. F. Starost, and D. D. Hickstein.** 2004. The genetic immunodeficiency disease, leukocyte adhesion deficiency, in humans, dogs, cattle, and mice. Comp Med **54:**363-372.

72. **Guiney, D. G.** 2005. The role of host cell death in Salmonella infections. Curr Top Microbiol Immunol **289:**131-150.

73. **Guiney, D. G., and M. Lesnick.** 2005. Targeting of the actin cytoskeleton during infection by Salmonella strains. Clin Immunol **114:**248-255.

74. **Hagemoser, W. A., J. A. Roth, J. Lofstedt, and J. A. Fagerland.** 1983. Granulocytopathy in a Holstein heifer. J Am Vet Med Assoc **183:**1093-1094.

75. **Hansen-Wester, I., and M. Hensel.** 2001. Salmonella pathogenicity islands encoding type III secretion systems. Microbes Infect **3:**549-559.

76. **Hapfelmeier, S., K. Ehrbar, B. Stecher, M. Barthel, M. Kremer, and W. D. Hardt.** 2004. Role of the Salmonella pathogenicity island 1 effector proteins SipA, SopB, SopE, and SopE2 in Salmonella enterica subspecies 1 serovar Typhimurium colitis in streptomycin-pretreated mice. Infect Immun **72:**795-809.

77. **Hapfelmeier, S., and W. D. Hardt.** 2005. A mouse model for S. typhimurium-induced enterocolitis. Trends Microbiol **13:**497-503.

78. **Haque, A., F. Bowe, R. J. Fitzhenry, G. Frankel, M. Thomson, R. Heuschkel, S. Murch, M. P. Stevens, T. S. Wallis, A. D. Phillips, and G. Dougan.** 2004. Early interactions of Salmonella enterica serovar typhimurium with human small intestinal epithelial explants. Gut **53:**1424-1430.

79. **Hayashi, F., K. D. Smith, A. Ozinsky, T. R. Hawn, E. C. Yi, D. R. Goodlett, J. K. Eng, S. Akira, D. M. Underhill, and A. Aderem.** 2001. The innate immune response to bacterial flagellin is mediated by toll-like receptor 5. Nature **410:**1099-1103.

80. **Hensel, M.** 2004. Evolution of pathogenicity islands of Salmonella enterica. Int J Med Microbiol **294:**95-102.

81. **Hernandez, L. D., K. Hueffer, M. R. Wenk, and J. E. Galan.** 2004. Salmonella modulates vesicular traffic by altering phosphoinositide metabolism. Science **304:**1805-1807.

82. **Hersh, D., D. M. Monack, M. R. Smith, N. Ghori, S. Falkow, and A. Zychlinsky.** 1999. The Salmonella invasin SipB induces macrophage apoptosis by binding to caspase-1. Proc Natl Acad Sci U S A **96:**2396-2401.

83. **Hilfiker-Kleiner, D., A. Hilfiker, K. Kaminski, A. Schaefer, J. K. Park, K. Michel, A. Quint, M. Yaniv, J. B. Weitzman, and H. Drexler.** 2005. Lack of JunD promotes pressure overload-induced apoptosis, hypertrophic growth, and angiogenesis in the heart. Circulation **112:**1470-1477.

84. **Hinton, M. H.** 1973. Salmonella dublin abortion in cattle. Vet Rec **93:**162.

85. **Hobbie, S., L. M. Chen, R. J. Davis, and J. E. Galan.** 1997. Involvement of mitogen-activated protein kinase pathways in the nuclear responses and cytokine production induced by Salmonella typhimurium in cultured intestinal epithelial cells. J Immunol **159:**5550-5559.

86. **Hohmann, E. L.** 2001. Nontyphoidal salmonellosis. Clin Infect Dis **32:**263-269.

87. **Hopkins, R. S., R. A. Jajosky, P. A. Hall, D. A. Adams, F. J. Connor, P. Sharp, W. J. Anderson, R. F. Fagan, J. J. Aponte, D. A. Nitschke, C. A.**

Worsham, N. Adekoya, and M. H. Chang. 2005. Summary of notifiable diseases--United States, 2003. MMWR Morb Mortal Wkly Rep **52:**1-85.

88. **Huang, F. C., A. Werne, Q. Li, E. E. Galyov, W. A. Walker, and B. J. Cherayil.** 2004. Cooperative interactions between flagellin and SopE2 in the epithelial interleukin-8 response to Salmonella enterica serovar typhimurium infection. Infect Immun **72:**5052-5062.

89. **Hueck, C. J.** 1998. Type III protein secretion systems in bacterial pathogens of animals and plants. Microbiol Mol Biol Rev **62:**379-433.

90. **Hughes, L. E., E. A. Gibson, H. E. Roberts, E. T. Davies, G. Davies, and W. J. Sojka.** 1971. Bovine salmonellosis in England and Wales. Br Vet J **127:**225-238.

91. **Humphries, A. D., M. Raffatellu, S. Winter, E. H. Weening, R. A. Kingsley, R. Droleskey, S. Zhang, J. Figueiredo, S. Khare, J. Nunes, L. G. Adams, R. M. Tsolis, and A. J. Baumler.** 2003. The use of flow cytometry to detect expression of subunits encoded by 11 Salmonella enterica serotype Typhimurium fimbrial operons. Mol Microbiol **48:**1357-1376.

92. **Hurley, B. P., and B. A. McCormick.** 2003. Translating tissue culture results into animal models: the case of Salmonella typhimurium. Trends Microbiol **11:**562-569.

93. **Jachak, S. M.** 2007. PGE synthase inhibitors as an alternative to COX-2 inhibitors. Curr Opin Investig Drugs **8:**411-415.

94. **Jarvelainen, H. A., A. Galmiche, and A. Zychlinsky.** 2003. Caspase-1 activation by Salmonella. Trends Cell Biol **13:**204-209.

95. **Jones, B. D., N. Ghori, and S. Falkow.** 1994. Salmonella typhimurium initiates murine infection by penetrating and destroying the specialized epithelial M cells of the Peyer's patches. J Exp Med **180:**15-23.

96. **Jones, M. A., M. W. Wood, P. B. Mullan, P. R. Watson, T. S. Wallis, and E. E. Galyov.** 1998. Secreted effector proteins of Salmonella dublin act in concert to induce enteritis. Infect Immun **66:**5799-5804.

97. **Jung, H. C., L. Eckmann, S. K. Yang, A. Panja, J. Fierer, E. Morzycka-Wroblewska, and M. F. Kagnoff.** 1995. A distinct array of proinflammatory cytokines is expressed in human colon epithelial cells in response to bacterial invasion. J Clin Invest **95:**55-65.

98. **Kehrli, M. E., Jr., M. R. Ackermann, D. E. Shuster, M. J. van der Maaten, F. C. Schmalstieg, D. C. Anderson, and B. J. Hughes.** 1992. Bovine leukocyte adhesion deficiency. Beta 2 integrin deficiency in young Holstein cattle. Am J Pathol **140:**1489-1492.

99. **Kehrli, M. E., Jr., F. C. Schmalstieg, D. C. Anderson, M. J. Van der Maaten, B. J. Hughes, M. R. Ackermann, C. L. Wilhelmsen, G. B. Brown, M. G. Stevens, and C. A. Whetstone.** 1990. Molecular definition of the bovine granulocytopathy syndrome: identification of deficiency of the Mac-1 (CD11b/CD18) glycoprotein. Am J Vet Res **51:**1826-1836.

100. **Kehrli, M. E., Jr., D. E. Shuster, and M. R. Ackermann.** 1992. Leukocyte adhesion deficiency among Holstein cattle. Cornell Vet **82:**103-109.

101. **Kiama, S. G., D. Dreher, L. Cochand, M. Kok, C. Obregon, L. Nicod, and P. Gehr.** 2006. Host cell responses of Salmonella typhimurium infected human dendritic cells. Immunol Cell Biol **84:**475-481.

102. **Klimpel, G. R., M. Asuncion, J. Haithcoat, and D. W. Niesel.** 1995. Cholera toxin and Salmonella typhimurium induce different cytokine profiles in the gastrointestinal tract. Infect Immun **63:**1134-1137.

103. **Knodler, L. A., and B. B. Finlay.** 2001. Salmonella and apoptosis: to live or let die? Microbes Infect **3:**1321-1326.

104. **Kuai, J., E. Nickbarg, J. Wooters, Y. Qiu, J. Wang, and L. L. Lin.** 2003. Endogenous association of TRAF2, TRAF3, cIAP1, and Smac with lymphotoxin beta receptor reveals a novel mechanism of apoptosis. J Biol Chem **278:**14363-14369.

105. **Kubori, T., A. Sukhan, S. I. Aizawa, and J. E. Galan.** 2000. Molecular characterization and assembly of the needle complex of the Salmonella typhimurium type III protein secretion system. Proc Natl Acad Sci U S A **97:**10225-10230.

106. **Kuhle, V., and M. Hensel.** 2004. Cellular microbiology of intracellular Salmonella enterica: functions of the type III secretion system encoded by Salmonella pathogenicity island 2. Cell Mol Life Sci **61:**2812-2826.

107. **Lee, C. A., M. Silva, A. M. Siber, A. J. Kelly, E. Galyov, and B. A. McCormick.** 2000. A secreted Salmonella protein induces a proinflammatory response in epithelial cells, which promotes neutrophil migration. Proc Natl Acad Sci U S A **97:**12283-12288.

108. **Livak, K. J., and T. D. Schmittgen.** 2001. Analysis of relative gene expression data using real-time quantitative PCR and the 2(-Delta Delta C(T)) Method. Methods **25:**402-408.

109. **Lundberg, U., U. Vinatzer, D. Berdnik, A. von Gabain, and M. Baccarini.** 1999. Growth phase-regulated induction of Salmonella-induced macrophage apoptosis correlates with transient expression of SPI-1 genes. J Bacteriol **181:**3433-3437.

110. **Luster, A. D.** 1998. Chemokines--chemotactic cytokines that mediate inflammation. N Engl J Med **338:**436-445.

111. **Ly, K. T., and J. E. Casanova.** 2007. Mechanisms of Salmonella entry into host cells. Cell Microbiol **9:**2103-2111.

112. **Madara, J. L., T. W. Patapoff, B. Gillece-Castro, S. P. Colgan, C. A. Parkos, C. Delp, and R. J. Mrsny.** 1993. 5'-adenosine monophosphate is the neutrophil-derived paracrine factor that elicits chloride secretion from T84 intestinal epithelial cell monolayers. J Clin Invest **91:**2320-2325.

113. **Manger, I. D., and D. A. Relman.** 2000. How the host 'sees' pathogens: global gene expression responses to infection. Curr Opin Immunol **12:**215-218.

114. **Marlovits, T. C., T. Kubori, A. Sukhan, D. R. Thomas, J. E. Galan, and V. M. Unger.** 2004. Structural insights into the assembly of the type III secretion needle complex. Science **306:**1040-1042.

115. **Martindale, J. L., and N. J. Holbrook.** 2002. Cellular response to oxidative stress: signaling for suicide and survival. J Cell Physiol **192:**1-15.

116. **Mastroeni, P., and N. Menager.** 2003. Development of acquired immunity to Salmonella. J Med Microbiol **52:**453-459.

117. **Mastroeni, P., A. Vazquez-Torres, F. C. Fang, Y. Xu, S. Khan, C. E. Hormaeche, and G. Dougan.** 2000. Antimicrobial actions of the NADPH phagocyte oxidase and inducible nitric oxide synthase in experimental salmonellosis. II. Effects on microbial proliferation and host survival in vivo. J Exp Med **192:**237-248.

118. **McCormick, B. A., S. P. Colgan, C. Delp-Archer, S. I. Miller, and J. L. Madara.** 1993. Salmonella typhimurium attachment to human intestinal epithelial monolayers: transcellular signalling to subepithelial neutrophils. J Cell Biol **123:**895-907.

119. **McCormick, B. A., P. M. Hofman, J. Kim, D. K. Carnes, S. I. Miller, and J. L. Madara.** 1995. Surface attachment of Salmonella typhimurium to intestinal epithelia imprints the subepithelial matrix with gradients chemotactic for neutrophils. J Cell Biol **131:**1599-1608.

120. **McCormick, B. A., C. A. Parkos, S. P. Colgan, D. K. Carnes, and J. L. Madara.** 1998. Apical secretion of a pathogen-elicited epithelial chemoattractant activity in response to surface colonization of intestinal epithelia by Salmonella typhimurium. J Immunol **160:**455-466.

121. **Mead, P. S., L. Slutsker, V. Dietz, L. F. McCaig, J. S. Bresee, C. Shapiro, P. M. Griffin, and R. V. Tauxe.** 1999. Food-related illness and death in the United States. Emerg Infect Dis **5:**607-625.

122. **Mehta, A., S. Singh, and N. K. Ganguly.** 1998. Role of reactive oxygen species in Salmonella typhimurium-induced enterocyte damage. Scand J Gastroenterol **33:**406-414.

123. **Meyerholz, D. K., and T. J. Stabel.** 2003. Comparison of early ileal invasion by Salmonella enterica serovars Choleraesuis and Typhimurium. Vet Pathol **40:**371-375.

124. **Meyerholz, D. K., T. J. Stabel, M. R. Ackermann, S. A. Carlson, B. D. Jones, and J. Pohlenz.** 2002. Early epithelial invasion by Salmonella enterica serovar Typhimurium DT104 in the swine ileum. Vet Pathol **39:**712-720.

125. **Mikulowska-Mennis, A., T. B. Taylor, P. Vishnu, S. A. Michie, R. Raja, N. Horner, and S. T. Kunitake.** 2002. High-quality RNA from cells isolated by laser capture microdissection. Biotechniques **33:**176-179.

126. **Minguet, S., M. Swamy, B. Alarcon, I. F. Luescher, and W. W. Schamel.** 2007. Full activation of the T cell receptor requires both clustering and conformational changes at CD3. Immunity **26:**43-54.

127. **Mirck, M. H., T. Von Bannisseht-Wijsmuller, W. J. Timmermans-Besselink, J. H. Van Luijk, J. B. Buntjer, and J. A. Lenstra.** 1995. Optimization of the PCR test for the mutation causing bovine leukocyte adhesion deficiency. Cell Mol Biol (Noisy-le-grand) **41:**695-698.

128. **Morgan, E.** 2007. *Salmonella* Pathonenicty Islands, p. 67-88. *In* M. Rhen, D. Maskell, P. Mastroeni, and J. Threlfall (ed.), *Salmonella*: Molecular Biology and Pathogenesis. Horizon Bioscience, Norfolk, UK.

129. **Mrsny, R. J., A. T. Gewirtz, D. Siccardi, T. Savidge, B. P. Hurley, J. L. Madara, and B. A. McCormick.** 2004. Identification of hepoxilin A3 in inflammatory events: a required role in neutrophil migration across intestinal epithelia. Proc Natl Acad Sci U S A **101:**7421-7426.

130. **Muller, K. E., W. E. Bernadina, H. C. Kalsbeek, A. Hoek, V. P. Rutten, and G. H. Wentink.** 1994. Bovine leukocyte adhesion deficiency--clinical course and laboratory findings in eight affected animals. Vet Q **16:**65-71.

131. **Muller, K. E., A. Hoek, V. P. Rutten, W. E. Bernadina, and G. H. Wentink.** 1997. Antigen-specific immune responses in cattle with inherited beta2-integrin deficiency. Vet Immunol Immunopathol **58:**39-53.

132. **Nagahata, H.** 2004. Bovine leukocyte adhesion deficiency (BLAD): a review. J Vet Med Sci **66:**1475-1482.

133. **Nagahata, H., K. Hatakeyama, Y. Izumisawa, H. Noda, H. Nochi, and K. Tamoto.** 1994. Two cases of Holstein calves with bovine leukocyte adhesion deficiency (BLAD) (case report). Dtsch Tierarztl Wochenschr **101:**53-56.

134. **Nagahata, H., H. Higuchi, N. Yamashiki, and M. Yamaguchi.** 2000. Analysis of the functional characteristics of L-selectin and its expression on normal and CD18-deficient bovine neutrophils. Immunol Cell Biol **78:**264-271.

135. **Nagahata, H., M. E. Kehrli, Jr., H. Murata, H. Okada, H. Noda, and G. J. Kociba.** 1994. Neurtrophil function and pathologic findings in Holstein calves with leukocyte adhesion deficiency. Am J Vet Res **55:**40-48.

136. **Nagahata, H., A. Masuyama, M. Masue, M. Yuki, H. Higuchi, H. Ohtsuka, T. Kurosawa, H. Sato, and H. Noda.** 1997. Leukocyte emigration in normal calves and calves with leukocyte adhesion deficiency. J Vet Med Sci **59:**1143-1147.

137. **Nagahata, H., H. Nochi, Y. Sanada, K. Tamoto, H. Noda, and G. J. Kociba.** 1994. Analysis of mononuclear cell functions in Holstein cattle with leukocyte adhesion deficiency. Am J Vet Res **55:**1101-1106.

138. **Nagahata, H., H. Noda, K. Takahashi, T. Kurosawa, and M. Sonoda.** 1987. A suspected case of neutrophil dysfunction in a Holstein heifer. Nippon Juigaku Zasshi **49:**1165-1167.

139. **Nagahata, H., H. Noda, K. Takahashi, T. Kurosawa, and M. Sonoda.** 1987. Bovine granulocytopathy syndrome: neutrophil dysfunction in Holstein Friesian calves. Zentralbl Veterinarmed A **34:**445-451.

140. **Nakajima, K., H. Hirose, M. Taniguchi, H. Kurashina, K. Arasaki, M. Nagahama, K. Tani, A. Yamamoto, and M. Tagaya.** 2004. Involvement of BNIP1 in apoptosis and endoplasmic reticulum membrane fusion. Embo J **23:**3216-3226.

141. **Nau, G. J., J. F. Richmond, A. Schlesinger, E. G. Jennings, E. S. Lander, and R. A. Young.** 2002. Human macrophage activation programs induced by bacterial pathogens. Proc Natl Acad Sci U S A **99:**1503-1508.

142. **Norris, F. A., M. P. Wilson, T. S. Wallis, E. E. Galyov, and P. W. Majerus.** 1998. SopB, a protein required for virulence of Salmonella

dublin, is an inositol phosphate phosphatase. Proc Natl Acad Sci U S A **95:**14057-14059.

143. **Pang, T., Z. A. Bhutta, B. B. Finlay, and M. Altwegg.** 1995. Typhoid fever and other salmonellosis: a continuing challenge. Trends Microbiol **3:**253-255.

144. **Patel, J. C., and J. E. Galan.** 2006. Differential activation and function of Rho GTPases during Salmonella-host cell interactions. J Cell Biol **175:**453-463.

145. **Patel, J. C., and J. E. Galan.** 2005. Manipulation of the host actin cytoskeleton by Salmonella--all in the name of entry. Curr Opin Microbiol **8:**10-15.

146. **Patel, R. K., K. M. Singh, K. J. Soni, J. B. Chauhan, and K. R. S. Rao.** 2007. Low incidence of bovine leukocyte adhesion deficiency (BLAD) carriers in Indian cattle and buffalo breeds. J Appl Genet **48:**153-155.

147. **Penheiter, K. L., N. Mathur, D. Giles, T. Fahlen, and B. D. Jones.** 1997. Non-invasive Salmonella typhimurium mutants are avirulent because of an inability to enter and destroy M cells of ileal Peyer's patches. Mol Microbiol **24:**697-709.

148. **Rabsch, W., H. Tschape, and A. J. Baumler.** 2001. Non-typhoidal salmonellosis: emerging problems. Microbes Infect **3:**237-247.

149. **Raffatellu, M., C. Tukel, D. Chessa, R. P. Wilson, and A. J. Baumler.** 2007. The intestinal phase of *Salmonella* infections, p. 31-51. *In* M. Rhen,

D. Maskell, P. Mastroeni, and J. Threlfall (ed.), *Salmonella*: Molecular Biology and Pathogenesis. Horizon Bioscience, Norfolk, UK.

150. **Raffatellu, M., R. P. Wilson, D. Chessa, H. Andrews-Polymenis, Q. T. Tran, S. Lawhon, S. Khare, L. G. Adams, and A. J. Baumler.** 2005. SipA, SopA, SopB, SopD, and SopE2 contribute to Salmonella enterica serotype typhimurium invasion of epithelial cells. Infect Immun **73:**146-154.

151. **Rakkola, R., S. Matikainen, and T. A. Nyman.** 2007. Proteome analysis of human macrophages reveals the upregulation of manganese-containing superoxide dismutase after toll-like receptor activation. Proteomics **7:**378-384.

152. **Rao, R. M., S. K. Shaw, M. Kim, and F. W. Luscinskas.** 2005. Emerging topics in the regulation of leukocyte transendothelial migration. Microcirculation **12:**83-89.

153. **Rezaei, N.** 2006. TNF-receptor-associated periodic syndrome (TRAPS): an autosomal dominant multisystem disorder. Clin Rheumatol **25:**773-777.

154. **Rings, D. M.** 1985. Salmonellosis in calves. Vet Clin North Am Food Anim Pract **1:**529-539.

155. **Rosenberger, C. M., M. G. Scott, M. R. Gold, R. E. Hancock, and B. B. Finlay.** 2000. Salmonella typhimurium infection and lipopolysaccharide stimulation induce similar changes in macrophage gene expression. J Immunol **164:**5894-5904.

156. **Rottner, K., S. Lommel, J. Wehland, and T. E. Stradal.** 2004. Pathogen-induced actin filament rearrangement in infectious diseases. J Pathol **204:**396-406.

157. **Sansonetti, P. J., J. Arondel, M. Huerre, A. Harada, and K. Matsushima.** 1999. Interleukin-8 controls bacterial transepithelial translocation at the cost of epithelial destruction in experimental shigellosis. Infect Immun **67:**1471-1480.

158. **Santos, R. L., and A. J. Baumler.** 2004. Cell tropism of Salmonella enterica. Int J Med Microbiol **294:**225-233.

159. **Santos, R. L., J. A. Schoffelmeer, R. M. Tsolis, J. A. Gutierrez-Pabello, A. J. Baumler, and L. G. Adams.** 2002. Salmonella serotype Typhimurium infection of bovine Peyer's patches down-regulates plasma membrane calcium-transporting ATPase expression. J Infect Dis **186:**372-378.

160. **Santos, R. L., R. M. Tsolis, A. J. Baumler, and L. G. Adams.** 2002. Hematologic and serum biochemical changes in Salmonella ser Typhimurium-infected calves. Am J Vet Res **63:**1145-1150.

161. **Santos, R. L., R. M. Tsolis, A. J. Baumler, and L. G. Adams.** 2003. Pathogenesis of Salmonella-induced enteritis. Braz J Med Biol Res **36:**3-12.

162. **Santos, R. L., R. M. Tsolis, A. J. Baumler, R. Smith III, and L. G. Adams.** 2001. Salmonella enterica serovar typhimurium induces cell

death in bovine monocyte-derived macrophages by early sipB-dependent and delayed sipB-independent mechanisms. Infect Immun **69:**2293-2301.

163. **Santos, R. L., R. M. Tsolis, S. Zhang, T. A. Ficht, A. J. Baumler, and L. G. Adams.** 2001. Salmonella-induced cell death is not required for enteritis in calves. Infect Immun **69:**4610-4617.

164. **Santos, R. L., S. Zhang, R. M. Tsolis, A. J. Baumler, and L. G. Adams.** 2002. Morphologic and molecular characterization of Salmonella typhimurium infection in neonatal calves. Vet Pathol **39:**200-215.

165. **Santos, R. L., S. Zhang, R. M. Tsolis, R. A. Kingsley, L. G. Adams, and A. J. Baumler.** 2001. Animal models of Salmonella infections: enteritis versus typhoid fever. Microbes Infect **3:**1335-1344.

166. **Schesser, K., J. M. Dukuzumuremyi, C. Cilio, S. Borg, T. S. Wallis, S. Pettersson, and E. E. Galyov.** 2000. The Salmonella YopJ-homologue AvrA does not possess YopJ-like activity. Microb Pathog **28:**59-70.

167. **Schmitt, C. K., J. S. Ikeda, S. C. Darnell, P. R. Watson, J. Bispham, T. S. Wallis, D. L. Weinstein, E. S. Metcalf, and A. D. O'Brien.** 2001. Absence of all components of the flagellar export and synthesis machinery differentially alters virulence of Salmonella enterica serovar Typhimurium in models of typhoid fever, survival in macrophages, tissue culture invasiveness, and calf enterocolitis. Infect Immun **69:**5619-5625.

168. **Seidel, G. E., Jr.** 1981. Superovulation and embryo transfer in cattle. Science **211:**351-358.

169. **Shiloh, M. U., J. D. MacMicking, S. Nicholson, J. E. Brause, S. Potter, M. Marino, F. Fang, M. Dinauer, and C. Nathan.** 1999. Phenotype of mice and macrophages deficient in both phagocyte oxidase and inducible nitric oxide synthase. Immunity **10:**29-38.

170. **Shoshani, T., A. Faerman, I. Mett, E. Zelin, T. Tenne, S. Gorodin, Y. Moshel, S. Elbaz, A. Budanov, A. Chajut, H. Kalinski, I. Kamer, A. Rozen, O. Mor, E. Keshet, D. Leshkowitz, P. Einat, R. Skaliter, and E. Feinstein.** 2002. Identification of a novel hypoxia-inducible factor 1-responsive gene, RTP801, involved in apoptosis. Mol Cell Biol **22:**2283-2293.

171. **Shuster, D. E., M. E. Kehrli, Jr., M. R. Ackermann, and R. O. Gilbert.** 1992. Identification and prevalence of a genetic defect that causes leukocyte adhesion deficiency in Holstein cattle. Proc Natl Acad Sci U S A **89:**9225-9229.

172. **Sipes, K. M., H. A. Edens, M. E. Kehrli, Jr., H. M. Miettinen, J. E. Cutler, M. A. Jutila, and M. T. Quinn.** 1999. Analysis of surface antigen expression and host defense function in leukocytes from calves heterozygous or homozygous for bovine leukocyte adhesion deficiency. Am J Vet Res **60:**1255-1261.

173. **Siu, P. M., R. W. Bryner, Z. Murlasits, and S. E. Alway.** 2005. Response of XIAP, ARC, and FLIP apoptotic suppressors to 8 wk of treadmill running in rat heart and skeletal muscle. J Appl Physiol **99:**204-209.

174. **Smith, B. P., L. Da Roden, M. C. Thurmond, G. W. Dilling, H. Konrad, J. A. Pelton, and J. P. Picanso.** 1994. Prevalence of salmonellae in cattle and in the environment on California dairies. J Am Vet Med Assoc **205:**467-471.

175. **Song, G., G. Ouyang, and S. Bao.** 2005. The activation of Akt/PKB signaling pathway and cell survival. J Cell Mol Med **9:**59-71.

176. **Springer, T. A.** 1990. Adhesion receptors of the immune system. Nature **346:**425-434.

177. **Srikanth, C. V., and B. J. Cherayil.** 2007. Intestinal innate immunity and the pathogenesis of salmonella enteritis. Immunol Res **37:**61-78.

178. **Stojiljkovic, I., A. J. Baumler, and F. Heffron.** 1995. Ethanolamine utilization in Salmonella typhimurium: nucleotide sequence, protein expression, and mutational analysis of the cchA cchB eutE eutJ eutG eutH gene cluster. J Bacteriol **177:**1357-1366.

179. **Sun, J., P. E. Fegan, A. S. Desai, J. L. Madara, and M. E. Hobert.** 2007. Flagellin-induced tolerance of the Toll-like receptor 5 signaling pathway in polarized intestinal epithelial cells. Am J Physiol Gastrointest Liver Physiol **292:**G767-778.

180. **Swaminathan, B., P. Gerner-Smidt, and T. Barrett.** 2006. Focus on Salmonella. Foodborne Pathog Dis **3:**154-156.

181. **Tajima, M., M. Irie, R. Kirisawa, K. Hagiwara, T. Kurosawa, and K. Takahashi.** 1993. The detection of a mutation of CD18 gene in bovine leukocyte adhesion deficiency (BLAD). J Vet Med Sci **55:**145-146.

182. **Takahashi, K., K. Miyagawa, S. Abe, T. Kurosawa, M. Sonoda, T. Nakade, H. Nagahata, H. Noda, Y. Chihaya, and E. Isogai.** 1987. Bovine granulocytopathy syndrome of Holstein-Friesian calves and heifers. Nippon Juigaku Zasshi **49:**733-736.

183. **Tallant, T., A. Deb, N. Kar, J. Lupica, M. J. de Veer, and J. A. DiDonato.** 2004. Flagellin acting via TLR5 is the major activator of key signaling pathways leading to NF-kappa B and proinflammatory gene program activation in intestinal epithelial cells. BMC Microbiol **4:**33.

184. **Tammen, I., H. Klippert, A. Kuczka, A. Treviranus, J. Pohlenz, M. Stober, D. Simon, and B. Harlizius.** 1996. An improved DNA test for bovine leucocyte adhesion deficiency. Res Vet Sci **60:**218-221.

185. **Tobar, J. A., L. J. Carreno, S. M. Bueno, P. A. Gonzalez, J. E. Mora, S. A. Quezada, and A. M. Kalergis.** 2006. Virulent Salmonella enterica serovar typhimurium evades adaptive immunity by preventing dendritic cells from activating T cells. Infect Immun **74:**6438-6448.

186. **Trigona, W. L., I. K. Mullarky, Y. Cao, and L. M. Sordillo.** 2006. Thioredoxin reductase regulates the induction of haem oxygenase-1 expression in aortic endothelial cells. Biochem J **394:**207-216.

187. **Tsolis, R. M., L. G. Adams, T. A. Ficht, and A. J. Baumler.** 1999. Contribution of Salmonella typhimurium virulence factors to diarrheal disease in calves. Infect Immun **67:**4879-4885.

188. **Tsolis, R. M., L. G. Adams, M. J. Hantman, C. A. Scherer, T. Kimbrough, R. A. Kingsley, T. A. Ficht, S. I. Miller, and A. J. Baumler.**

2000. SspA is required for lethal Salmonella enterica serovar Typhimurium infections in calves but is not essential for diarrhea. Infect Immun **68:**3158-3163.

189. **Tsolis, R. M., R. A. Kingsley, S. M. Townsend, T. A. Ficht, L. G. Adams, and A. J. Baumler.** 1999. Of mice, calves, and men. Comparison of the mouse typhoid model with other Salmonella infections. Adv Exp Med Biol **473:**261-274.

190. **Tukel, C., M. Raffatellu, D. Chessa, R. P. Wilson, M. Akcelik, and A. J. Baumler.** 2006. Neutrophil influx during non-typhoidal salmonellosis: who is in the driver's seat? FEMS Immunol Med Microbiol **46:**320-329.

191. **Tukel, C., M. Raffatellu, A. D. Humphries, R. P. Wilson, H. L. Andrews-Polymenis, T. Gull, J. F. Figueiredo, M. H. Wong, K. S. Michelsen, M. Akcelik, L. G. Adams, and A. J. Baumler.** 2005. CsgA is a pathogen-associated molecular pattern of Salmonella enterica serotype Typhimurium that is recognized by Toll-like receptor 2. Mol Microbiol **58:**289-304.

192. **Uzzau, S., D. J. Brown, T. Wallis, S. Rubino, G. Leori, S. Bernard, J. Casadesus, D. J. Platt, and J. E. Olsen.** 2000. Host adapted serotypes of Salmonella enterica. Epidemiol Infect **125:**229-255.

193. **Uzzau, S., G. S. Leori, V. Petruzzi, P. R. Watson, G. Schianchi, D. Bacciu, V. Mazzarello, T. S. Wallis, and S. Rubino.** 2001. Salmonella enterica serovar-host specificity does not correlate with the magnitude of intestinal invasion in sheep. Infect Immun **69:**3092-3099.

194. **van den Heuvel, A. P., A. M. de Vries-Smits, P. C. van Weeren, P. F. Dijkers, K. M. de Bruyn, J. A. Riedl, and B. M. Burgering.** 2002. Binding of protein kinase B to the plakin family member periplakin. J Cell Sci **115:**3957-3966.

195. **van der Velden, A. W., M. K. Copass, and M. N. Starnbach.** 2005. Salmonella inhibit T cell proliferation by a direct, contact-dependent immunosuppressive effect. Proc Natl Acad Sci U S A **102:**17769-17774.

196. **Van der Vieren, M., H. Le Trong, C. L. Wood, P. F. Moore, T. St John, D. E. Staunton, and W. M. Gallatin.** 1995. A novel leukointegrin, alpha d beta 2, binds preferentially to ICAM-3. Immunity **3:**683-690.

197. **van Garderen, E., K. E. Muller, G. H. Wentink, and T. S. van den Ingh.** 1994. Post-mortem findings in calves suffering from bovine leukocyte adhesion deficiency (BLAD). Vet Q **16:**24-26.

198. **Vazquez-Torres, A., and F. C. Fang.** 2001. Oxygen-dependent anti-Salmonella activity of macrophages. Trends Microbiol **9:**29-33.

199. **Vazquez-Torres, A., and F. C. Fang.** 2001. Salmonella evasion of the NADPH phagocyte oxidase. Microbes Infect **3:**1313-1320.

200. **Wallis, T. S.** 2006. Host-specificity of Salmonella infections in animal species, p. 57-88. *In* P. Mastroeni and D. Maskell (ed.), Salmonella Infections: Clinical, Immunological and Molecular Aspects. Cambridge University Press, Cambridge, UK.

201. **Wallis, T. S., and E. E. Galyov.** 2000. Molecular basis of Salmonella-induced enteritis. Mol Microbiol **36:**997-1005.

202. **Wallis, T. S., A. T. Vaughan, G. J. Clarke, G. M. Qi, K. J. Worton, D. C. Candy, M. P. Osborne, and J. Stephen.** 1990. The role of leucocytes in the induction of fluid secretion by Salmonella typhimurium. J Med Microbiol **31:**27-35.

203. **Wallis, T. S., M. Wood, P. Watson, S. Paulin, M. Jones, and E. Galyov.** 1999. Sips, Sops, and SPIs but not stn influence Salmonella enteropathogenesis. Adv Exp Med Biol **473:**275-280.

204. **Wang, X., M. Narayanan, J. M. Bruey, D. Rigamonti, E. Cattaneo, J. C. Reed, and R. M. Friedlander.** 2006. Protective role of Cop in Rip2/caspase-1/caspase-4-mediated HeLa cell death. Biochim Biophys Acta **1762:**742-754.

205. **Waterman, S. R., and D. W. Holden.** 2003. Functions and effectors of the Salmonella pathogenicity island 2 type III secretion system. Cell Microbiol **5:**501-511.

206. **Watson, P. R., E. E. Galyov, S. M. Paulin, P. W. Jones, and T. S. Wallis.** 1998. Mutation of invH, but not stn, reduces Salmonella-induced enteritis in cattle. Infect Immun **66:**1432-1438.

207. **Watson, P. R., S. M. Paulin, A. P. Bland, P. W. Jones, and T. S. Wallis.** 1995. Characterization of intestinal invasion by Salmonella typhimurium and Salmonella dublin and effect of a mutation in the invH gene. Infect Immun **63:**2743-2754.

208. **Weiss, D. S., B. Raupach, K. Takeda, S. Akira, and A. Zychlinsky.** 2004. Toll-like receptors are temporally involved in host defense. J Immunol **172:**4463-4469.

209. **Wesche-Soldato, D. E., R. Z. Swan, C. S. Chung, and A. Ayala.** 2007. The apoptotic pathway as a therapeutic target in sepsis. Curr Drug Targets **8:**493-500.

210. **WHO.** 2005. World Health Organization Drug-Resistant *Salmonella*. http://www.who.int/mediacentre/factsheets/fs139/en/.

211. **Wick, M. J.** 2004. Living in the danger zone: innate immunity to Salmonella. Curr Opin Microbiol **7:**51-57.

212. **Wilson, H. L., P. Aich, F. M. Roche, S. Jalal, P. D. Hodgson, F. S. Brinkman, A. Potter, L. A. Babiuk, and P. J. Griebel.** 2005. Molecular analyses of disease pathogenesis: application of bovine microarrays. Vet Immunol Immunopathol **105:**277-287.

213. **Wood, M. W., M. A. Jones, P. R. Watson, A. M. Siber, B. A. McCormick, S. Hedges, R. Rosqvist, T. S. Wallis, and E. E. Galyov.** 2000. The secreted effector protein of Salmonella dublin, SopA, is translocated into eukaryotic cells and influences the induction of enteritis. Cell Microbiol **2:**293-303.

214. **Wray, C., and H. D. Robert.** 2000. Salmonella infections in cattle, p. 169-190. *In* C. Wray and A. Wray (ed.), Salmonella in Domestic Animals. CABI Publishing, Wallingford, UK.

215. **Wray, C., and W. J. Sojka.** 1978. Experimental Salmonella typhimurium infection in calves. Res Vet Sci **25:**139-143.

216. **Wray, C., and W. J. Sojka.** 1981. Salmonella dublin infection of calves: use of small doses to simulate natural infection on the farm. J Hyg (Lond) **87:**501-509.

217. **Wray, C., J. N. Todd, and M. Hinton.** 1987. Epidemiology of Salmonella typhimurium infection in calves: excretion of S typhimurium in the faeces of calves in different management systems. Vet Rec **121:**293-296.

218. **Wu, M. S., Y. S. Lin, Y. T. Chang, C. T. Shun, M. T. Lin, and J. T. Lin.** 2005. Gene expression profiling of gastric cancer by microarray combined with laser capture microdissection. World J Gastroenterol **11:**7405-7412.

219. **Young, B., and J. W. Heath.** 2000. Gastrointestinal tract, p. 249-273. *In* C. Livingstone (ed.), Wheater's Functional Histology. Sydney, Australia.

220. **Zeng, H., A. Q. Carlson, Y. Guo, Y. Yu, L. S. Collier-Hyams, J. L. Madara, A. T. Gewirtz, and A. S. Neish.** 2003. Flagellin is the major proinflammatory determinant of enteropathogenic Salmonella. J Immunol **171:**3668-3674.

221. **Zhang, S., L. G. Adams, J. Nunes, S. Khare, R. M. Tsolis, and A. J. Baumler.** 2003. Secreted effector proteins of Salmonella enterica serotype typhimurium elicit host-specific chemokine profiles in animal models of typhoid fever and enterocolitis. Infect Immun **71:**4795-4803.

222. **Zhang, S., R. A. Kingsley, R. L. Santos, H. Andrews-Polymenis, M. Raffatellu, J. Figueiredo, J. Nunes, R. M. Tsolis, L. G. Adams, and A.**

J. Baumler. 2003. Molecular pathogenesis of Salmonella enterica serotype typhimurium-induced diarrhea. Infect Immun **71:**1-12.

223. **Zhang, S., R. L. Santos, R. M. Tsolis, S. Stender, W. D. Hardt, A. J. Baumler, and L. G. Adams.** 2002. The Salmonella enterica serotype typhimurium effector proteins SipA, SopA, SopB, SopD, and SopE2 act in concert to induce diarrhea in calves. Infect Immun **70:**3843-3855.

224. **Zhou, D., and J. Galan.** 2001. Salmonella entry into host cells: the work in concert of type III secreted effector proteins. Microbes Infect **3:**1293-1298.

225. **Zhou, D., M. S. Mooseker, and J. E. Galan.** 1999. An invasion-associated Salmonella protein modulates the actin-bundling activity of plastin. Proc Natl Acad Sci U S A **96:**10176-10181.

226. **Zhou, D., M. S. Mooseker, and J. E. Galan.** 1999. Role of the S. typhimurium actin-binding protein SipA in bacterial internalization. Science **283:**2092-2095.

APPENDIX A

Table A.1. Host genes differentially expressed in *S. typhimurium*-infected bovine ligated ileal loops from Control calves (CD18 +/+) at 1, 4, 8, and 12 hours post-infection (HPI). The numbers show the fold change of infected over control uninfected samples with positive values representing up-regulation and negative values representing down-regulation. Underlined fold change values represent statistically different gene expression ($p \leq 0.025$).

Gene symbol	1 HPI	4 HPI	8 HPI	12 HPI	Gene description[a]
Abcg8	-1.05	-1.21	-1.33	-1.80	ATP-binding cassette, sub-family G (WHITE), member 8
Ace2	-2.84	-1.16	-1.40	-4.31	angiotensin I converting enzyme (peptidyl-dipeptidase A) 2
ADAMTSL4	1.04	1.06	1.47	2.01	Thrombospondin repeat containing 1Bos taurus, 219 sequence(s)
ADFP	-1.37	-1.03	1.49	1.45	adipophilin (fragment).
Adm	1.20	1.45	2.37	2.66	adrenomedullin
Agr2	-2.66	1.48	1.34	1.28	anterior gradient 2 homologue
ALDOC	2.05	1.29	-1.25	1.15	fructose-bisphosphate aldolase c (ec 4.1.2.13) (brain-type aldolase).
ANKRD1	1.32	-1.06	-1.22	1.51	nuclear protein
Ankrd25	1.19	1.25	1.84	5.03	ankyrin repeat domain 25
ANKRD46	1.54	-1.15	1.01	1.15	ankyrin repeat domain 46 Other Aliases: MGC129030
ANPEP	-3.04	-1.38	-2.75	-8.09	microsomal aminopeptidase N; myeloid plasma membrane glycoprotein CD13
ANXA2	2.16	1.00	1.20	2.12	annexin II (ANX2); lipocortin II; calpactin I heavy subunit; chromobindin 8; protein I
ANXA8	2.30	1.02	-1.27	1.40	annexin VIII (ANX8)
Apoa1	-3.44	-2.62	-3.66	-16.17	apolipoprotein A-I
Apoc3	-2.18	-1.91	-2.12	-9.60	apolipoprotein C-III
ARG2	-1.37	1.24	1.29	1.56	ARG2 (Arginase II, non-hepatitic arginase, kidney-type arginase)

Table A.1. (continued)

Gene Symbol	1 HPI	4 HPI	8 HPI	12 HPI	Gene description
ATP1B3	-2.71	-1.23	-1.09	-2.59	sodium/potassium-transporting ATPase beta 3 subunit (ATPB3)
Atp5g1	1.54	-1.29	-1.54	-2.55	ATP synthase, H+ transporting, mitochondrial F0 complex, subunit C1(subunit 9)
B4galt1	-1.19	1.51	1.84	1.78	UDP-Gal:betaGlcNAc beta 1,4- galactosyltransferase, polypeptide 1
BCL2A1	-1.34	1.15	3.03	3.09	BCL-2-related protein A1 (BCL2A1)
BHLHB2	1.42	2.57	3.95	6.04	basic helix-loop-helix domain containing, class B, 2
BoLA-DRB3	-3.27	1.73	1.16	-1.31	major histocompatibility complex, class II, DRB3
Bzw2	1.73	1.15	1.50	1.64	basic leucine zipper and W2 domains 2
C14orf147	-1.09	1.50	1.79	1.52	chromosome 14 open reading frame 147
C2	-1.74	1.15	-1.11	1.21	complement component 2
C3	-1.80	-1.92	2.43	2.40	complement component 3
C8orf4	1.07	-1.12	1.65	1.86	chromosome 8 open reading frame 4
CAPN2	1.29	-1.03	1.53	2.92	calpain 2, (m/II) large subunit
CASP4	-1.21	-1.13	1.59	1.52	caspase 4, apoptosis-related cysteine protease
CCL2	1.61	3.72	6.07	13.60	chemokine (C-C motif) ligand 2
CCL20	-1.27	2.02	1.41	1.31	chemokine (C-C motif) ligand 20
CCL8	-1.03	3.26	3.91	4.86	chemokine (C-C motif) ligand 8
Ccrn4l	1.08	1.78	1.67	1.98	carbon catabolite repression 4-like
CD1E	1.92	-1.17	-1.06	1.16	T-cell surface glycoprotein CD1E precursor; R2G1
cd21	-1.27	1.28	1.52	-1.15	complement receptor type 2
CD3D	-2.18	1.11	1.00	-1.22	T-cell surface glycoprotein CD3 delta subunit precursor (CD3D; T3D)
CD3E	-1.90	1.15	-1.41	1.19	T-cell surface glycoprotein CD3 epsilon subunit precursor; T-cell surface antigen T3/leu-4
CD44	2.26	-1.35	-1.07	1.20	CD44 antigen hematopoietic form precursor (CD44H) phagocytic glycoprotein I (PGP-1)
CD48	-1.46	1.21	1.87	1.76	B-lymphocyte activation marker BLAST-1 precursor; bcm1 surface antigen
CD79A	-2.46	1.32	-1.13	-2.12	B-cell antigen receptor complex associated protein alpha-chain DE precursor
CDX2	-3.37	1.02	-1.36	-1.12	homeobox protein cdx-2 (caudal-type homeobox protein 2) (cdx-3)

Table A.1. (continued)

Gene Symbol	1 HPI	4 HPI	8 HPI	12 HPI	Gene description
Cebpd	1.20	2.78	3.28	3.20	CCAAT/enhancer binding protein (C/EBP), delta
Cenph	-1.77	1.21	-1.45	-1.15	centromere autoantigen H
CFLAR	-1.26	1.17	1.69	1.58	CASP8 and FADD-like apoptosis regulator
Chrne	2.61	2.45	1.63	1.69	cholinergic receptor, nicotinic, epsilon polypeptide
CLDN2	-1.58	1.02	-1.47	-2.22	claudin 2
COMP	-1.22	1.65	2.02	3.51	cartilage oligomeric matrix protein
CORO1A	-2.85	1.07	-1.12	-1.81	coronin-like protein P57
Cplx2	2.02	1.00	1.14	-1.11	complexin 2
Crip1	-1.60	-1.85	-1.58	-3.32	cysteine-rich protein 1 (intestinal)
CSF1	1.45	-1.03	1.57	2.08	colony stimulating factor 1 (macrophage)
CSN3	1.71	-1.27	1.10	1.17	casein kappa
CSRP2	1.00	1.30	1.69	2.48	smooth muscle cell lim protein (cysteine-rich protein 2) (crp2)
CTGF	1.33	-1.06	-1.02	1.59	connective tissue growth factor precursor (CTGF)
CTSL	1.29	-1.14	-1.48	-1.03	cathepsin L precursor major excreted protein (MEP)
CXCL6	1.16	2.88	5.15	4.96	chemokine (C-X-C motif) ligand 6 (granulocyte chemotactic protein 2)
Cyb5r1	-1.74	1.01	-1.28	-1.20	NAD(P)H:quinone oxidoreductase type 3, polypeptide A2
CYLC1	2.43	1.82	1.79	1.66	cylicin, basic protein of sperm head cytoskeleton 1
DGAT1	-2.24	1.16	1.03	-1.73	similiar to sterol O-acyltransferase (SOAT); acyl-CoA cholesterol acyltransferase (ACAT)
DPP4	-1.63	-1.52	-1.33	-2.58	dipeptidyl peptidase IV (DPP IV DPP4) T-cell activation CD26 antigen TP103 adenosine
DUSP6	1.07	1.20	2.50	1.36	dual specificity phosphatase 6
Eaf2	1.50	-1.32	1.55	-1.25	ELL associated factor 2
EGR1	1.93	1.67	3.27	2.41	early growth response protein 1 (hEGR1) transcription factor ETR103
Ehf	-1.25	1.35	1.71	2.16	ets homologous factor
Eif3s3	-1.88	1.34	-1.18	-1.43	eukaryotic translation initiation factor 3, subunit 3 (gamma)
EIF4A1	1.32	-1.21	1.07	1.87	eukaryotic initiation factor 4a-i (eif-4a-i).

Table A.1. (continued)

Gene Symbol	1 HPI	4 HPI	8 HPI	12 HPI	Gene description
Elac1	2.13	1.78	1.54	1.83	elaC homolog 1 (E. coli)
F2RL2	1.39	1.20	1.50	1.75	coagulation factor II (thrombin) receptor-like 2
F3	1.49	2.01	3.16	6.08	coagulation factor III (thromboplastin, tissue factor)
FBL	-1.84	1.28	-1.23	-1.19	fibrillarin (34 kd nucleolar scleroderma antigen).
FCGR3A	-1.21	1.34	1.71	1.63	Fc fragment of IgG, low affinity IIIa, receptor (CD16a)
FDPS	2.24	1.11	-1.02	1.49	farnesyl pyrophosphate synthetase
FGF1	2.04	-1.03	-1.23	1.01	fibroblast growth factor 1 (acidic)
FGF2	1.28	1.17	2.36	1.94	fibroblast growth factor 2 (basic)
FGFR3	-1.21	-1.47	-1.55	-2.03	fibroblast growth factor receptor 3
5-OPase	-1.82	1.28	-1.15	-1.35	5-oxo-L-prolinase
FOS	-1.00	3.09	3.07	4.28	v-fos FBJ murine osteosarcoma viral oncogene homolog
Gabarapl1	1.13	1.12	1.24	1.58	GABA(A) receptor-associated protein like 1
GABRA1	1.80	1.20	-1.16	1.09	gamma-aminobutyric acid (GABA) A receptor, alpha 1
GADD45B	1.27	1.04	1.52	1.85	growth arrest and DNA-damage-inducible, beta
GALT	-1.38	1.04	-1.32	-1.80	galactose-1-phosphate uridyl transferase
GFAP	1.70	-1.18	-1.16	1.03	glial fibrillary acidic protein
GJA1	1.31	1.27	1.33	1.70	gap junction protein, alpha 1
GNAO1	1.87	-1.15	-1.23	1.11	guanine nucleotide-binding protein g(o) alpha subunit 1 (gnao1)
Gng3	2.17	1.05	1.21	-1.20	guanine nucleotide binding protein (G protein), gamma 3 subunit
Gng5	-1.14	1.22	1.15	1.84	guanine nucleotide binding protein (G protein), gamma 5 subunit
GPC	-2.55	1.30	-1.08	-2.25	glycophorin C
GPX4	-2.38	1.39	-1.09	-1.06	glutathione peroxidase 4 (phospholipid hydroperoxidase)
Gsta4	1.59	-1.26	-1.29	-1.37	glutathione S-transferase, alpha 4
Gucy2c	-1.21	-1.01	-1.30	-1.91	guanylate cyclase 2c
HIF1A	1.56	1.62	2.62	3.70	hypoxia-inducible factor 1 alpha (HIF1 alpha)

Table A.1. (continued)

Gene Symbol	1 HPI	4 HPI	8 HPI	12 HPI	Gene description
HNF4A	-1.95	-1.36	1.09	-1.18	hepatocyte nuclear factor 4 (HNF4) transcription factor 14
Hpse	-1.50	1.79	1.57	-1.05	heparanase
HSPA1A	1.31	-1.08	1.16	1.74	heat shock 70kDa protein 1A
HSPA3	-1.14	-1.32	1.10	2.83	heat shock 70kDa protein 3
ICAM1	-1.48	1.84	1.90	2.99	intercellular adhesion molecule-1 precursor (ICAM1)
IER2	-1.07	1.58	1.90	1.06	transcription factor ETR101
Ifi30	-2.09	1.79	2.36	1.49	interferon gamma inducible protein 30
IFNG	1.58	1.43	5.70	7.37	interferon, gamma
IGFBP2	1.86	1.27	-2.05	-1.47	insulin-like growth factor binding protein 2
IGFBP3	-1.32	1.30	2.43	2.88	insulin-like growth factor-binding protein 3 precursor (IGF-binding protein 3 IGFBP3 IBP3)
IGIP	1.22	1.15	1.60	2.02	IgA regulatory protein
Igj	-1.30	1.03	2.47	1.23	immunoglobulin joining chain
IL17	1.17	1.38	3.05	4.52	interleukin 17
IL1A	1.25	2.10	3.21	11.97	interleukin 1, alpha
IL1B	1.42	3.68	4.97	9.03	interleukin 1, beta
il-1r2	1.18	1.59	1.96	2.40	IL-1 receptor 2
IL22RA1	-2.44	1.09	-1.53	-1.05	interleukin 22 receptor, alpha 1
IL6	1.32	1.51	1.59	4.92	interleukin 6 (interferon, beta 2)
IL8	-1.23	6.34	8.07	13.52	interleukin 8
IL8RB	-1.05	1.43	2.35	2.71	interleukin 8 receptor, beta
IRF1	-2.18	1.81	2.08	1.56	interferon regulatory factor 1 (IRF1)
Isg15	-1.24	1.22	2.32	3.99	ubiquitin-like modifier
ITGA2	1.25	2.11	2.05	3.58	integrin, alpha 2 (CD49B, alpha 2 subunit of VLA-2 receptor)
ITGB1	1.32	1.10	1.56	2.27	integrin, beta 1
ITGB5	1.56	-1.13	-1.01	1.14	integrin, beta 5

Table A.1. (continued)

Gene Symbol	1 HPI	4 HPI	8 HPI	12 HPI	Gene description
ITPR3	-2.44	1.47	-1.09	-1.36	inositol 1,4,5-triphosphate receptor, type 3
Klhdc3	1.52	-1.12	-1.06	1.33	kelch domain containing 3
Lap3	-1.19	1.01	2.35	2.90	leucine aminopeptidase 3
Laptm4b	-1.42	-1.33	-1.25	-2.09	lysosomal associated protein transmembrane 4 beta
LDHA	1.11	1.20	1.62	2.21	L-lactate dehydrogenase M subunit (LDHA)
Ldlr	1.35	1.49	1.19	1.73	low density lipoprotein receptor
LEAP-2	-1.28	-1.39	-1.29	-2.06	liver-expressed antimicrobial peptide 2
LIF	1.24	1.31	1.88	3.01	leukemia inhibitory factor
LOC404122	1.12	1.32	1.55	2.50	actin, cytoplasmic 2
LOC407131	1.13	1.07	1.73	1.15	CD80 anitgen
LOC407235	1.11	-1.04	1.03	1.47	adiponectin receptor-1
LOC408018	1.17	1.32	2.30	3.43	C-C motif chemokine receptor 3
LOC414347	-1.11	1.34	1.23	1.59	putative MIP1-beta protein
LOC504364	1.88	-1.04	1.17	-1.04	similar to Riken cDNA C230021P08 gene
LOC504650	-1.14	-1.18	1.72	-1.31	similar to choline/ethanolaminephosphotransferase 1
LOC505214	-2.50	1.14	1.37	-1.24	similar to cytokeratin 20
LOC505518	-2.85	-1.24	-1.28	-2.16	similar to placenta expressed transcript protein
LOC505691	-1.40	1.06	-1.22	-1.76	similar to p18
LOC505890	1.04	1.83	2.58	1.31	similar to ADAM DEC1 precursor
LOC506029	1.74	1.26	-1.07	-1.04	similar to amyotrophic lateral sclerosis 2
LOC506118	-1.35	1.19	1.47	-1.03	similar to glycosyltransferase 28 domain containing 1
LOC506406	-1.38	1.26	1.51	1.89	similar to mitochondrial glutathione reductase
LOC506692	-2.42	-1.30	-1.38	-3.64	similar to N-acetylated alpha-linked acidic dipeptidase-like 1
LOC506924	2.07	1.12	-1.11	1.25	similar to fibroblast growth factor 13
LOC507193	2.16	-1.16	-1.09	1.14	similar to ADD1 protein

Table A.1. (continued)

Gene Symbol	1 HPI	4 HPI	8 HPI	12 HPI	Gene description
LOC507436	-1.27	1.46	1.78	2.49	similar to Putative lymphocyte G0/G1 switch protein 2
LOC508133	1.04	2.08	2.20	2.40	similar to syndecan 4
LOC508162	-2.31	1.38	-1.28	-1.61	similar to Nuclear receptor coactivator 2
LOC508490	1.13	-1.06	-1.29	1.75	similar to integrin alpha 3
LOC508658	-1.04	1.19	1.53	1.55	similar to Tyrosine-protein phosphatase non-receptor type 1
LOC508666	1.29	1.57	2.77	2.47	similar to MPIF-1
LOC509471	-3.04	-1.19	-1.06	1.10	similar to ubiquitin-conjugating enzyme RIG-B
LOC509501	-1.34	1.56	5.23	6.91	proteoglycan 1 precursor-like
LOC509642	-2.29	1.25	-1.00	-1.34	similar to oxidized-LDL responsive gene 2
LOC509774	1.15	1.44	1.71	2.37	similar to Ibrdc3 protein
LOC510165	-1.93	1.03	-1.06	-1.18	similar to HPS5 protein major form
LOC510341	-2.08	1.50	-1.12	-1.12	similar to AHNAK nucleoprotein
LOC510506	-2.53	1.05	-1.19	-2.47	similar to carbamoyl phosphate synthetase 1
LOC510833	-1.12	-1.46	2.06	-1.41	similar to Collagen alpha 1(III) chain precursor
LOC510923	-1.12	1.14	1.68	1.89	similar to estrogen responsive finger protein
LOC511106	1.04	1.10	1.83	1.68	similar to SCCA2/SCCA1 fusion protein
LOC511224	-2.55	1.01	-1.05	-1.24	similar to transcription factor NFATmac
LOC511245	2.16	1.22	1.22	-1.04	similar to sulfotransferase N4h
LOC511430	-1.82	1.31	3.03	1.50	similar to down-regulated in colon cancer 1
LOC511511	1.48	1.22	1.93	1.59	similar to granulocyte colony stimulating factor receptor
LOC511591	-1.23	-1.22	-1.58	-1.86	similar to sortilin 1 preproprotein
LOC512355	2.32	-1.08	1.24	1.08	similar to TNF receptor-associated factor 2
LOC512726	1.87	1.03	1.04	-1.21	similar to Src homology 2 domain containing F
LOC512846	2.46	1.22	1.33	1.05	similar to ubiquitin-conjugating enzyme E2-like
LOC512975	-2.23	1.02	1.84	-1.08	similar to Claudin-7

Table A.1. (continued)

Gene Symbol	1 HPI	4 HPI	8 HPI	12 HPI	Gene description
LOC513478	-1.39	1.19	1.64	1.59	similar to interleukin-10 receptor
LOC513497	1.12	1.20	1.91	1.93	similar to p21/WAF1
LOC513513	1.05	1.01	1.47	1.67	similar to chitinase
LOC513526	1.79	1.17	-1.04	1.00	similar to U11/U12 snRNP 25K protein
LOC513848	-1.20	1.40	1.49	1.57	similar to abhydrolase domain containing 13
LOC513856	-1.33	-1.05	1.44	1.39	similar to alpha-2-macroglobulin
LOC513990	-1.06	-1.02	1.67	3.45	similar to interferon-gamma induced monokine CXCL9
LOC514108	2.91	2.72	1.99	1.88	similar to Eukaryotic translation initiation factor 4E transporter
LOC514613	-1.04	1.45	1.45	2.09	similar to cyclin L ania-6a
LOC514812	-5.48	-1.12	1.05	2.11	cytokeratin 19
LOC514835	-2.17	1.13	-1.08	-1.79	similar to T-cell leukemia/lymphoma 1B
LOC515088	2.05	-1.01	1.10	-1.08	similar to G protein-coupled receptor kinase interactor
LOC515917	1.54	1.01	-1.03	1.01	similar to trophoblast Kunitz domain protein 2
LOC516104	1.16	1.42	2.30	4.34	similar to putative alpha chemokine
LOC516689	1.34	1.12	-1.77	1.03	similar to proteolipid M6B isoform TMD-omega
LOC516781	2.42	-1.05	1.14	1.33	similar to transcriptional regulatory protein p54
LOC517192	1.01	2.11	1.50	1.22	similar to jun D proto-oncogene
LOC518258	-1.21	1.23	1.52	2.08	similar to FUN14 domain containing 1
LOC518849	2.33	-1.19	-1.15	1.20	similar to Slc17a7 protein
LOC520842	-1.75	1.21	1.09	-1.45	similar to kruppel-like factor 4
LOC521424	-1.50	2.95	2.65	7.23	similar to squamous cell-specific protein
LOC522372	-2.04	1.15	-1.00	-1.02	similar to GCIP-interacting protein p29 (P29)
LOC522692	-1.07	1.68	1.70	1.67	similar to platelet glycoprotein V
LOC522886	1.77	1.10	-1.27	1.26	similar to periplakin
LOC523542	-1.79	1.20	-1.10	-1.16	similar to casein kinase I delta

Table A.1. (continued)

Gene Symbol	1 HPI	4 HPI	8 HPI	12 HPI	Gene description
LOC525795	1.72	1.13	-1.17	-1.03	similar to agrin
LOC525869	1.13	-1.05	1.56	1.48	similar to Ankycorbin
LOC526585	-1.97	1.49	1.35	1.25	similar to Coagulation factor II (thrombin) receptor
LOC526865	1.26	1.30	1.16	1.49	similar to poliovirus receptor
LOC527520	1.05	1.30	2.99	2.55	similar to HERC6
LOC530884	-3.63	-1.64	1.33	1.17	similar to receptor activator of nuclear factor-kappa B
LOC532569	1.75	4.07	7.61	18.15	similar to Calgranulin B
LOC532671	-2.00	1.24	1.54	-1.07	similar to mucolipin 2
LOC533243	-1.07	1.23	1.48	1.04	similar to zinc finger protein 143
LOC533264	1.01	1.00	1.41	1.37	similar to sulfatase 2
LOC534258	-1.76	-1.16	1.13	1.16	similar to paired related homeobox protein
LOC534360	-1.13	1.27	1.68	1.81	similar to nectin 3; PRR3
LOC534497	-1.31	-1.79	-1.67	-1.74	similar to peripheral myelin protein 22
LOC534793	-1.08	-1.08	1.24	1.51	similar to Inositol polyphosphate-4-phosphatase, type II
LOC534799	1.01	1.62	1.96	2.58	similar to DNA topoisomerase I
LOC534923	2.10	1.08	1.39	-1.28	similar to protein serine/threonine kinase
LOC535692	2.19	1.12	-1.15	1.26	similar to SMAP-1b
LOC536011	1.57	1.11	-1.11	1.04	similar to Cdon homolog (mouse)
LOC537282	-1.42	1.20	1.52	2.40	similar to Myosin IB
LOC538536	-2.56	-1.22	-1.28	-1.04	similar to seven-transmembrane receptor Frizzled-5
LOC538606	-1.84	1.21	-1.26	-1.17	similar to myosin phosphatase target subunit 1
LOC539109	-1.56	1.92	1.86	1.05	similar to stromelysin-3
LOC539143	1.85	-1.24	1.48	-1.06	ATP binding protein
LOC539145	1.06	1.11	1.51	2.80	similar to OTU domain containing 5
LOC539360	1.91	1.68	1.45	1.20	similar to calpain 6

Table A.1. (continued)

Gene Symbol	1 HPI	4 HPI	8 HPI	12 HPI	Gene description
LOC539533	-1.85	1.62	1.44	2.18	similar to Nedd4 binding protein 2
LOC539700	-2.81	-1.09	-1.14	-1.17	similar to A-kinase anchor protein-like protein 8
LOC540135	1.85	2.25	3.27	4.85	similar to pleckstrin homology-like domain, family A, member 1
LOC540147	-2.07	-1.03	-1.07	1.28	similar to CDH22
LOC540789	-1.44	1.31	1.56	1.54	similar to poly (ADP-ribose) polymerase family, member 14
LOC540869	1.15	1.06	1.44	1.59	similar to Solute carrier family 30 (zinc transporter), member 4
LOC540895	1.93	1.75	2.15	1.74	similar to cardiac voltage gated potassium channel modulatory
LOC615037	-1.56	1.21	1.68	1.57	similar to Bone morphogenetic protein 2
LOC617313	1.71	1.03	1.53	1.18	similar to Granzyme H precursor
LOC617552	-1.01	-1.01	1.02	1.57	similar to connector enhancer of kinase suppressor of Ras 1
LOC617832	-1.27	2.05	2.40	2.83	similar to Ankyrin repeat domain 22
LOC618267	1.19	1.11	1.30	1.69	similar to adaptor-related protein complex 4, sigma 1 subunit
Lrp8	1.14	-1.07	1.36	1.57	low density lipoprotein receptor-related protein 8, apolipoprotein e receptor
LUM	-2.30	1.25	1.04	-1.68	lumican precursor (LUM); keratan sulfate proteoglycan; LDC
Mail	-2.26	1.42	1.01	-1.63	molecule possessing ankyrin repeats induced by lipopolysaccharide
MAP1B	1.98	1.03	-1.39	1.00	microtubule-associated protein 1B
MAPK13	-1.20	1.29	1.82	1.62	mitogen-activated protein kinase 13
Mbd4	-1.86	1.09	1.01	-1.46	methyl-CpG binding domain protein 4
Mcoln1	-1.10	-2.49	1.00	-1.22	mucolipin 1
MGC126940	1.79	1.29	-1.18	1.12	similar to receptor expression enhancing protein
MGC126950	-3.23	1.67	-1.03	-1.02	similar to 39S ribosomal protein L28, mitochondrial precursor
MGC127229	-1.44	-2.25	-1.29	-7.40	similar to Fructose-bisphosphate aldolase B (Liver-type aldolase)
MGC127493	-1.03	-2.18	-1.08	2.33	similar to transgelin
MGC127572	1.08	1.26	1.96	3.29	similar to Diamine acetyltransferase 1
MGC127582	1.54	1.09	1.15	1.11	similar to putative S1 RNA binding domain protein

Table A.1. (continued)

Gene Symbol	1 HPI	4 HPI	8 HPI	12 HPI	Gene description
MGC127813	-3.76	-1.17	-1.48	-4.04	similar to Apolipoprotein A-IV precursor
MGC127814	-2.55	1.19	-1.01	-1.82	similar to Complement component C9 precursor
MGC127936	2.97	1.53	2.01	5.13	similar to S100 calcium-binding protein A2
MGC128147	-1.45	1.66	2.24	2.66	similar to threonyl-tRNA synthetase
MGC128242	2.14	1.03	-1.44	-1.26	similar to neuronal protein
MGC128290	1.18	1.22	1.54	1.05	similar to tumor necrosis factor receptor superfamily, member 9
MGC128467	1.28	2.91	5.04	5.47	similar to Nuclear factor 1 A-type (Nuclear factor 1/A) (NF1-A)
MGC128573	1.09	1.49	2.19	1.95	similar to radical S-adenosyl methionine domain containing 2
MGC128596	1.78	1.16	1.32	1.75	similar to Zinc finger protein 696
MGC128881	2.07	-1.08	1.03	-1.44	similar to solute carrier family 22 (organic cation transporter), member 17
MGC128885	-1.92	-1.05	-1.15	1.11	similar to thyroid hormone receptor interactor 6
MGC129043	1.73	-1.27	1.19	1.21	similar to U4/U6 small nuclear ribonucleoprotein Prp4
MGC133836	1.74	-1.25	1.24	-1.01	similar to translation factor sui1 homolog
MGC133896	2.47	-1.33	1.17	-1.01	similar to elongation protein 4 homolog
MGC133975	-1.72	1.10	1.06	-1.09	similar to BCL2/adenovirus E1B 19kD interacting protein 1 isoform BNIP1-c
MGC133989	-1.04	-1.17	-1.30	-3.06	similar to C44B7.7
MGC134216	1.22	1.03	-1.67	-1.06	similar to testicular cell adhesion molecule 1
MGC134468	-1.12	1.31	1.80	2.02	similar to SWI/SNF-related matrix-associated actin-dependent regulator of chromatin
MGC137146	1.70	1.12	1.23	-1.04	similar to ribonuclease P (predicted)
MGC137208	1.64	1.15	1.68	2.22	similar to phosphoserine phosphatase
MGC137223	1.12	1.18	1.02	1.84	similar to RAB3A interacting protein isoform alpha 1
MGC137270	-1.48	1.02	-1.31	-2.65	similar to Tissue alpha-L-fucosidase precursor
MGC137945	1.02	1.30	-1.09	-2.63	similar to F-box only protein 25
MGC138118	-2.17	1.01	-1.04	-1.12	similar to SPRY domain-containing SOCS box protein SSB-2
MGC139086	2.67	1.04	-1.24	-1.03	similar to Follistatin-related protein 3 precursor

Table A.1. (continued)

Gene Symbol	1 HPI	4 HPI	8 HPI	12 HPI	Gene description
MGC139116	1.31	1.12	1.67	1.51	similar to SINK-homologous serine/threonine kinase
MGC139302	1.78	1.11	-1.05	1.11	similar to KDEL (Lys-Asp-Glu-Leu) containing 1
MGC139434	1.06	-1.05	1.00	1.40	similar to F46F6.4
MGC139459	1.25	1.63	2.49	2.97	similar to RTP801
MGC139487	1.05	-1.10	1.65	2.44	similar to interferon-induced protein with tetratricopeptide repeats
MGC139527	1.54	1.03	1.90	1.92	similar to Sorting nexin-10
MGC139630	1.17	-1.24	1.02	1.55	similar to Transcription elongation factor A protein 2
MGC139917	1.14	-1.02	-1.54	1.00	similar to NipSnap1 protein
MGC140483	1.69	-1.07	1.02	1.15	similar to methylenetetrahydrofolate dehydrogenase (NADP+ dependent)1-like
MGC140497	-1.29	-1.37	-1.57	-2.10	similar to cytochrome P450, family 2, subfamily U, polypeptide 1
MGC140534	-1.13	-1.49	-1.18	-2.58	similar to solute carrier family 43, member 2
MGC140560	1.08	1.00	1.15	1.78	imilar to protein phosphatase 1, regulatory (inhibitor) subunit 5
MGC140612	2.07	-1.03	-1.09	-1.26	similar to synuclein, beta
MGC140677	1.89	1.09	1.15	1.20	similar to CG11448-PA
MGC140747	1.09	1.00	-1.03	1.48	similar to ankyrin repeat and MYND domain containing 2
MGC140786	-1.17	1.04	1.43	2.22	similar to regulator of G-protein signalling 2
MGC142335	-1.93	1.23	-1.33	-1.43	similar to HP1-BP74
MGC142357	-2.47	1.20	1.12	-1.13	similar to solute carrier family 26, member 6
MGC142452	-1.78	1.18	-1.19	-1.06	similar to transcriptional regulator protein
MGC142482	-2.24	1.41	1.25	-1.58	imilar to Derlin-3 (Der1-like protein 3)
MGC142499	-1.33	2.20	3.03	3.22	similar to SAM domain and HD domain-containing protein 1
MGC142651	1.33	1.67	2.33	3.17	similar to CG3717-PA
MGC142672	1.32	1.77	2.29	1.82	similar to core 1 synthase, glycoprotein-N-acetylgalactosamine
MGC142673	1.33	1.33	1.82	2.24	similar to pleckstrin homology-like domain family A member 2
MGC142715	1.21	1.04	1.32	1.91	similar to COX15 homolog isoform 1 precursor

Table A.1. (continued)

Gene Symbol	1 HPI	4 HPI	8 HPI	12 HPI	Gene description
MGC142786	-1.05	1.41	2.06	2.47	similar to MARCKS-like protein
MGC142842	1.30	1.71	3.10	2.72	similar to guanylate-binding protein 5
MGC143284	1.24	-1.10	-1.87	1.27	similar to cullin 2
MGC143369	1.52	-1.04	1.29	1.16	similar to ankyrin repeat domain 16
MGC143451	2.13	1.32	1.48	-1.07	similar to Rho GTPase activating protein 10
MGC151889	1.14	-1.25	-1.02	1.51	similar to Pancreatic secretory granule membrane major glycoprotein GP2 precursor
MGC29891	1.97	-1.01	-1.19	1.02	GA repeat binding protein, beta 2
MIA	-2.42	-1.21	-1.23	-1.31	melanoma-derived growth regulatory protein precursor; melanoma inhibitory activity (MIA)
MKP-1	1.30	1.62	2.46	5.30	MAP kinase phosphatase-1
Mpeg1	-1.42	1.89	2.27	1.66	macrophage expressed gene 1
Mrgprf	2.00	2.00	1.38	1.08	MAS-related GPR, member F
Mrpl48	1.69	1.24	1.01	-1.22	mitochondrial ribosomal protein L48
Mtf2	-2.27	-1.09	-1.25	-1.32	metal response element binding transcription factor 2
MX2	-1.20	1.41	2.79	2.76	interferon-regulated resistance GTP-binding protein MXAB
MYOC	1.07	1.00	1.27	1.68	myocilin
MyoD1	-1.64	1.09	-1.10	-1.05	myogenic differentiation 1
NCR3	1.09	-1.21	1.73	-1.02	natural cytotoxicity triggering receptor 3
NFKBIA	-1.06	1.13	3.03	3.35	nuclear factor of kappa light polypeptide gene enhancer in B-cells inhibitor, alpha
NMB	1.54	-1.08	-1.02	1.06	neuromedin B
NNAT	2.08	1.07	-1.22	1.04	neuronatin brain-specific mammalian developmental gene
Nnt	-1.57	1.20	-1.23	-2.21	nicotinamide nucleotide transhydrogenase
NOS2A	-1.28	2.54	3.22	2.74	inducible nitric oxide synthase (INOS) type II NOS hepatocyte NOS (HEP-NOS)
NPB	-1.90	1.09	-1.24	-1.59	preproneuropeptide B
Nppc	-2.15	-1.17	-1.14	-1.01	natriuretic peptide precursor type C
NRXN3	1.69	1.12	1.03	1.09	neurexin III alpha

Table A.1. (continued)

Gene Symbol	1 HPI	4 HPI	8 HPI	12 HPI	Gene description
Nxt1	1.70	1.02	-1.11	1.22	NTF2-related export protein 1
OAS1	-1.40	1.91	2.47	2.22	(2'-5')oligoadenylate synthetase 1 ((2-5')oligo(A) synthetase 1; 2-5A synthetase 1)
Ogn	-1.08	-1.14	-1.51	-3.05	osteoglycin
OTC	-1.24	-1.34	-1.62	-2.98	ornithine carbamoyltransferase precursor (ec 2.1.3.3) (otcase) (ornithine transcarbamylase).
PAG7	-1.61	1.56	1.39	-1.15	pregnancy-associated glycoprotein 7
PDPN	2.21	1.98	2.28	3.07	podoplanin
PDZK1	-1.73	-1.10	-1.70	-2.23	pdz domain containing-protein.
Peg3	1.83	-1.13	-1.10	-1.23	paternally expressed 3
PEPT1	-1.34	-1.52	-1.93	-2.46	proton-dependent gastrointestinal peptide transporter 1
Pfdn2	1.67	-1.19	-1.10	1.05	prefoldin 2
PHB2	2.43	-1.01	1.08	1.47	B-cell associated protein
Phgdh	2.10	1.11	1.42	1.01	phosphoglycerate dehydrogenase
PIGS	1.90	-1.05	1.22	1.15	phosphatidylinositol glycan, class S
PIK4CA	-1.10	-2.07	-1.06	1.18	phosphatidylinositol 4-kinase, catalytic, alpha polypeptide
Plac8	1.14	1.08	1.69	2.54	placenta-specific 8
PLAT	1.79	1.26	1.78	2.04	plasminogen activator, tissue
PLAU	1.36	1.91	2.61	5.64	plasminogen activator, urokinase
PLAUR	1.38	1.17	1.49	3.56	plasminogen activator, urokinase receptor
PP	1.23	1.09	2.64	3.04	pyrophosphatase (inorganic)
Ppp1r16a	-2.54	1.78	-1.39	-2.19	protein phosphatase 1, regulatory (inhibitor) subunit 16A
PTGS2	1.67	2.97	4.18	12.59	prostaglandin G/H synthase 2 precursor; cyclooxygenase 2 (COX2)
RAB13	-1.88	1.21	-1.19	1.02	RAB13, member RAS oncogene family
Rab8b	1.04	1.09	1.59	1.63	member RAS oncogene family
RAP1A	1.54	-1.09	1.68	1.03	RAP1A, member of RAS oncogene family
RBMS1	-1.15	1.26	1.37	2.45	single-stranded DNA-binding protein MSSP-1

Table A.1. (continued)

Gene Symbol	1 HPI	4 HPI	8 HPI	12 HPI	Gene description
Retn	-1.05	-1.36	1.26	1.48	resistin
RHOB	1.40	1.59	1.73	2.56	ras homolog gene family, member B
Rnf141	-2.08	1.05	-1.56	-1.70	ring finger protein 141
S100A10	-1.80	1.27	-1.28	1.42	calpactin I light chain
S100A11	1.71	1.28	1.53	2.86	calgizzarin; S100C protein; MLN70
S100A4	2.14	-1.22	-1.05	1.11	placental calcium-binding protein; calvasculin; S100 calcium-binding protein A4
Sdbcag84	-2.18	-1.04	-1.06	-1.11	serologically defined breast cancer antigen 84
SELP	1.18	1.83	2.84	2.71	P-selectin precursor (SELP); granule membrane protein 140 (GMP140)
SERPINB8	1.16	-1.07	1.33	1.55	cytoplasmic antiproteinase 2 (CAP2) protease inhibitor 8
SIAT4B	-1.68	1.10	-1.02	-1.18	sialyltransferase 4B (beta-galactoside alpha-2,3-sialyltransferase)
SIAT8A	1.65	-1.04	-1.04	1.04	alpha-N-acetylneuraminnide alpha-2,8-sialyltransferase; ganglioside GD3/GT3 synthase
SLC11A1	1.08	1.27	1.67	2.48	natural resistance-associated macrophage protein 1 (NRAMP1)
SLC1A1	-1.14	-1.07	-1.63	-3.03	high-affinity glutamate transporter excitatory amino acid transporter 3 sodium-dependent
SLC1A3	-1.08	-1.06	-1.77	-1.22	excitatory amino acid transporter 1; sodium-dependent glutamate/aspartate transporter 1
SLC2A1	1.05	1.13	1.23	2.11	erythrocyte glucose transporter 1 (GLUT1)
SLC2A3	1.25	1.16	1.48	1.77	brain glucose transporter 3 (GTR3)
Slc34a2	-1.29	-1.64	-2.10	-1.85	solute carrier family 34 (sodium phosphate), member 2
SLC7A7	-1.71	1.03	-1.26	-2.99	glycoprotein-associated amino acid transporter.
Smc4l1	-2.33	1.27	-1.26	-1.33	SMC4 structural maintenance of chromosomes 4-like 1 (yeast)
SNAI2	-1.04	1.12	1.39	2.14	snail homolog 2 (Drosophila)
Sncg	1.54	1.06	-1.21	1.00	synuclein, gamma
SOCS3	1.02	1.95	1.92	2.55	suppressor of cytokine signaling 3
Sod2	1.96	3.69	8.53	15.05	superoxide dismutase 2, mitochondrial
SPINK1	-2.42	-1.49	1.16	-1.46	serine peptidase inhibitor, Kazal type 1
Spint1	-2.13	1.23	1.05	-1.21	serine protease inhibitor, Kunitz type 1

Table A.1. (continued)

Gene Symbol	1 HPI	4 HPI	8 HPI	12 HPI	Gene description
Stxbp1	2.10	-1.07	-1.02	1.14	syntaxin binding protein 1
SV2	1.59	-1.01	-1.33	-1.05	synaptic vesicle glycoprotein 2 Other Aliases: KIAA0736
Tacstd1	-1.01	-1.10	2.68	3.10	tumor-associated calcium signal transducer 1
Tbca	1.74	1.11	-1.21	-1.09	tubulin cofactor a
TFPI2	1.56	1.31	1.44	2.37	tissue factor pathway inhibitor 2
THBS	1.78	1.60	2.63	8.55	thrombospondin
TICAM2	1.09	-1.11	1.41	1.28	toll-like receptor adaptor molecule 2
TIMP1	1.37	1.35	2.66	4.37	metalloproteinase inhibitor 1 precursor (TIMP1) erythroid potentiating activity (EPA)
TLR4	1.11	1.36	2.33	2.73	toll-like receptor 4
TNFAIP6	1.37	1.14	1.42	2.51	tumor necrosis factor-inducible protein TSG-6 hyaluronate-binding protein
TNFRSF1A	-1.03	1.41	2.06	2.22	tumor necrosis factor receptor superfamily, member 1A
TNFRSF6	1.02	-1.10	1.40	1.61	tumor necrosis factor receptor superfamily, member 6
TNFRSF8	-1.77	1.07	1.07	-1.05	tumor necrosis factor receptor superfamily, member 8
Tspan1	-2.97	-1.02	1.31	1.03	tetraspanin 1
Tspan33	1.67	1.21	1.13	-1.12	tetraspanin 33
TUBB	1.75	-1.18	1.02	-1.04	tubulin, beta
TXNRD1	-1.08	1.01	1.43	2.37	thioredoxin reductase
TYROBP	1.12	-1.17	1.94	1.45	DNAX activation protein 12
UBE1L	-2.40	1.25	1.19	1.17	ubiquitin-activating enzyme E1-related protein
UCHL1	2.12	1.18	-1.86	1.06	ubiquitin carboxyl-terminal esterase L1 (ubiquitin thiolesterase)
VCAM1	-1.80	1.14	1.57	1.07	vascular cell adhesion protein 1 precursor (V-CAM 1) CD106 antigen
Vldlr	1.13	1.00	1.37	1.18	very low density lipoprotein receptor
Wars	1.31	1.73	7.34	12.58	tryptophanyl-tRNA synthetase
XDH	-1.49	1.02	1.81	1.32	xanthine dehydrogenase/oxidase
XRCC1	-1.91	-1.14	-1.39	-1.36	DNA-repair protein XRCC1

Table A.1. (continued)

Gene Symbol	1 HPI	4 HPI	8 HPI	12 HPI	Gene description
zo2	-1.04	-1.06	1.11	1.68	tight junction protein 2

[a]278 differentially expressed genes of unknown description are not listed.

APPENDIX B

Table B.1. Host genes differentially expressed in *S. typhimurium*-infected bovine ligated ileal loops from BLAD calves (CD18 -/-) at 1, 4, 8, and 12 hours post-infection (HPI). The numbers show the fold change of infected over control uninfected samples with positive values representing up-regulation and negative values representing down-regulation. Underlined fold change values represent statistically different gene expression ($p \leq 0.025$).

Gene symbol	1 HPI	4 HPI	8 HPI	12 HPI	Gene description[a]
AADAT	1.11	1.42	1.58	-1.17	aminoadipate aminotransferase
Abcc5	1.08	2.41	1.02	-1.01	ATP-binding cassette, sub-family C (CFTR/MRP), member 5
Abcg2	-1.24	-1.61	-2.40	-3.19	ATP-binding cassette, sub-family G (white), member 2
Abhd4	-1.32	1.12	1.73	-2.16	abhydrolase domain containing 4
Ace2	-2.50	-2.90	-2.07	-6.16	angiotensin I converting enzyme (peptidyl-dipeptidase A) 2
Acp6	-1.20	1.20	2.28	-2.38	lysophosphatidic acid phosphatase protein
ACR	-1.02	1.52	1.02	-2.13	acrosin precursor
Acta1	1.00	1.89	1.70	-1.24	actin, alpha 1, skeletal muscle
ACTB	-1.10	-1.21	-1.33	3.97	actin, beta
Actr3	1.03	-1.21	-1.01	2.17	ARP3 actin-related protein 3 homolog (yeast)
Adam2	-1.18	2.12	1.46	-1.12	a disintegrin and metalloprotease domain 2
ADAMTSL4	1.21	1.59	1.98	1.40	Thrombospondin repeat containing 1Bos taurus, 219 sequence(s)
ADCY1	1.06	2.13	1.30	-1.20	adenylate cyclase 1 (brain)
ADCYAP1R1	1.16	2.66	1.80	1.53	adenylate cyclase activating polypeptide 1 (pituitary) receptor type I
ADFP	-1.03	1.70	1.03	-1.43	adipophilin (fragment).
AEBP1	1.01	1.71	1.17	-1.25	aortic carboxypeptidase-like protein aclp (aebp1).

Table B.1. (continued)

Gene Symbol	1 HPI	4 HPI	8 HPI	12 HPI	Gene description
ALAS2	1.00	1.43	1.60	-1.05	5-aminolevulinic acid synthase, erythroid-specific
ALDH5	-1.03	2.28	1.18	-1.21	aldehyde dehydrogenase 5, mitochondrial X Chromosome
Aldh7a1	1.22	2.03	1.70	1.31	aldehyde dehydrogenase 7 family, member A1
ALDOC	1.21	3.04	2.39	1.54	fructose-bisphosphate aldolase c (brain-type aldolase).
Amotl2	1.37	2.58	1.53	-1.08	angiomotin like 2
ANPEP	-1.72	-6.39	-9.91	-11.68	microsomal aminopeptidase N; myeloid plasma membrane glycoprotein CD13
ANXA5	1.14	1.60	1.35	2.99	annexin V; lipocortin V; endonexin II; calphobindin I (CBP-I)
ANXA8	1.34	2.40	1.23	1.93	annexin VIII (ANX8)
APEX1	1.18	1.34	1.41	2.28	DNA-lyase AP endonuclease 1 APEX nuclease (APEN APE1) REF-1 protein
Apoa1	-1.55	-4.88	-7.01	-8.87	apolipoprotein A-I
APOB	1.13	-1.34	1.08	-3.08	apolipoprotein B
Apoc3	1.43	-5.06	-7.25	-12.24	apolipoprotein C-III
Apoh	-1.64	1.58	1.62	1.00	apolipoprotein H
ARFRP1	1.18	-1.54	1.32	2.49	ARF-related protein (ARP).
ARL2	1.00	1.35	-1.01	2.36	ADP-ribosylation factor-like protein 2
ARNT	-1.14	1.70	1.52	1.00	aryl hydrocarbon receptor nuclear translocator
Arr3	-1.04	2.11	1.60	1.34	arrestin 3, retinal
Arv1	1.01	2.17	1.29	-1.03	ARV1 homolog (S. cerevisiae)
ASMT	1.01	2.85	1.20	-1.07	acetylserotonin O-methyltransferase
ASMTL	-1.04	1.29	1.30	-2.00	acetylserotonin O-methyltransferase-like
at2	-1.03	1.85	1.67	-1.12	angiotensin receptor 2
ATP1B3	-1.41	-1.51	-2.39	-3.81	sodium/potassium-transporting ATPase beta 3 subunit (ATPB3)
ATP2B4	1.21	2.06	1.20	1.35	ATPase, Ca++ transporting, plasma membrane 4
ATP6D	-1.05	2.03	1.21	-1.30	vacuolar proton-ATPase, subunit D; V-ATPase, subunit D
Atp6v0a2	-1.03	1.99	1.20	-1.27	ATPase, H+ transporting

Table B.1. (continued)

Gene Symbol	1 HPI	4 HPI	8 HPI	12 HPI	Gene description
Atp6v0b	1.04	2.42	1.32	1.66	ATPase, H+ transporting, V0 subunit B
Atp6v0e	-1.06	1.88	1.21	-1.13	ATPase, H+ transporting, V0 subunit
Atp6v1e1	1.04	-1.21	1.03	2.61	ATPase, H+ transporting, V1 subunit E isoform 1
Atp6v1h	1.05	1.89	1.25	1.01	ATPase, H+ transporting, lysosomal 50/57kDa, V1 subunit H
AVPR2	1.03	1.45	1.87	-1.08	arginine vasopressin receptor 2 (nephrogenic diabetes insipidus)
B4GALT5	1.19	1.74	1.11	-1.27	UDP-Gal:betaGlcNAc beta 1,4- galactosyltransferase, polypeptide 5
Basp1	1.29	1.53	1.50	4.11	brain abundant, membrane attached signal protein 1
BCL2A1	-1.44	1.20	1.56	3.29	BCL-2-related protein A1 (BCL2A1)
BCORL1	-1.24	2.33	1.32	-1.19	BCL6 co-repressor-like 1
BHLHB2	1.32	2.02	1.29	2.91	basic helix-loop-helix domain containing, class B, 2
Bmp15	1.09	1.87	-1.02	1.03	bone morphogenetic protein 15
BoLA	-1.30	-2.58	-3.66	1.36	MHC class I antigen
BYSL	1.14	2.02	1.30	-1.04	bystin
BZRP	1.12	1.52	1.35	1.96	benzodiazapine receptor (peripheral)
C1QBP	1.09	1.37	1.42	2.17	complement component 1, Q subcomponent binding protein
CA6	-1.05	2.00	1.38	-1.37	carbonic anhydrase VI
CACNA1G	1.08	1.25	2.02	-1.53	calcium channel, voltage-dependent, alpha 1G subunit
Calb3	1.81	1.18	-1.12	-3.67	S100 calcium binding protein G
CAPNS1	1.09	1.46	1.22	3.03	calpain, small subunit 1
CAR-XI	-1.32	1.31	1.70	-1.43	carbonic anhydrase-related XI protein
Cbx6	1.07	2.08	1.44	1.18	chromobox homolog 6
CCKBR	1.05	1.79	1.24	-1.28	cholecystokinin B receptor
CCL2	1.93	1.56	-1.43	2.72	chemokine (C-C motif) ligand 2
CCL20	1.95	1.21	-1.04	1.27	chemokine (C-C motif) ligand 20
CCL8	1.12	1.97	-1.45	1.89	chemokine (C-C motif) ligand 8

Table B.1. (continued)

Gene Symbol	1 HPI	4 HPI	8 HPI	12 HPI	Gene description
CCNA2	1.34	1.57	2.09	1.87	cyclin A2
Ccrl1	-1.27	1.84	1.15	-1.34	chemokine (C-C motif) receptor-like 1
Cd28	1.00	2.33	1.73	1.06	CD28 antigen
CD36	1.46	2.15	1.63	-1.29	platelet glycoprotein IV (GPIV; PAS IV; PAS4); GPIIIB; CD36 antigen
CD37	-1.21	1.68	2.17	-1.06	leukocyte CD37 antigen
CD48	-1.04	-1.23	-1.06	2.08	B-lymphocyte activation marker BLAST-1 precursor; CD48 antigen
CD79A	-1.06	1.21	1.80	3.12	B-cell antigen receptor complex; CD79A antigen
CD9	1.55	1.58	-1.00	3.67	CD9 antigen; p24; leukocyte antigen MIC3; motility-related protein (MRP-1)
CDK11	-1.03	1.97	1.38	-1.40	PITSLRE protein kinase beta 1
CDK5R1	1.17	1.70	1.55	1.06	cyclin-dependent kinase 5 activator precursor (CDK5 activator)
CDX2	-1.70	-1.82	-1.56	-2.72	homeobox protein CDX-2 (caudal-type homeobox protein 2) (CDX-3)
Ceacam1	-1.57	-1.32	-1.42	-2.17	CEA-related cell adhesion molecule 1
Cenph	1.04	1.11	1.38	2.52	centromere autoantigen H
CGA	1.00	1.42	1.66	-1.45	glycoprotein hormone alpha subunit precursor
CHS1	1.25	1.63	1.29	1.14	lysosomal trafficking regulator
CHUK	-1.13	1.82	1.27	-1.50	conserved helix-loop-helix ubiquitous kinase
CLDN2	-1.70	-2.23	-3.14	-4.46	claudin 2
CLDN3	1.83	-1.74	1.29	2.84	claudin 3
CLECSF1	-1.09	2.29	1.33	-1.07	lectin, superfamily member 1(cartilage-derived)
Clic1	1.28	1.46	1.29	2.73	chloride intracellular channel 1
Clstn3	1.08	2.54	1.26	1.05	calsyntenin 3
c-met	1.04	1.78	1.35	-1.17	HGF receptor c-Met
Coch	1.16	1.71	1.73	1.00	coagulation factor C homolog, cochlin
Cog6	1.01	-1.30	3.10	-1.31	component of oligomeric golgi complex 6
Col1a1	-1.29	1.39	1.10	-2.72	collagen, type I, alpha 1

Table B.1. (continued)

Gene Symbol	1 HPI	4 HPI	8 HPI	12 HPI	Gene description
COL1A2	-1.09	1.58	1.86	-1.54	procollagen 1 alpha 2 subunit precursor (COL1A2)
COQ7	-1.05	1.90	1.51	-1.08	timing protein CLK-1
CPGES	1.06	1.65	1.13	2.50	cytosolic prostaglandin E synthase
Cplx2	1.15	1.94	3.36	1.23	complexin 2
CPSF1	1.48	-1.58	-1.01	2.25	cleavage and polyadenylation specificity factor, 160 kd subunit
Cpsf3	-1.10	1.77	1.31	1.22	cleavage and polyadenylation specificity factor 3
CR452642	-1.17	1.71	1.31	-1.42	similar to DnaJ (Hsp40) homolog, subfamily C, member 17
Crebl1	-1.12	2.26	1.46	1.07	cAMP responsive element binding protein-like 1
CRHR1	-1.09	1.99	2.08	-1.33	corticotropin releasing hormone receptor 1
Crip1	-1.14	-1.34	-2.54	-2.01	cysteine-rich protein 1 (intestinal)
CROT	-1.17	2.13	1.33	-1.64	carnitine O-octanoyltransferase
CSN1S2	1.10	1.92	1.26	-1.37	casein alpha-S2
CSRP2	-1.01	1.70	1.34	1.14	smooth muscle cell lim protein (cysteine-rich protein 2) (CRP2)
CTLA4	1.24	1.87	1.04	2.25	cytotoxic T-lymphocyte-associated protein 4
CTNNBIP1	-1.16	1.68	1.23	-1.56	catenin, beta interacting protein 1
CTSC	1.11	1.70	1.27	2.19	dipeptidyl-peptidase I precursor (DPP-I) cathepsin C cathepsin J
CTSL	1.19	2.28	-1.10	-1.14	cathepsin L precursor major excreted protein (MEP)
CXCR6	-1.15	2.03	1.33	-1.33	chemokine (C-X-C motif) receptor 6
CYP11A1	-1.06	1.66	1.48	-1.09	mitochondrial cytochrome P450 XIA1 precursor P450
DBI	-1.61	2.01	1.67	-1.49	acyl-CoA-binding protein (ACBP) diazepam binding inhibitor (DBI) endozepine
Ddef1	1.11	1.64	1.71	1.15	development and differentiation enhancing factor 1
Denr	-1.06	1.94	1.45	1.10	density-regulated protein
DGKH	-1.14	2.18	1.29	-1.12	diacylglycerol kinase, eta
Dlg5	1.04	1.84	1.10	-1.05	discs, large homolog 5 (Drosophila)
DLK1	-1.13	-1.06	2.81	-1.62	delta-like protein precursor (DLK)

Table B.1. (continued)

Gene Symbol	1 HPI	4 HPI	8 HPI	12 HPI	Gene description
Dnajb11	1.16	1.76	1.25	1.72	DnaJ (Hsp40) homolog, subfamily B, member 11
Dnajb6	1.08	1.34	1.13	2.19	Dnajb6
Dnajc14	-1.30	1.81	1.13	-1.37	DnaJ (Hsp40) homolog, subfamily C, member 14
Dpysl2	1.24	1.40	1.69	1.92	dihydropyrimidinase-like 2
Dspg3	1.06	1.69	1.64	-1.15	dermatan sulphate proteoglycan 3
EGR1	1.92	1.56	1.38	1.68	early growth response protein 1 (hEGR1) transcription factor ETR103
EIF1AX	1.20	1.14	1.13	2.54	eukaryotic translation initiation factor 1A
Eif3s3	-1.08	1.55	1.26	1.99	eukaryotic translation initiation factor 3, subunit 3 (gamma)
EIF4A1	1.12	2.03	-1.06	4.05	eukaryotic initiation factor 4A-I (EIF-4A-I).
EIF4E	1.20	1.53	1.42	2.24	translation initiation factor eIF-4E
Elac1	-1.10	1.97	1.33	-1.29	elaC homolog 1 (E. coli)
Eno1	1.05	1.41	1.20	2.68	enolase 1, alpha non-neuron
Epsti1	1.21	1.61	1.39	3.06	epithelial stromal interaction 1 (breast)
Evc	1.00	1.53	2.03	-1.16	Ellis van Creveld gene homolog (human)
F3	1.29	1.73	1.47	3.27	coagulation factor III (thromboplastin, tissue factor)
FABP	1.21	1.43	2.14	1.65	fatty acid binding protein (heart) like
FBXL6	-1.32	1.55	2.79	-1.66	F-box and leucine-rich repeat protein 6
FECH	1.21	2.14	1.82	1.12	ferrochelatase precursor protoheme ferro-lyase heme synthetase
FES	1.78	2.25	-1.37	-1.07	C-fes proto-oncogene
FEZ1	1.12	2.34	1.47	-1.01	zygini; FEZ1-T
FGFR1OP	1.08	1.92	1.68	-1.15	FGFR1 oncogene partner
FGFR3	1.13	-1.34	-1.00	-2.07	fibroblast growth factor receptor 3 (achondroplasia, thanatophoric dwarfism)
FGIF	1.00	1.73	1.49	-1.08	fetal globin inducing factor
5HTR2A	1.00	1.66	1.80	1.29	5-hydroxytryptamine receptor 2A
FN1	1.38	2.99	1.08	2.57	fibronectin 1

Table B.1. (continued)

Gene Symbol	1 HPI	4 HPI	8 HPI	12 HPI	Gene description
FOS	1.17	2.69	1.19	3.14	v-fos FBJ murine osteosarcoma viral oncogene homolog
Fts	1.18	1.82	-1.15	2.14	fused toes homolog
FUT	-1.86	-1.31	1.41	-2.52	alpha 1,3 fucosyltransferase
Gabarapl1	1.03	1.93	1.28	2.53	GABA(A) receptor-associated protein like 1
GABRA2	1.26	1.57	2.16	1.06	gamma-aminobutyric acid (GABA) A receptor, alpha 2
GABRA3	1.23	1.73	2.17	-1.05	gamma-aminobutyric acid (GABA) A receptor, alpha 3
GABRB1	1.25	2.12	2.02	-1.34	gamma-aminobutyric acid (GABA) A receptor, beta 1
GABRG2	1.00	2.45	3.13	1.26	gamma-aminobutyric acid (GABA) A receptor, gamma 2
GAL	-1.06	2.05	1.29	-1.65	galanin
GAPD	1.00	1.36	1.25	3.84	glyceraldehyde-3-phosphate dehydrogenase
Gapdhs	1.49	-1.35	1.07	-2.22	glyceraldehyde-3-phosphate dehydrogenase, spermatogenic
GDF8	1.03	1.52	1.67	-1.17	growth/differentiation factor 8 precursor (GDF8); myostatin (MSTN)
Ggta1	1.15	-1.20	-2.63	-3.02	glycoprotein galactosyltransferase alpha 1, 3
GLB1	-1.10	1.69	1.34	-1.48	beta-D-galactosidase precursor; lactase; acid beta-galactosidase; GLB1
GNAS1	1.01	1.53	-1.15	2.75	guanine nucleotide binding protein (G protein)
Gng2	1.63	2.59	2.11	3.17	guanine nucleotide binding protein (G protein), gamma 2 subunit
Gng3	1.29	2.66	3.68	1.40	guanine nucleotide binding protein (G protein), gamma 3 subunit
Gnptg	1.07	1.74	1.16	1.03	N-acetylglucosamine-1-phosphate transferase, gamma subunit
Golga7	-1.17	2.05	1.34	1.49	golgi autoantigen, golgin subfamily a, 7
Gpr114	1.98	-1.29	1.15	-1.36	G-protein coupled receptor 114
Gpr89	1.15	1.81	1.16	1.39	G protein-coupled receptor 89
Gprc5b	1.27	2.37	1.96	1.70	G protein-coupled receptor, family C, group 5, member B
GRP	-1.02	1.85	1.42	-1.38	gastrin-releasing peptide
GRP58	1.13	1.12	1.09	2.43	probable protein disulfide isomerase ER-60 precursor (ERP60)
Gsta4	1.71	3.16	2.66	1.58	glutathione S-transferase, alpha 4

Table B.1. (continued)

Gene Symbol	1 HPI	4 HPI	8 HPI	12 HPI	Gene description
GUCY1A3	1.11	2.64	-1.10	1.09	guanylate cyclase 1, soluble, alpha 3
H2AFZ	1.14	1.36	1.56	2.02	histone H2A.Z.
HBE4	1.08	1.65	1.48	-1.17	hemoglobin, beta, epsilon 4 Other Designations: globin, beta,epsilon 4
HDAC2	-1.25	1.93	-1.15	1.42	histone deacetylase 2
HIF1A	1.36	1.65	2.15	3.82	hypoxia-inducible factor 1 alpha (HIF1 alpha)
HNF4A	-2.37	-2.23	-1.26	-3.12	hepatocyte nuclear factor 4 (HNF4) transcription factor 14
HNF4G	-1.60	-2.50	-1.65	-5.71	hepatocyte nuclear factor 4-gamma (HNF4-gamma).
HNT	1.32	1.82	2.24	-1.03	neurotrimin
Hoxc6	1.34	-1.63	-1.01	-1.99	homeo box C6
HPD	1.06	1.77	1.75	1.00	4-hydroxyphenylpyruvate dioxygenase (4HPPD)
HRMT1L2	1.09	1.30	1.43	2.56	suppressor for yeast mutant
hrp-4	1.20	2.51	1.30	-1.49	hepatoma derived growth factor related protein 4
Hsd3b	-1.03	1.90	1.62	3.43	hydroxysteroid dehydrogenase-1, delta<5>-3-beta
HSPA8	-1.00	1.35	1.04	3.34	heat shock 70kDa protein 8
HSPBAP1	-1.07	1.45	1.84	-1.40	HSPB (heat shock 27kDa) associated protein 1
HSPCA	1.23	1.44	1.15	3.58	heat shock 90-kDa protein A (HSP90A HSPCA) HSP86
HTATIP2	-1.47	1.22	1.10	-1.98	CC3 (CC3)
HYAL2	-1.02	2.14	1.15	-1.76	LUCA2 lysosomal hyaluronidase 2 (HYAL2) PH-20 homolog
ID1	1.02	2.34	1.06	-1.04	inhibitor of DNA binding 1, dominant negative helix-loop-helix protein
ID3	-1.27	1.29	-1.04	-2.40	inhibitor of DNA binding 3, dominant negative helix-loop-helix protein
Idh3a	-1.01	2.03	1.38	1.32	isocitrate dehydrogenase 3 (NAD+) alpha
Ifi30	-2.18	-1.55	-1.13	-1.34	interferon gamma inducible protein 30
IFNG	1.15	1.99	1.56	4.34	interferon, gamma
IGF2	-1.18	1.20	3.40	-1.34	insulin-like growth factor II (IGF2) somatomedin A
IGFBP2	1.32	2.06	-1.13	2.19	insulin-like growth factor binding protein 2 (IGFBP2)

Table B.1. (continued)

Gene Symbol	1 HPI	4 HPI	8 HPI	12 HPI	Gene description
IGIP	1.01	1.67	1.16	2.12	IgA regulatory protein
Igj	1.05	-4.73	1.39	-3.51	immunoglobulin joining chain
IL10	1.45	1.10	-1.45	-2.28	interleukin 10
IL17	1.00	1.80	1.30	2.68	interleukin 17 (cytotoxic T-lymphocyte-associated serine esterase 8)
IL18	-1.27	1.20	1.32	-2.00	interleukin 18 (interferon-gamma-inducing factor)
IL1A	2.51	2.07	1.04	2.62	interleukin 1, alpha
il-1r2	1.10	1.10	1.10	-2.50	IL-1 receptor 2
IL22RA1	-1.62	-2.03	-1.88	-2.63	interleukin 22 receptor, alpha 1
IL8	2.41	1.41	-1.25	1.96	interleukin 8
ITGA2	1.03	1.51	1.01	2.27	integrin, alpha 2 (CD49B, alpha 2 subunit of VLA-2 receptor)
ITPR3	-1.26	-1.43	2.49	-1.44	inositol 1,4,5-triphosphate receptor, type 3
JOSD1	1.08	1.95	1.36	1.02	Josephin domain containing 1
KCNH1	-1.03	1.74	1.29	-1.28	voltage-gated potassium channel eagb
Kcnk2	-1.02	1.71	1.11	-1.24	potassium channel, subfamily K, member 2
KERA	-1.09	2.41	1.69	-1.12	keratocan precursor (corneal keratan sulfate proteoglycan 3)
KIF5A	1.20	1.55	1.14	3.83	neuronal kinesin heavy chain (NKHC).
KLP1	-1.01	1.90	1.12	-1.31	K562 cell-derived leucine-zipper-like protein 1
LAMR1	-2.30	1.20	1.09	-1.11	laminin receptor 1 (ribosomal protein SA, 67kDa)
LCP1	1.03	-1.06	-1.04	2.87	L-plastin; lymphocyte cytosolic protein 1 (LCP-1); LC64P
LDHA	1.06	1.60	1.58	2.82	L-lactate dehydrogenase M subunit (LDHA)
Ldlr	1.28	1.82	1.16	-1.13	low density lipoprotein receptor
Lgals8	-1.04	-1.38	2.00	-1.17	lectin, galactoside-binding, soluble, 8 (galectin 8)
LIF	1.04	2.33	1.76	3.26	leukemia inhibitory factor (cholinergic differentiation factor)
LIPF	1.04	1.48	1.96	-1.15	gastric triacylglycerol lipase
LOC282859	-1.01	2.06	1.17	1.00	cytosolic leucine-rich protein

Table B.1. (continued)

Gene Symbol	1 HPI	4 HPI	8 HPI	12 HPI	Gene description
LOC286871	-1.16	2.05	1.67	-1.01	uterine milk protein precursor
LOC404111	-1.03	1.34	1.19	-1.83	epidermal keratin VII
LOC404122	1.12	1.35	1.29	5.92	actin, cytoplasmic 2
LOC404176	1.80	-1.47	1.10	1.72	T-cell receptor delta chain
LOC408018	-1.18	-1.51	1.53	-1.33	C-C motif chemokine receptor 3
LOC493778	-1.36	1.15	1.90	-1.76	up-regulated during vascular calcification
LOC504285	1.03	2.81	1.31	-1.32	similar to presenilin-like protein 1
LOC504323	1.08	1.31	1.20	-2.07	similar to thrombospondin 3
LOC504481	-1.01	2.26	1.65	-1.30	similar to methyl sterol oxidase
LOC504650	-1.11	-1.59	-1.40	-2.05	similar to choline/ethanolaminephosphotransferase 1
LOC504823	-1.07	1.30	-1.09	1.81	similar to nuclear pore complex protein
LOC504856	-1.02	1.30	1.34	-2.10	similar to myeloid/lymphoid or mixed-lineage leukemia
LOC505044	1.23	-1.02	2.14	2.05	similar to Transmembrane protein 123
LOC505214	-1.66	-5.95	1.32	-4.01	similar to cytokeratin 20
LOC505477	1.09	2.38	1.72	1.09	similar to regulator of G protein signaling RGS12
LOC505507	1.01	1.24	1.02	2.98	similar to ribosomal protein S7
LOC505573	-1.13	2.19	1.11	-1.58	similar to Cartilage intermediate layer protein
LOC505740	-1.18	2.07	1.68	-1.48	similar to adenylate cyclase 5
LOC505750	-1.03	1.86	1.17	-1.15	similar to membrane glycoprotein LRIG1
LOC505846	-1.32	1.66	1.39	-2.68	similar to UTP18, small subunit (SSU) processome component
LOC505890	1.49	-2.36	-2.20	-2.29	similar to ADAM DEC1 precursor (ADAM-like protein decysin 1)
LOC505945	1.16	1.11	2.52	1.46	similar to serine/arginine-rich protein specific kinase 2
LOC506423	-1.29	1.14	1.18	-2.01	similar to Glucose 6-phosphate translocase
LOC506606	-1.02	1.84	1.94	-1.37	similar to heterochromatin protein 1 beta
LOC506628	1.45	1.87	1.63	-1.20	chromobox-like protein 2

Table B.1. (continued)

Gene Symbol	1 HPI	4 HPI	8 HPI	12 HPI	Gene description
LOC506692	1.06	-3.40	-3.00	-9.19	similar to N-acetylated alpha-linked acidic dipeptidase-like 1
LOC506751	1.19	2.00	2.28	1.31	similar to Laminin alpha-5 chain
LOC506908	1.35	1.58	2.10	1.04	similar to cytoplasmic linker 2
LOC507032	1.28	2.10	2.00	1.14	similar to Programmed cell death 2-like
LOC507041	1.24	1.41	2.07	-1.15	similar to protein kinase C epsilon
LOC507149	1.06	2.16	1.03	1.23	similar to Cyclin-dependent kinase 8
LOC507478	1.25	1.56	1.22	1.94	similar to RNA U, small nuclear RNA export adaptor
LOC507969	-1.30	1.39	1.18	-2.11	similar to Solute carrier organic anion transporter family
LOC508025	1.03	2.21	1.54	1.00	similar to zinc finger protein 423
LOC508108	-2.60	1.56	1.62	-2.26	beta-4-N-acetylgalactosaminyltransferase
LOC508133	1.14	1.80	1.91	2.31	similar to syndecan 4
LOC508169	1.21	1.37	-1.01	2.57	similar to zinc transporter 5
LOC508208	-1.00	1.84	1.01	-1.03	similar to LATS, large tumor suppressor, homolog 2
LOC508245	-1.25	1.72	1.00	-1.49	similar to Ribonuclease T2 precursor
LOC508291	1.01	1.27	1.60	-1.18	similar to Huntingtin-interacting protein 1-related protein
LOC508490	1.61	1.73	1.50	1.97	similar to integrin alpha 3
LOC508637	-1.03	2.16	-1.07	2.42	similar to Sushi domain containing 4
LOC508781	-1.03	1.92	1.77	-1.51	similar to Dimethylaniline monooxygenase [N-oxide-forming] 1
LOC508935	1.13	1.45	1.30	-1.90	similar to Symplekin
LOC509302	-1.03	2.07	1.69	1.58	similar to DnaJ homology subfamily A member 5
LOC509566	1.00	1.16	1.28	2.43	similar to fructose-1,6-bisphosphate aldolase A
LOC509885	1.02	2.75	1.53	1.02	similar to isoleucyl-tRNA synthetase
LOC510050	1.10	1.18	1.21	2.84	similar to TG-interacting factor
LOC510095	-1.04	1.82	1.06	-1.30	similar to retinoblastoma-associated protein RAP140
LOC510267	1.23	-1.04	1.41	2.21	similar to thymopoietin isoform gamma

Table B.1. (continued)

Gene Symbol	1 HPI	4 HPI	8 HPI	12 HPI	Gene description
LOC510361	1.25	1.66	1.94	-1.16	similar to HIV-1 Rev binding protein-like
LOC510413	1.13	1.69	1.10	1.03	similar to PCAF associated factor 65 beta
LOC510417	-1.32	-3.12	-2.38	1.26	MHC class I heavy chain
LOC510486	1.08	1.82	1.14	1.20	similar to Transmembrane and coiled-coil domain family 1
LOC510506	1.13	-2.45	1.07	-6.55	similar to carbamoyl phosphate synthetase 1
LOC510801	1.00	1.47	1.94	-1.42	similar to Carbonic anhydrase I
LOC510879	1.27	1.85	2.78	-1.42	similar to intersectin long
LOC510923	-1.05	2.78	1.60	1.99	similar to estrogen responsive finger protein
LOC511045	-1.14	1.33	1.75	-1.32	similar to dynactin 1 p150
LOC511329	1.01	1.75	1.78	-1.16	similar to poly (ADP-ribose) polymerase family, member 6
LOC511430	-1.40	-2.46	-4.10	-2.48	similar to down-regulated in colon cancer 1
LOC511558	-1.44	1.43	1.24	-2.09	similar to glycerol 3-phosphate permease
LOC511619	-1.17	2.00	1.28	-1.28	similar to conductin
LOC512082	-1.04	2.17	1.49	-1.17	not available
LOC512110	1.02	2.66	1.17	-1.47	similar to Protein KIAA0195 (Transmembrane protein 94)
LOC512459	1.00	1.64	1.45	1.00	similar to glutamic acid decarboxylase
LOC512512	-2.21	-1.43	1.32	-1.63	similar to DNase1-Like III protein
LOC512524	-1.06	-1.44	1.68	-1.11	similar to Sushi domain containing 3
LOC512653	-1.11	1.86	1.90	-1.30	similar to Prenylated Rab acceptor protein 1
LOC512779	1.21	1.74	3.02	1.28	similar to chromosome 18 open reading frame 21
LOC512958	1.05	2.23	-4.07	-1.12	similar to delta8-delta7 sterol isomerase related protein EBRP
LOC513251	1.00	1.03	1.77	-1.50	similar to Chromosome 4 open reading frame 33
LOC513270	-1.08	-1.44	1.80	-1.09	similar to nucleoporin 153kDa
LOC513412	1.09	1.39	1.69	1.00	similar to junctional adhesion molecule 3
LOC513554	-1.03	1.69	1.79	-1.57	similar to acyl-CoA:cholesterol acyltransferase 2

Table B.1. (continued)

Gene Symbol	1 HPI	4 HPI	8 HPI	12 HPI	Gene description
LOC513641	-1.28	-1.02	2.70	-1.29	similar to hematopoietic protein 1
LOC513855	1.00	1.53	1.70	-1.02	similar to delta 4-3-oxosteroid 5 beta-reductase
LOC513856	-1.96	1.32	1.56	-2.03	similar to alpha-2-macroglobulin
LOC513990	1.14	1.45	2.02	5.43	similar to interferon-gamma induced monokine CXCL9
LOC514192	-1.06	1.77	1.26	-1.15	similar to YEATS domain containing 2
LOC514269	-1.15	1.63	-1.00	-1.05	similar to nephrocystin
LOC514644	-1.16	-1.09	1.71	-1.23	similar to phosphatase and actin regulator 4
LOC514819	1.00	1.79	2.10	-1.15	similar to transmembrane receptor
LOC514947	-1.00	1.75	-1.35	-1.26	similar to zinc finger protein ZNF287
LOC515078	-1.09	1.88	1.41	-1.20	similar to transmembrane protein 62
LOC515578	-1.20	1.42	1.24	-2.45	similar to C-terminal binding protein 1
LOC515593	1.39	2.24	-1.35	1.50	similar to microtubule-associated protein 1A
LOC515860	1.02	3.00	1.06	-1.10	similar to peroxidasin homolog
LOC516008	1.00	1.62	1.50	-1.05	similar to CD200 cell surface glycoprotein receptor
LOC516104	-1.09	2.53	-1.89	1.98	similar to putative alpha chemokine
LOC516630	-1.19	1.01	1.33	1.89	imilar to SNF2 histone linker PHD RING helicase
LOC516689	1.51	2.25	1.80	2.07	similar to proteolipid M6B isoform TMD-omega
LOC517531	1.10	1.64	1.46	1.10	similar to Mitochondrial intermediate peptidase
LOC518274	1.38	1.61	1.62	1.16	similar to actin binding protein anillin
LOC518974	1.05	1.05	1.55	-2.19	similar to vacuolar proton pump 116 kDa accessory subunit
LOC519018	-1.19	1.54	1.59	-1.49	similar to S-phase kinase-associated protein 2
LOC520178	1.07	2.01	-2.23	1.10	similar to protein-tyrosine-phosphatase
LOC520842	-1.82	-1.20	-1.20	-3.72	similar to kruppel-like factor 4
LOC521318	1.19	-1.03	1.59	-1.21	similar to cardiotrophin-2
LOC521424	-1.36	1.61	1.31	2.99	similar to squamous cell-specific protein

Table B.1. (continued)

Gene Symbol	1 HPI	4 HPI	8 HPI	12 HPI	Gene description
LOC521728	1.27	1.84	1.67	-1.34	similar to cation-transporting P5-ATPase
LOC521784	1.12	1.84	1.25	1.36	similar to Transmembrane protein 16F
LOC521939	1.10	-1.08	1.15	-2.00	similar to Cyclin A1
LOC523542	1.79	-1.42	1.13	3.47	similar to casein kinase I delta
LOC525095	-1.07	1.70	1.70	-1.14	similar to Phosphatidylinositol glycan anchor biosynthesis
LOC525427	-1.36	-1.19	1.34	-2.76	similar to engulfment and cell motility 3
LOC525835	1.00	2.64	1.90	1.97	similar to heparan sulfate D-glucosaminyl 3-O-sulfotransferase 4
LOC526544	-1.25	1.30	2.28	-1.10	frequenin-like protein
LOC527732	1.20	2.28	-1.06	-1.08	similar to plakophilin 4
LOC528252	1.23	1.22	1.71	-1.22	similar to talin 2
LOC530050	-2.29	-1.55	1.06	-2.21	similar to smooth muscle myosin heavy chain 11 isoform SM2A
LOC530659	1.09	2.12	1.25	1.11	similar to integral inner nuclear membrane protein MAN1
LOC530884	2.43	1.62	1.14	1.56	similar to receptor activator of nuclear factor-kappa B
LOC532569	1.04	2.02	1.19	5.08	similar to Calgranulin B (Migration inhibitory factor-related protein 14) (MRP-14)
LOC532671	2.05	-1.38	1.24	-1.19	similar to mucolipin 2
LOC532944	1.03	1.77	1.11	-1.28	similar to lipoma HMGIC fusion partner
LOC533187	1.21	1.70	1.56	-1.06	similar to HMG-BOX transcription factor BBX
LOC533199	1.12	2.65	1.29	2.31	similar to Dual specificity mitogen-activated protein kinase kinase 1 (MAPKK 1)
LOC533243	-1.02	1.72	1.43	-1.06	similar to zinc finger protein 143
LOC533248	1.25	1.97	1.54	1.78	similar to Hook-related protein 1
LOC533449	-1.04	1.25	1.88	-2.19	similar to ten integrin EGF-like repeat domains protein
LOC533590	1.02	1.46	1.29	2.50	similar to protein-tyrosine phosphatase
LOC533634	1.12	1.60	1.83	1.15	similar to oxysterol-binding protein-like protein 6
LOC533642	-1.02	1.56	1.63	1.21	similar to Procollagen-lysine, 2-oxoglutarate 5-dioxygenase 2
LOC533669	1.08	1.61	1.16	2.24	similar to ATP-binding cassette, sub-family B (MDR/TAP)

Table B.1. (continued)

Gene Symbol	1 HPI	4 HPI	8 HPI	12 HPI	Gene description
LOC533823	1.26	1.57	-1.04	2.33	similar to Rho guanine nucleotide exchange factor 6 (Rac/Cdc42)
LOC534010	-1.01	1.79	1.78	-1.34	similar to HMG-box transcription factor
LOC534185	-1.31	1.73	1.14	1.29	similar to 28S ribosomal protein S31, mitochondrial precursor
LOC534594	-1.04	1.92	1.37	-1.23	similar to dTDP-D-glucose 4,6-dehydratase
LOC534661	1.20	1.33	2.06	1.68	similar to Paired box protein Pax-8
LOC534815	-1.05	1.36	1.70	1.21	similar to Phosphoinositide-3-kinase, class 3
LOC534850	1.02	1.81	1.14	-1.56	similar to chromosome 10 open reading frame 38
LOC534891	1.18	1.95	1.10	-1.31	similar to transmembrane protein 63B
LOC534896	1.82	-1.32	1.25	-1.42	similar to centrosome-associated protein 350
LOC534970	-1.26	1.57	1.16	-1.32	similar to ribosomal protein L26 homolog
LOC535138	1.29	1.97	1.11	1.28	similar to CDC91 cell division cycle 91-like 1
LOC535152	-1.10	-1.02	1.23	2.36	similar to DEAD box RNA helicase DP97
LOC535399	1.25	2.26	1.22	-1.01	similar to lymphoid enhancer binding factor-1
LOC535490	1.07	1.23	-1.03	-2.27	similar to melanoma differentiation associated protein-5
LOC536307	-1.36	1.66	-1.05	-2.38	KRAB domain-containing zinc finger protein
LOC536989	1.06	1.45	1.90	-1.19	similar to tumor endothelial marker 7
LOC537246	1.20	1.96	1.45	1.27	similar to Transcription intermediary factor 1-alpha (TIF1-alpha)
LOC537280	1.04	1.77	1.50	-1.26	similar to solute carrier 19A3
LOC537487	-1.09	1.36	1.73	-1.18	similar to bone specific CMF608
LOC537631	1.02	2.49	2.70	1.21	similar to JNK3 beta2 protein kinase
LOC538576	1.81	-1.20	1.18	-1.44	similar to oxysterol-binding protein-like protein
LOC538754	-1.10	1.97	1.19	-1.19	similar to Protein phosphatase 1
LOC538905	-1.21	2.08	1.40	-1.24	similar to peroxisomal protein (PeP)
LOC538924	-1.13	2.42	2.05	-1.05	similar to cadherin 20, type 2 preproprotein
LOC538983	-1.01	1.35	2.16	1.29	similar to transcription associated factor TAFII31L

Table B.1. (continued)

Gene Symbol	1 HPI	4 HPI	8 HPI	12 HPI	Gene description
LOC539106	1.10	2.02	1.22	-1.18	similar to Centrobin, centrosomal BRCA2 interacting protein
LOC539139	-1.21	1.81	1.09	-1.31	similar to Kruppel-like factor 9
LOC539145	1.10	1.84	1.67	2.07	similar to OTU domain containing 5
LOC539270	-1.21	1.31	1.09	-2.05	similar to activator of basal transcription 1
LOC539312	1.00	1.17	2.30	-1.57	similar to zinc finger protein of the cerebellum 4
LOC539449	1.68	2.15	1.14	1.12	similar to serum-inducible kinase
LOC539689	-1.41	1.41	1.50	-1.86	similar to Cartilage paired-class homeoprotein 1
LOC539797	1.00	1.36	1.70	-1.15	similar to rhotekin-2
LOC539882	1.41	2.88	1.72	2.13	similar to tubulin, alpha 1
LOC539899	-1.00	1.85	1.14	-1.97	similar to ryanodine receptor 3
LOC540002	-1.21	2.27	1.33	-1.28	similar to Chondroitin polymerizing factor
LOC540007	-1.20	1.10	2.02	-2.35	similar to fatty acid amide hydrolase
LOC540135	1.62	1.21	-2.79	2.42	similar to pleckstrin homology-like domain, family A, member 1
LOC540376	-1.07	1.96	1.34	-1.03	similar to Alpha-methylacyl-CoA racemase
LOC540481	-1.26	1.05	1.88	-2.20	similar to T-cell transcription factor-4 long C-terminal
LOC540568	-1.09	1.56	-1.01	2.44	Atp2a2
LOC540642	1.07	2.07	1.32	1.31	similar to F-box and WD-40 domain protein 11
LOC540768	-1.08	1.94	1.50	-1.17	similar to voltage-gated potassium channel
LOC540789	-1.19	2.03	1.45	1.03	similar to poly (ADP-ribose) polymerase family, member 14
LOC540853	-1.04	2.69	1.27	1.00	similar to synaptosomal-associated protein 25
LOC541143	1.19	2.00	1.21	1.04	similar to zinc finger protein 131
LOC613326	1.44	1.18	1.22	2.17	similar to tyrosine phosphatase
LOC613527	-1.12	1.41	1.87	-1.36	similar to cystinosin
LOC613767	-1.06	1.90	1.00	1.24	similar to Cyclin-dependent kinase 2-interacting protein
LOC613886	-1.27	-1.22	2.90	-2.05	similar to protein tyrosine phosphatase-like

Table B.1. (continued)

Gene Symbol	1 HPI	4 HPI	8 HPI	12 HPI	Gene description
LOC614612	2.03	1.05	2.13	-1.06	similar to Steroid 5 alpha-reductase 1
LOC614661	-1.14	1.55	1.77	-1.15	similar to coronin 6
LOC614716	-1.04	1.74	1.40	-1.07	similar to Chain A, Crystal Structure Of Human Auh Protein
LOC615223	-1.22	-1.02	-1.10	-3.34	similar to butyrophilin-like 9
LOC615232	1.07	1.67	-1.08	-1.40	similar to inositol 1,4,5-triphophate 5-phosphatase
LOC615390	-1.06	-1.29	-1.43	-2.30	similar to Brain protein I3
LOC615430	1.08	1.33	1.37	2.06	similar to Parvin, alpha
LOC615890	1.05	1.59	-1.10	1.10	similar to glycerophosphodiester phosphodiesterase domain containing 1
LOC616048	1.00	1.98	1.24	-1.23	similar to testis and skeletal muscle-specific dual specificity phosphatase
LOC616089	-1.51	-1.39	-1.21	-2.26	similar to PDZ domain containing 6
LOC617531	-1.15	1.99	2.08	-1.26	similar to Calcium and integrin binding family member 2
LOC617927	1.00	1.93	-1.03	-1.12	similar to beta1-syntrophin
LOC618631	-1.26	1.13	2.02	-1.54	similar to serine/threonine protein kinase
Lrp8	1.05	1.95	1.12	1.87	low density lipoprotein receptor-related protein 8, apolipoprotein e receptor
Lsm1	1.19	2.36	1.12	1.48	LSM1 homolog, U6 small nuclear RNA associated (S. cerevisiae)
Lsm3	1.20	1.25	1.19	2.72	LSM3 homolog, U6 small nuclear RNA associated (S. cerevisiae)
LUM	-1.91	-1.26	-1.05	-2.19	lumican precursor (LUM); keratan sulfate proteoglycan; LDC
MAGP2	-1.09	1.63	1.33	-1.49	microfibril-associated glycoprotein-2
MAP1B	1.21	3.35	1.07	-1.05	microtubule-associated protein 1B
MDH2	-1.10	2.26	1.39	-1.40	malate dehydrogenase precursor
Mdk	-1.25	1.96	1.82	-1.34	midkine
MDP-1	-1.16	1.71	1.18	-1.29	magnesium-dependent phosphatase 1
Mest	1.26	1.71	1.75	1.27	mesoderm specific transcript homolog (mouse)
MGC127016	1.88	1.32	-1.34	-1.43	similar to Cell death activator CIDE-B
MGC127133	-1.49	-1.34	-1.61	-2.68	20-beta-hydroxysteroid dehydrogenase-like

Table B.1. (continued)

Gene Symbol	1 HPI	4 HPI	8 HPI	12 HPI	Gene description
MGC127182	-1.41	-1.07	-1.33	-3.08	similar to sulfotransferase family, cytosolic, 1B, member 1
MGC127210	-1.04	1.19	1.35	2.01	similar to OTU domain, ubiquitin aldehyde binding 1
MGC127229	-1.75	-2.89	-2.80	-8.61	similar to Fructose-bisphosphate aldolase B (Liver-type aldolase)
MGC127247	1.21	1.39	1.56	2.10	similar to interferon-related developmental regulator 1
MGC127304	-1.01	1.85	1.54	1.07	similar to eukaryotic translation initiation factor 3
MGC127325	-1.50	-1.16	1.58	-2.71	similar to CNDP dipeptidase 2
MGC127374	-1.10	1.65	1.22	-1.41	similar to Adipocyte plasma membrane-associated protein
MGC127438	1.03	-1.21	-2.20	3.43	similar to ribosomal protein L28
MGC127494	1.08	1.47	1.41	2.19	similar to SPARC-like protein 1 precursor (High endothelial venule protein)
MGC127504	-1.14	1.46	-1.04	2.12	similar to Lysyl-tRNA synthetase
MGC127555	-1.17	1.68	1.12	1.24	similar to Probable rRNA processing protein EBP2
MGC127635	1.11	1.51	1.56	2.49	similar to Ran-specific GTPase-activating protein
MGC127744	1.27	2.77	-2.19	-1.02	similar to Carbonic anhydrase III (Carbonate dehydratase III)
MGC127769	1.62	1.24	1.91	-1.02	similar to cAMP responsive element modulator
MGC127813	-1.30	-3.59	-2.20	-7.39	similar to Apolipoprotein A-IV precursor (Apo-AIV)
MGC127814	-1.33	-3.76	1.44	-6.61	similar to Complement component C9 precursor
MGC127936	-1.02	3.23	1.80	3.50	similar to S100 calcium-binding protein A2 (S-100L protein)
MGC127996	-1.18	1.77	1.35	-1.33	similar to poly(rC) binding protein 2
MGC128000	-1.20	2.75	1.32	-1.52	similar to nuclear protein E3-3
MGC128059	1.18	1.34	1.12	2.25	similar to ADP-ribosylation factor 4
MGC128147	-1.22	1.71	-1.31	3.59	similar to threonyl-tRNA synthetase
MGC128158	1.02	2.00	1.90	1.00	similar to optineurin
MGC128237	-1.22	1.99	-1.02	2.05	similar to ubiquinol-cytochrome c reductase binding protein
MGC128370	-1.07	-1.04	1.28	2.26	similar to Polyadenylate-binding protein-interacting protein 2
MGC128467	1.22	3.28	1.77	2.75	similar to Nuclear factor 1 A-type (Nuclear factor 1/A) (NF1-A)

Table B.1. (continued)

Gene Symbol	1 HPI	4 HPI	8 HPI	12 HPI	Gene description
MGC128573	-1.31	2.23	2.16	1.81	similar to radical S-adenosyl methionine domain containing 2
MGC128669	1.15	1.83	1.91	1.09	similar to HIV-1 Rev-binding protein 2
MGC128683	1.78	-1.28	1.18	2.45	similar to Nucleolar protein 11
MGC128711	1.30	2.96	1.22	-1.07	similar to Ribonuclease P protein subunit p30 (RNaseP protein p30)
MGC128732	-1.11	3.03	1.24	-1.14	similar to Cell division cycle 7-related protein kinase (CDC7-related kinase)
MGC128745	1.14	2.00	1.67	1.90	similar to CUE domain containing 2
MGC128752	1.14	1.51	1.70	-1.04	similar to 26S proteasome non-ATPase regulatory subunit 9
MGC128827	1.39	1.29	1.09	2.81	similar to proliferation-associated 2G4
MGC128838	1.15	1.31	-1.13	2.04	similar to peroxisomal LON protease-like
MGC128881	1.00	1.21	2.70	1.31	similar to solute carrier family 22 (organic cation transporter)
MGC128932	-1.02	1.79	-1.23	-1.26	similar to RAB28, member RAS oncogene family
MGC128970	1.13	1.62	1.11	-1.36	similar to T-cell immunomodulatory protein
MGC129048	1.09	1.29	1.91	1.93	similar to Annexin A3 (Annexin III)
MGC129081	-1.22	2.03	1.39	-1.30	similar to family with sequence similarity 48, member A
MGC129121	1.20	1.67	1.47	2.51	similar to Myeloid leukemia factor 2
MGC133516	1.17	1.01	-1.07	3.29	similar to Transcription initiation factor IIA gamma chain
MGC133675	1.11	1.62	1.71	-1.18	similar to CD59 antigen p18-20
MGC133868	-1.04	1.65	1.43	2.47	similar to basic transcription factor 3-like 4
MGC133975	-1.21	1.30	1.92	1.29	similar to BCL2/adenovirus E1B 19kD interacting protein 1 isoform
MGC134157	-1.02	2.18	1.44	-1.05	imilar to DnaJ (Hsp40) homolog, subfamily C, member 11
MGC134255	-1.00	1.60	1.39	-1.14	similar to Propionyl-CoA carboxylase beta chain
MGC134308	-1.03	2.33	1.52	-1.23	similar to Nit protein 2
MGC134398	-1.18	1.77	-1.10	-1.49	similar to mitogen-activated protein kinase kinase 2
MGC134600	1.22	1.47	1.76	1.60	similar to Stomatin-like protein 2 (SLP-2)
MGC137117	-1.11	1.17	1.05	-2.17	similar to unc-51-like kinase 3

Table B.1. (continued)

Gene Symbol	1 HPI	4 HPI	8 HPI	12 HPI	Gene description
MGC137132	-1.44	-2.37	-3.12	-3.69	similar to Dehydrogenase/reductase SDR family member 8 precursor
MGC137138	-1.03	1.87	1.12	1.03	similar to transcription elongation factor B
MGC137242	-1.05	1.93	2.37	1.29	similar to DnaJ (Hsp40) homolog, subfamily C, member 17
MGC137296	-1.07	1.99	1.46	-1.18	similar to peroxisomal biogenesis factor 16
MGC137365	-1.08	2.01	1.45	1.18	similar to four and a half LIM domains 2
MGC137449	1.15	1.65	1.07	1.94	similar to putative MAPK activating protein PM20
MGC137500	1.06	1.69	1.25	2.28	similar to Serine/threonine-protein kinase 16
MGC137522	-1.08	1.80	1.25	1.16	similar to glucocerebrosidase precursor
MGC137635	-1.16	1.70	1.34	-1.20	similar to ubiquitin specific protease 2
MGC137760	1.18	1.34	1.69	-1.11	similar to Mitochondrial 28S ribosomal protein S21
MGC137952	1.20	1.27	-1.05	2.16	similar to ubiquitin carboxyl-terminal hydrolase
MGC138046	1.07	2.53	-1.05	-1.04	similar to chromatin modifying protein 4C
MGC138937	1.16	1.74	1.45	1.56	similar to zinc finger, CSL domain containing 2
MGC139005	1.08	1.14	1.52	-1.02	similar to DNMT1 associated protein-1
MGC139009	-1.01	1.49	1.74	-1.01	similar to family with sequence similarity 82, member C
MGC139067	1.05	2.48	1.33	-1.01	similar to potassium channel modulatory factor 1
MGC139256	1.30	1.97	1.78	-1.01	similar to Probable G-protein coupled receptor 37 precursor
MGC139258	-1.18	2.01	1.27	1.05	similar to Zinc-finger protein RFP (Ret finger protein)
MGC139294	1.15	2.24	1.36	1.19	similar to immunoglobulin superfamily, member 4B
MGC139338	-1.12	2.02	1.67	1.19	similar to nuclear receptor subfamily 4
MGC139346	-1.03	1.68	1.14	-1.12	similar to Sphingomyelin phosphodiesterase 2
MGC139360	-1.16	1.24	3.00	-2.15	similar to sulfatase modifying factor 1
MGC139389	1.23	1.23	1.84	1.08	similar to B-cell CLL/lymphoma 11A
MGC139473	1.27	1.49	1.77	1.40	similar to PRP19/PSO4 homolog (Nuclear matrix protein 200)
MGC139803	1.15	1.80	1.08	1.05	similar to Ras-related protein Rab-5A

Table B.1. (continued)

Gene Symbol	1 HPI	4 HPI	8 HPI	12 HPI	Gene description
MGC139829	1.14	2.59	1.42	1.06	similar to stromal cell derived factor receptor 1
MGC139875	-1.24	2.34	1.15	-1.21	similar to anti-silencing function 1B
MGC139976	-1.06	2.15	1.24	1.05	similar to Syndecan-1 precursor (SYND1) (CD138 antigen)
MGC140041	-1.04	1.31	1.43	3.27	similar to Alpha-actinin 3
MGC140052	-1.07	-1.24	2.00	-1.14	similar to ubiquitin-activating enzyme E1C
MGC140063	-1.10	1.78	1.67	-1.20	similar to Transmembrane protein 45a
MGC140228	1.25	-1.38	1.02	2.39	similar to aplysia ras-related homolog A2
MGC140497	-1.31	1.39	-1.01	-2.09	similar to cytochrome P450, family 2, subfamily U, polypeptide 1
MGC140534	-1.08	-1.74	-1.12	-2.42	similar to solute carrier family 43, member 2
MGC140571	-1.02	1.33	-1.02	-1.90	similar to Cbp/p300-interacting transactivator
MGC140605	-1.09	1.26	-1.14	2.59	similar to S100 calcium binding protein A16
MGC140624	1.36	1.84	1.40	-1.13	similar to Septin-8
MGC140634	-1.04	1.78	1.46	-1.10	similar to Olfactomedin-like protein 3 precursor
MGC140655	-1.30	1.87	1.68	-1.22	similar to LIM and cysteine-rich domains 1 (predicted)
MGC140671	-1.01	1.89	1.32	-1.38	similar to lactamase, beta 2
MGC140687	1.05	1.04	1.99	2.32	similar to Telomeric repeat binding factor 2 interacting protein 1
MGC140699	1.39	1.86	1.69	1.22	similar to p53-induced protein
MGC140755	1.00	2.13	1.49	-1.10	similar to TatD DNase domain containing 1
MGC142416	-1.08	2.16	1.40	-1.29	similar to Calcium/calmodulin-dependent protein kinase type 1B
MGC142546	-1.01	1.89	1.30	-1.61	similar to chromosome 9 open reading frame 19
MGC142566	-1.22	-1.39	-1.95	-3.64	similar to retinoic acid receptor responder
MGC142585	1.05	1.96	1.31	1.09	similar to Leucine zipper-EF-hand containing transmembrane protein
MGC142613	1.00	2.15	1.51	-1.27	similar to Nucleolar protein 10
MGC142672	1.45	1.96	1.24	2.64	similar to core 1 synthase
MGC142673	1.10	1.48	1.17	2.17	similar to pleckstrin homology-like domain family A member 2

Table B.1. (continued)

Gene Symbol	1 HPI	4 HPI	8 HPI	12 HPI	Gene description
MGC142842	1.12	2.97	2.55	3.08	similar to guanylate-binding protein 5
MGC143166	1.14	1.50	1.97	-1.34	similar to Fetal brain protein 239
MGC143250	1.00	1.35	1.79	-1.21	kelch repeat and BTB (POZ) domain containing 4
MGC143259	1.67	-1.65	1.00	1.03	similar to DNA polymerase gamma subunit 2, mitochondrial precursor
MGC143385	1.06	1.88	1.68	1.26	similar to MANSC domain containing 1
MGC152096	1.32	2.09	1.93	1.40	similar to oxidation resistance 1
MMP13	-1.02	2.08	1.81	5.61	matrix metalloproteinase 13 (MMP13) collagenase 3 precursor
Mpeg1	-2.28	-1.71	-1.41	-1.35	macrophage expressed gene 1
MPV17	1.22	1.26	1.98	1.33	MPV17 protein
Mpzl1	1.07	3.04	1.09	-1.16	myelin protein zero-like 1
Mrpl19	-1.03	2.29	1.24	1.31	DEP domain containing 6
Mrpl20	-1.04	2.02	1.24	1.12	mitochondrial ribosomal protein L20
Mrpl30	1.22	2.63	1.51	1.41	mitochondrial ribosomal protein L30
Mrpl9	-1.25	2.21	1.23	-2.02	mitochondrial ribosomal protein L9
MTCBP-1	1.20	-1.15	1.07	-2.12	membrane-type 1 matrix metalloproteinase cytoplasmic tail binding protein-1
MUC15	-1.29	1.20	1.66	-1.11	mucin 15
MX1	1.14	1.43	1.31	2.89	interferon-regulated resistance GTP-binding protein MXA (IFI-78K)
MYB	1.49	1.88	2.52	1.72	myb proto-oncogene c-myb
MYL1	-1.13	2.13	1.24	-1.11	myosin, light polypeptide 1, alkali; skeletal, fast
Myo1a	-1.20	1.00	1.13	-2.29	myosin IA
NASP	1.05	1.43	1.33	2.14	nuclear autoantigenic sperm protein (NASP)
NDUFV3	-1.14	2.30	1.20	-1.22	NADH dehydrogenase (ubiquinone) flavoprotein 3
NFKBIA	1.32	1.25	1.27	3.05	nuclear factor of kappa light polypeptide gene enhancer in B-cells inhibitor, alpha
NMB	-1.08	1.90	1.28	-1.59	neuromedin B
NQO1	1.11	3.05	1.86	1.06	NAD(P)H dehydrogenase quinone reductase DT-diaphorase azoreductase

Table B.1. (continued)

Gene Symbol	1 HPI	4 HPI	8 HPI	12 HPI	Gene description
Nr2e3	1.01	1.81	1.19	-1.27	nuclear receptor subfamily 2, group E, member 3
NRXN3	-1.33	1.23	1.07	2.09	neurexin III alpha
NSEP1	1.13	1.27	-1.09	5.83	nuclease-sensitive element DNA-binding protein (NSEP)
NUDT21	-1.03	1.96	1.28	1.52	nudix (nucleoside diphosphate linked moiety X)-type motif 21
Nusap1	1.32	1.23	1.78	1.56	nucleolar and spindle associated protein 1
OAS1	-1.06	1.40	1.41	3.43	(2'-5')oligoadenylate synthetase 1 ((2-5')oligo(A) synthetase 1; 2-5A synthetase 1)
Ociad1	-1.02	1.99	1.93	2.49	OCIA domain containing 1
OCLN	1.07	-1.04	-1.19	-2.55	occludin
Ogn	1.06	-1.79	-2.21	-5.69	osteoglycin
OSTF1	1.20	2.22	1.27	1.32	osteoclast stimulating factor
OTC	-1.29	-1.21	-1.41	-2.05	ornithine carbamoyltransferase precursor
PAG7	3.13	1.31	1.71	-1.09	pregnancy-associated glycoprotein 7
PDC-109	1.00	1.83	1.33	-1.13	seminal vesicle secretory protein 109
Pde6a	1.00	1.52	1.57	-1.14	phosphodiesterase 6A, cGMP-specific, rod, alpha
PDE9A	1.28	1.00	1.19	-2.89	phosphodiesterase 9A
PDPN	1.29	2.76	1.95	2.88	podoplanin Other Designations: aggrus
Pdxp	1.01	1.99	1.57	1.99	pyridoxal (pyridoxine, vitamin B6) phosphatase
PEPT1	1.31	-1.53	-1.24	-3.09	proton-dependent gastrointestinal peptide transporter 1
PGAM1	1.17	1.50	-1.02	2.12	brain-form phosphoglycerate mutase; PGAM-B; BPG-dependent PGAM
pgk1	1.05	1.73	1.17	2.40	phosphoglycerate kinase 1
Plac8	1.09	4.37	3.04	3.58	placenta-specific 8
PLAU	1.02	2.42	1.76	1.93	plasminogen activator, urokinase
PLCB1	1.29	1.72	1.89	1.17	phospholipase C, beta 1 (phosphoinositide-specific)
Plp2	1.01	1.55	1.55	2.06	proteolipid protein 2
Pnn	-1.13	2.36	1.51	-1.48	pinin

Table B.1. (continued)

Gene Symbol	1 HPI	4 HPI	8 HPI	12 HPI	Gene description
POLR2F	-1.23	1.80	1.24	-1.34	DNA-directed rna polymerase ii 14.4 kd polypeptide (RPB6)
PP	1.00	2.95	2.07	5.54	pyrophosphatase (inorganic)
Ppargc1a	1.00	1.41	1.72	-1.62	peroxisome proliferative activated receptor, gamma, coactivator 1 alpha
Ppia	-1.01	1.35	-1.16	2.92	peptidylprolyl isomerase A
PPID	-1.04	2.25	1.26	1.17	peptidylprolyl isomerase D (cyclophilin D)
PPM1A	-1.07	1.45	2.49	-1.98	protein phosphatase 1A (formerly 2C), magnesium-dependent, alpha isoform
PPP2CA	-1.04	1.60	1.12	-1.39	protein phosphatase 2 (formerly 2A), catalytic subunit, alpha isoform
Prdx5	-1.14	2.13	1.19	1.05	peroxiredoxin 5
PREP	1.08	2.16	1.20	1.27	prolyl endopeptidase
PRKACA	-1.16	2.00	-1.04	-1.19	protein kinase, cAMP-dependent, catalytic, alpha
PRKAR2B	1.45	1.56	1.73	1.90	protein kinase, cAMP-dependent, regulatory, type II, beta
PRKR	1.12	2.73	1.81	1.51	interferon-inducible RNA-dependent protein kinase (P68 kinase)
PRKRA	1.00	2.07	2.07	-1.08	protein kinase, interferon-inducible double stranded RNA dependent activator
PSMB2	-1.11	1.02	1.12	3.07	proteasome component C7-I (macropain subunit C7-I)
PTGS1	-1.02	1.40	1.29	-1.77	prostaglandin G/H synthase 1 precursor; cyclooxygenase 1 (COX1)
PTGS2	1.31	3.58	3.02	6.67	prostaglandin G/H synthase 2 precursor; cyclooxygenase 2 (COX2)
Rab8b	-1.09	1.18	2.13	-1.44	member RAS oncogene family
Rabggtb	1.20	1.31	1.01	2.45	RAB geranylgeranyl transferase, b subunit
Raly	-1.21	1.22	-1.32	2.33	hnRNP-associated with lethal yellow
RASA1	-1.01	1.97	1.24	1.08	RAS p21 protein activator (GTPase activating protein) 1
RBP1	1.00	3.25	1.44	-1.63	retinol-binding protein i, cellular (CRBP)
RCN1	1.10	2.25	1.15	1.81	RETICULOCALBIN 1 PRECURSOR.
Rnf11	1.15	1.60	1.08	2.03	RING finger protein 11
RPIA	1.03	2.52	1.27	1.10	ribose 5-phosphate isomerase A (ribose 5-phosphate epimerase)
RPL10	1.04	-1.15	-1.08	4.24	60S ribosomal protein L10; tumor suppressor QM; laminin receptor homolog

Table B.1. (continued)

Gene Symbol	1 HPI	4 HPI	8 HPI	12 HPI	Gene description
RPL5	-1.01	1.08	-1.16	3.85	60S ribosomal protein L5
RPS27A	-1.16	1.30	-1.11	3.07	H.sapiens Uba80 mRNA for ubiquitin
RPS28	-1.04	1.19	2.01	-1.55	40S RIBOSOMAL PROTEIN S28.
Rtn3	1.29	2.34	1.86	1.60	reticulon 3
S100A10	-1.25	1.76	1.03	2.44	calpactin I light chain
S100A11	-1.01	2.08	-1.11	3.26	calgizzarin; S100C protein; MLN70
S100A12	1.57	1.09	1.24	4.91	S100 calcium binding protein A12 (calgranulin C)
SARS	-1.30	1.29	-1.12	2.97	seryl-trna synthetase (serine--trna ligase) (SERRS).
Sec61g	1.02	2.21	1.27	2.26	SEC61, gamma subunit
SERPINE2	1.01	1.77	1.36	1.98	glia-derived neurite-promoting factor (GDNPF)
Sf3b5	-1.20	1.64	1.23	-1.23	splicing factor 3b, subunit 5
SFRS2	1.14	1.32	-1.05	2.43	splicing factor, arginine/serine-rich 2 (splicing factor SC35)
SIAT8A	-1.26	2.63	1.91	-1.45	alpha-N-acetylneuraminnide alpha-2,8-sialyltransferase
SIAT8D	1.38	1.66	-1.01	2.29	alpha-2,8-sialyltransferase
SLC14A1	1.00	2.90	2.23	1.20	erythrocyte urea transporter (UTE UT1) SLC14A1 HUT11 RACH1
SLC1A1	1.17	1.04	-1.00	-2.47	high-affinity glutamate transporter excitatory amino acid transporter 3
SLC1A3	1.67	1.98	1.34	2.09	sodium-dependent glutamate/aspartate transporter 1 (GLAST1)
Slc1a5	-1.36	1.74	1.44	-1.18	solute carrier family 1 (neutral amino acid transporter), member 5
Slc24a1	-1.08	1.16	1.99	-1.84	solute carrier family 24 (sodium/potassium/calcium exchanger), member 1
Slc25a25	1.14	1.39	1.62	1.08	solute carrier family 25 (mitochondrial carrier, phosphate carrier), member 25
SLC25A4	1.10	2.10	-1.06	-1.02	solute carrier family 25 (mitochondrial carrier; adenine nucleotide translocator)
SLC2A1	1.12	1.99	1.68	1.62	erythrocyte glucose transporter 1 (GLUT1)
Slc35a1	1.20	2.10	1.41	-1.21	solute carrier family 35 (CMP-sialic acid transporter), member 1
Slc38a2	1.03	2.55	1.35	1.96	solute carrier family 38, member 2
SLC6A2	-1.15	2.16	1.36	-1.06	sodium-dependent noradrenaline transporter norepinephrine transporter (NET)

Table B.1. (continued)

Gene Symbol	1 HPI	4 HPI	8 HPI	12 HPI	Gene description
SLC6A9	-1.10	1.52	1.65	-1.33	sodium- & chloride-dependent glycine transporter 1 (GLYT-1)
SLC7A5	1.04	2.61	1.34	1.01	E16 amino acid transporter
SNAI2	-1.49	1.67	1.69	-1.11	snail homolog 2 (Drosophila)
SNRPB	1.21	1.55	1.59	2.75	SNRNP POLYPEPTIDE B.
Sod2	1.11	2.43	1.48	5.28	superoxide dismutase 2, mitochondrial
SPARC	-1.04	1.83	-1.06	-1.11	secreted protein acidic and rich in cysteine precursor (SPARC)
Spint1	-1.01	-1.77	1.16	-2.69	serine protease inhibitor, Kunitz type 1
Ssna1	-1.17	2.15	1.42	-1.42	Sjogren's syndrome nuclear autoantigen 1
Ssrp1	-1.00	1.23	1.21	3.39	structure specific recognition protein 1
st6GalNAc-VI	1.12	1.32	1.71	1.08	beta-galactosamide alpha-2,6-sialyltransferase
Stxbp1	1.67	2.72	3.34	2.04	syntaxin binding protein 1
Tacstd1	1.33	1.43	2.62	1.57	tumor-associated calcium signal transducer 1
Taldo1	-1.16	1.18	1.06	2.07	transaldolase 1
TBCE	1.09	1.52	1.76	1.41	cofactor E
TERF1	1.15	1.94	1.18	1.36	telomeric repeat binding factor 1 (TRF1)
Tfb1m	-1.08	1.70	1.55	-1.30	transcription factor B1, mitochondrial
TFPI2	1.55	1.94	1.92	1.81	tissue factor pathway inhibitor 2
THBS	1.41	2.23	1.83	3.22	thrombospondin
TIMP1	-1.30	2.28	1.51	3.00	metalloproteinase inhibitor 1 precursor (TIMP1)
TIMP2	1.15	2.52	-1.01	1.08	tissue inhibitor of metalloproteinases 2 (TIMP2)
TIMP3	1.13	1.74	1.26	2.11	tissue inhibitor of metalloproteinases 3 (TIMP3)
TLR4	1.30	1.72	1.41	1.38	toll-like receptor 4
Tmed1	-1.02	2.05	1.19	-1.09	transmembrane emp24 protein transport domain containing 1
TNS	-1.16	1.64	1.09	1.08	tensin
TOLLIP	-1.24	1.61	1.12	-1.47	toll interacting protein

Table B.1. (continued)

Gene Symbol	1 HPI	4 HPI	8 HPI	12 HPI	Gene description
TPI1	-1.13	1.04	1.37	2.91	triosephosphate isomerase 1
TPM1	1.13	1.78	-1.19	2.85	tropomyosin alpha chain, skeletal muscle
Tpm3	-1.03	1.42	1.40	3.39	tropomyosin 3, gamma
TPPP	1.23	1.75	1.29	1.18	tropomyosin 1 (alpha)
TRB2	1.57	1.92	1.39	1.19	TRB-2 protein
TREM-1	1.03	2.34	-2.00	-1.13	triggering receptor expressed on myeloid cells-1
Tspan1	-2.74	-1.37	-1.54	-2.78	tetraspanin 1
Tspan33	1.58	1.68	1.91	-1.06	tetraspanin 33
TUBB	1.06	2.18	2.93	1.86	tubulin, beta
TUBB2A	-1.03	-1.09	1.21	3.69	tubulin, beta 2A
UBE2F	-1.01	1.69	1.33	1.03	ubiquitin-conjugating enzyme E2F (UBC6 homolog, C. elegans)
Ube2i	-1.57	1.02	2.94	-2.43	ubiquitin-conjugating enzyme E2I
Ubl5	1.10	1.14	1.15	2.26	ubiquitin-like 5
UBX8	1.02	1.99	1.46	1.35	UBX domain-containing protein 8
UCHL1	1.30	2.42	-1.23	1.93	ubiquitin carboxyl-terminal esterase L1 (ubiquitin thiolesterase)
VIM	-1.06	-1.07	-1.16	4.94	vimentin (VIM)
VIT	-1.30	1.55	1.31	-2.74	vitrin
Vsnl1	1.47	2.07	1.79	1.99	visinin-like 1
Wars	1.24	2.87	1.59	5.01	tryptophanyl-tRNA synthetase
Wsb2	1.04	2.40	1.06	2.12	WD repeat and SOCS box-containing 2
Yars	1.06	2.02	1.49	1.44	tyrosyl-tRNA synthetase
YWHAH	1.39	1.85	1.22	2.18	14-3-3n protein eta protein AS1 YWHAH YWHA1
ZBTB16	-1.26	2.08	-1.05	-2.46	promyelocytic leukemia zinc finger protein (PLZF); zinc finger protein 145 (ZNF145)
ZDHHC4	1.06	2.06	1.50	1.55	zinc finger, DHHC domain containing 4
Zdhhc6	1.13	1.31	1.75	1.35	zinc finger, DHHC-type containing 6

Table B.1. (continued)

Gene Symbol	1 HPI	4 HPI	8 HPI	12 HPI	Gene description
ZNF622	1.12	2.13	1.26	1.34	zinc finger protein 622

[a]837 differentially expressed genes of unknown description are not listed.

APPENDIX C

Table C.1. Mechanistic host genes differentially expressed in *S. typhimurium*-infected bovine ligated ileal loops from BLAD (CD18 -/-) and Control calves (CD18 +/+) at 1, 4, 8, and 12 hours post-infection (HPI) compared to uninfected control samples. The letter N represents gene expression with no statistical significance ($p \leq 0.025$). Blank spaces represent no detected gene expression.

	1 HPH		4 HPI		8 HPI		12 HPI		
Gene symbol	BLAD	Control	BLAD	Control	BLAD	Control	BLAD	Control	Gene description
AHSG		Up	N	Up	N				alpha-2-hs-glycoprotein precursor (fetuin)
AKT1	Up	Down					Up	Down	v-akt murine thymoma viral oncogene homolog 1
ALDH1A1	Up	N	N	Down	N	Down	N	Down	alcohol dehydrogenase 6 + aldehyde dehydrogenase 1
ALPL	Up	N	Up	N	Up	No			alkaline phosphatase
ANPEP	Down	Down	Down	N	Down	Down	Down	Down	myeloid plasma membrane glycoprotein CD13
ARRB1	Up	N	Up	N	Up	N	N	Down	arrestin, beta 1
ATP5H	N	Up	Down	No					ATP synthase, H+ transporting, mitochondrial F0 complex
Abcd4			Up	N					ATP-binding cassette, sub-family D (ALD), member 4
Ace2	Down	Down	Down	N	Down	Down	Down	Down	angiotensin I converting enzyme (peptidyl-dipeptidase A) 2

Table C.1. (continued)

	1 HPH		4 HPI		8 HPI		12 HPI		
Gene symbol	BLAD	Control	BLAD	Control	BLAD	Control	BLAD	Control	Gene description
Aldh7a1			Up	N	Up	N	N	Down	aldehyde dehydrogenase 7 family, member A1
Apoc3	N	Down	Down	Down	Down	Down	Down	Down	apolipoprotein C-III
Aqp4	Up	N	Up	N	Up	Down	N	Down	aquaporin 4
Atp6v0a2			Up	N	Up	N			ATPase, H+ transporting, lysosomal V0 subunit a2
BHLHB2	N	Up	Up	Up	N	Up	Up	Up	basic helix-loop-helix domain containing, class B, 2
C1R	Down	Down	Down	N	Down	Up	Down	N	complement component 1, r subcomponent
CASP6	N	N	Down	N	N	Up	Down	Down	caspase 6, apoptosis-related cysteine protease
CCL2	Up	Up	N	Up	Down	Up	Up	Up	chemokine (C-C motif) ligand 2
CCL5	Up	Down					N	Up	chemokine (C-C motif) ligand 5
CCL8			Up	Up	Down	Up	Up	Up	chemokine (C-C motif) ligand 8
CCNA2	Up	Down	Up	Up	Up	N	Up	Down	cyclin A2
CD9	Up	N	Up	N			Up	Up	CD9 antigen; p24; leukocyte antigen MIC3
CFLAR	N	Down	Down	Up	N	Up	N	Up	CASP8 and FADD-like apoptosis regulator
CHRNA3			N	Up			N	Up	neuronal acetylcholine receptor protein alpha-3 subunit precursor
CHUK	N	Down	Up	N	Up	N	Down	N	conserved helix-loop-helix ubiquitous kinase

Table C.1. (continued)

	1 HPH		4 HPI		8 HPI		12 HPI		
Gene symbol	BLAD	Control	BLAD	Control	BLAD	Control	BLAD	Control	Gene description
CROT			Up	N			N	Down	carnitine O-octanoyltransferase
CSNK2A2			Up	N	Up	N			casein kinase 2, alpha prime polypeptide
Cacnb2			Up	N	Up	N			calcium channel, voltage-dependent, beta 2 subunit
Cebpd	Up	N	N	Up	Down	Up	N	Up	CCAAT/enhancer binding protein (C/EBP), delta
Chrne	Up	Up	N	Up	Down	Up	N	Up	cholinergic receptor, nicotinic, epsilon polypeptide
Ciapin1			Up	N	Up	Down	N	Down	cytokine induced apoptosis inhibitor 1
Cspg6	Up	Down	N	Up	Up	Up	Up	N	chondroitin sulfate proteoglycan 6
Cyhr1	N	Up	Down	N			Down	N	cysteine and histidine rich 1
DBI	Down	Down	Up	N	Up	N	Up	Up	acyl-CoA-binding protein (ACBP) diazepam binding inhibitor (DBI)
DUSP6					N	Up			dual specificity phosphatase 6
EGR1	Up	Up	Up	Up	N	Up	Up	Up	early growth response protein 1 (hEGR1) transcription factor ETR103
Eif3s3	N	Down	Up	Up	N	Down	Up	Down	eukaryotic translation initiation factor 3, subunit 3 (gamma)
F2			Down	Up	Down	N			coagulation factor II (thrombin)
F5	Up	N	Up	N	N	Up			coagulation factor V (proaccelerin, labile factor)
FBP2	Down	Down					Down	N	folate receptor 2 (fetal)

Table C.1. (continued)

	1 HPH		4 HPI		8 HPI		12 HPI		
Gene symbol	BLAD	Control	BLAD	Control	BLAD	Control	BLAD	Control	Gene description
FDX1	Up	N	Up	N					adrenodoxin
FECH	Up	N	Up	N	Up	N	N	Down	ferrochelatase precursor protoheme ferro-lyase heme synthetase
FES	Up	N	Up	Down	Down	Up			C-fes proto-oncogene
FN1	Up	N	Up	N	Up	Down	Up	N	fibronectin 1
FOS	N	Up	Up	Up	N	Up	Up	Up	v-fos FBJ murine osteosarcoma viral oncogene homolog
FUT4	Down	N			N	Up	Down	Up	fucosyltransferase 4 (alpha (1,3) fucosyltransferase, myeloid-specific)
GRP58	N	Up			N	Down	Up	N	probable protein disulfide isomerase ER-60 precursor (ERP60)
GUCY1B3	Up	N	Up	N	Up	N			guanylate cyclase soluble beta-1 subunit guanylate cyclase
Gltp			Up	N	Up	N			glycolipid transfer protein
Got2			Up	N	Up	N			glutamic-oxaloacetic transaminase 2
HNF4A	Down	Down	Down	Down	Down	N	Down	N	hepatocyte nuclear factor 4 (HNF4) transcription factor 14
HNF4G	Down	Down	Down	Up	Down	N	Down	Down	hepatocyte nuclear factor 4-gamma
ICAM1	N	Down	N	Up	Down	Up	Up	Up	intercellular adhesion molecule-1 precursor
IFNAR2			Up	Up	N	Up	N	Up	interferon (alpha, beta and omega) receptor 2
IFNG	N	Up	Up	Up	Up	Up	Up	Up	interferon, gamma

Table C.1. (continued)

	1 HPH		4 HPI		8 HPI		12 HPI		
Gene symbol	BLAD	Control	BLAD	Control	BLAD	Control	BLAD	Control	Gene description
IGFBP2	N	Up	Up	N	N	Down	Up	Down	insulin-like growth factor binding protein 2
IGFBP3	Down	Down	Down	Up	Down	Up	Down	Up	insulin-like growth factor-binding protein 3 precursor
IKBKB	Down	Up	Up	N	Up	N			inhibitor of kappa light polypeptide gene enhancer in B-cells, kinase beta
IKBKG	Down	Down	Up	N	Up	N	N	Down	inhibitor of kappa light polypeptide gene enhancer in B-cells
IL1B	N	Up	Up	Up	N	Up	Up	Up	interleukin 1, beta
IL6	N	Up	Up	Up	N	Up	Up	Up	interleukin 6 (interferon, beta 2)
IL8	Up	Down	N	Up	N	Up	N	Up	interleukin 8
IRF1	Down	Down	N	Up	Down	Up	Up	Up	interferon regulatory factor 1 (IRF1)
ITGB2	N	Down	Down	N			Up	N	integrin, beta 2 (lymphocyte function-associated antigen 1)
ITPR2	Down	Down			N	Up	N	Down	inositol 1,4,5-triphosphate receptor, type 2
Idh3a			Up	N	Up	N			isocitrate dehydrogenase 3 (NAD+) alpha
LDHB	N	Down	N	Down	N	Down	N	Down	L-lactate dehydrogenase H subunit (LDHB)
Lmo4			Up	Down			Up	N	LIM domain only 4
Lu	N	Up	Down	N					Lutheran blood group (Auberger b antigen included)
MAPK13					N	Up	Down	Up	mitogen-activated protein kinase 13

Table C.1. (continued)

	1 HPH		4 HPI		8 HPI		12 HPI		
Gene symbol	BLAD	Control	BLAD	Control	BLAD	Control	BLAD	Control	Gene description
MMP14	Down	N			Up	Up	N	Up	matrix metalloproteinase 14 precursor
MSX1			Up	Down					MSX-1 homeobox protein HOX7
MYB	Up	Up	Up	N	Up	N	Up	Down	myb proto-oncogene c-myb
Mgst3	Down	N			Down	N			microsomal glutathione S-transferase 3
Mrpl30			Up	N	Up	N	Up	N	mitochondrial ribosomal protein L30
Ndufs3	N	Down	Up	N			N	Down	NADH dehydrogenase (ubiquinone) Fe-S protein 3
Nnt	Down	Down			Up	Down	Up	Down	nicotinamide nucleotide transhydrogenase
PAFAH1B1	Up	N	Up	N	N	Down	N	Down	platelet-activating factor acetylhydrolase IB alpha subunit
PIK3CA			Up	Down	Up	N			phosphoinositide-3-kinase, catalytic, alpha polypeptide
PLAU	N	Up	Up	Up	Up	Up	Up	Up	plasminogen activator, urokinase
PLCB1	Up	Down	Up	Up	Up	N	N	Down	phospholipase C, beta 1 (phosphoinositide-specific)
PP			Up	N	Up	Up	Up	Up	pyrophosphatase (inorganic)
PRKAR2B	Up	N	Up	Up	Up	Down	Up	Down	protein kinase, cAMP-dependent, regulatory, type II, beta
PRKCA			Up	N	Up	N	N	Down	protein kinase C, alpha
PTGDS	N	Up	Up	Down	N	Down	N	Down	prostaglandin-H2 D-isomerase precursor; prostaglandin-D synthase

Table C.1. (continued)

	1 HPH		4 HPI		8 HPI		12 HPI		
Gene symbol	BLAD	Control	BLAD	Control	BLAD	Control	BLAD	Control	Gene description
Plac8		Up	N	Up	Up	Up	Up	Up	placenta-specific 8
Ppargc1a	N	Down	Up	N	Up	Down	N	Down	peroxisome proliferative activated receptor, gamma, coactivator 1 alpha
RAB13	N	Down	Up	Up	Up	Down			RAB13, member RAS oncogene family
RAD21	Up	Down	N	Up			Up	Down	RAD21 homolog (S. pombe)
RAP1A	N	Up			N	Up	Dow	N	RAP1A, member of RAS oncogene family
RBP1			Up	Down	Up	N	Down	Up	retinol-binding protein i, cellular (CRBP)
RPL21	N	Down					Up	Down	60S ribosomal protein L21.
RPL5	N	Down			Down	N	Up	N	60S ribosomal protein L5
RRAS	Up	N	Up	N	N	Down			related RAS viral (r-ras) oncogene homolog
Rps29	Down	N			Down	N	Up	N	ribosomal protein S29
SERPINE2			Down	N			Down	N	glia-derived neurite-promoting factor (GDNPF)
SLC5A2	Up	N			Up	N	Up	N	sodium/glucose cotransporter 2
SLC6A9			Up	N	Up	N			sodium- & chloride-dependent glycine transporter 1 (GLYT-1)
SMAD4	N	Down	Up	N	Up	Down	N	Down	SMAD, mothers against DPP homolog 4 (Drosophila)
SMC1L1	N	Down	Up	N	Up	N	Up	Down	SMC1 structural maintenance of chromosomes 1-like 1 (yeast)

Table C.1. (continued)

	1 HPH		4 HPI		8 HPI		12 HPI		
Gene symbol	BLAD	Control	BLAD	Control	BLAD	Control	BLAD	Control	Gene description
SOCS3			N	Up	Down	Up	N	UP	suppressor of cytokine signaling 3
Sod2	Up	Up	Up	Up	N	Up	Up	Up	superoxide dismutase 2, mitochondrial
Ssbp2			Up	N	Up	Down			single-stranded DNA binding protein 2
Stxbp1	Up	Up	Up	Down	Up	N	Up	Up	syntaxin binding protein 1
TNFRSF1A			Up	Up	N	Up	Down	Up	tumor necrosis factor receptor superfamily, member 1A
TOLLIP	Down	Up	Up	N			Down	N	toll interacting protein
TPM1			Up	Down	N	Down	Up	N	tropomyosin alpha chain, skeletal muscle
TRAF6			Up	N					TNF receptor-associated factor 6
TUBB	N	Up	Up	N	Up	N	Up	N	beta tubulin
TXNRD2	Up	Down			Up	Down			thioredoxin reductase 2
Txn2	N	Down			N	Down			thioredoxin 2
Vapb	N	Down	Up	N	Up	Down	N	Down	vesicle-associated membrane protein, associated protein B and C
Vps16	N	Down	Up	N	N	Down	Up	Down	vacuolar protein sorting 16 (yeast)
YWHAE	N	Up	N	Up	N	Up	N	Down	protein epsilon (mitochondrial import stimulation factor l subunit)
YWHAH	Up	Down	Up	N	N	Down	Up	N	14-3-3n protein eta protein AS1 YWHAH YWHA1

VITA

Name: Jairo Eduardo dos Santos Nunes

Address: 893 S Delaware St
Eli Lilly Corporate Center
Indianapolis, IN, USA 46285

Email Address: jnunes@cvm.tamu.edu

Education: D.V.M, 1998
Universidade Federal de Uberlandia, Brazil

M.Sc., 2001, General Pathology
Faculdade de Medicina
Universidade Federal de Minas Gerais, Brazil